3

AEDC-TR-71-258
AD-737 367

ARCHIVE COPY
DO NOT LOAN

cy. 1

RESEARCH ON STORAGE HEATERS FOR HIGH TEMPERATURE WIND TUNNELS - FINAL REPORT

D. E. Hagford and D. G. DeCoursin

FluiDyne Engineering Corporation

February 1972

Approved for public release; distribution unlimited.

ARNOLD ENGINEERING DEVELOPMENT CENTER
AIR FORCE SYSTEMS COMMAND
ARNOLD AIR FORCE STATION, TENNESSEE

PROPERTY OF U.S. AIR FORCE
AEDC LIBRARY
F40600-72-C-0003

AEDC TECHNICAL LIBRARY
5 0720 00033 2884

NOTICES

When U. S. Government drawings specifications, or other data are used for any purpose other than a definitely related Government procurement operation, the Government thereby incurs no responsibility nor any obligation whatsoever, and the fact that the Government may have formulated, furnished, or in any way supplied the said drawings, specifications, or other data, is not to be regarded by implication or otherwise, or in any manner licensing the holder or any other person or corporation, or conveying any rights or permission to manufacture, use, or sell any patented invention that may in any way be related thereto.

Qualified users may obtain copies of this report from the Defense Documentation Center.

References to named commercial products in this report are not to be considered in any sense as an endorsement of the product by the United States Air Force or the Government.

RESEARCH ON STORAGE HEATERS FOR HIGH TEMPERATURE WIND TUNNELS - FINAL REPORT

D. E. Hagford and D. G. DeCoursin
FluiDyne Engineering Corporation

Approved for public release; distribution unlimited.

FOREWORD

The work reported herein was sponsored by Arnold Engineering Development Center (AEDC), Air Force Systems Command (AFSC), Arnold Air Force Station, Tennessee, under the following contracts with FluiDyne Engineering Corporation, Minneapolis, Minnesota: AF 40(600)-1094, Program Elements 62410034 and 63101F, Project 7778, Task 05; F40600-68-C-0002; and F40600-70-C-0006, Program Elements 62402F and 63723F, Project 3012, Task 07.

The work was performed from January 1964 to September 1971. The manuscript was submitted for publication on 20 August 1971.

The cooperation and assistance of several individuals and corporations has been invaluable in carrying out the work covered in the subject report. Dr. J. D. Plunkett, Materials Consultants, Inc., has provided technical interpretation of test results and analyses throughout the program while serving as a consultant to FluiDyne. Dr. L. L. Fehrenbacher has provided the majority of the material analyses both in his present position with the Aerospace Research Laboratory, WPAFB and in his previous position with the Air Force Materials Laboratory, WPAFB. Dr. Fehrenbacher has also served, throughout the program, as a consultant to the Air Force on zirconia materials, Dr. R. Ruh, Air Force Materials Laboratory, WPAFB, has provided both analytical services and has assisted in the interpretation of these data. Coors Porcelain Company and Zirconium Corporation of America (Zircoa) have contributed as the major material suppliers and the Arnold Research Organization (ARO), AEDC, as the operator of the Pilot Heater Facility.

The reproducibles used in the reproduction of this report were supplied by the authors.

This technical report has been reviewed and is approved.

G. M. ARNOLD, Chief
Facility Development Division
Directorate of Civil Engineering

ERNEST F. MOORE
Colonel, USAF
Director of Civil Engineering

ABSTRACT

The results from the materials development program for the ceramics of the storage heater system for high temperature wind tunnels are presented. A number of ceramic oxides were evaluated includign magnesia, zirconia, and alumina. Magnesia was dropped as a candidate early in the program because of the high vaporization rate experienced in a flowing combustion gas atmosphere. Zirconia was evaluated in its stabilized form using calcia, magnesia, and yttria as the stabilizing oxides. Yttria-stabilized zirconia evolved as the candidate material for the upper portion of the heater matrix (2800°F to 4200°F) and alumina for the lower portion (1000°F to 2800°F).

The development program evaluated materials in both subscale and pilot scale tests. The performance of the individual materials during the various subscale tests is discussed. The design basis for a pilot facility is presented along with the material performances following the 85 run, pilot heater test program.

Specifications for materials used in the pilot facility are presented along with a cored block specification prepared based on the development program.

TABLE OF CONTENTS

Page

LIST OF TABLES

LIST OF FIGURES

NOMENCLATURE

A	Cross section area of bed
D	Diameter of holes in cored brick
E	Modulus of elasticity
L	Length in direction of flow
R_a	= 1.05 x hole spacing-to-hole diameter ratio
R_1	$= \frac{R_a^4 (\ln R_a - 3/4) + R_a^2 - 1/4}{R_a^2 - 1}$
R_3	$= \frac{R_a^2 R_1}{R_a^2 - 1}$
S	Tensile stress
T	Temperature
T_{ave}	Average temperature in web
$T_{surface}$	Surface temperature of hole
a	Thermal diffusivity
C_p	Specific heat of air
k_s	Thermal conductivity of ceramic
$\dot{m}$	Mass flow rate
p	Porosity of ceramic material
α	Coefficient of expansion
θ	Time
ν	Poisson's ratio

Subscript o refers to zero material porosity

1.0 INTRODUCTION

The design and development of advanced air breathing propulsion systems for operation at high supersonic and hypersonic flight conditions will demand the development of test facilities capable of simulating the actual flight conditions. These facilities would have the capability of providing stagnation conditions corresponding to simulated flight conditions at hypersonic Mach numbers. A blowdown type facility involving a large regenerative storage heater can be employed to provide these stagnation conditions at reasonable power inputs.

The work covered in this report was directed toward the evaluation and specification of high temperature materials for use in the storage heater system. Several materials were evaluated under the subject contracts on the basis of their comparative performance, life, availability, and costs. The combination of thermal stresses (which are inherent in heat exchangers) and brittle materials (a category within which all ceramics fall) represents the major general limitation in the design and operation of ceramic heat exchangers. Both factors are discussed in the following text, along with other critical material, performance, and evaluation test considerations. A unified discussion of thermal stress design considerations has been included as Appendix C.

The evaluation involved tests designed to expose the materials to simulated test conditions and observe their performance rather than attempt to measure the materials' properties and calculate a performance. The tests were conducted both on a subscale basis and in a pilot heater. The subscale tests exposed small quantities of material to one test parameter at a time, such as temperature, pressure, and mechanical loads. Subsequent tests in the pilot heater combined these tests by exposing relatively large quantities of materials to operating conditions very similar to those anticipated in a full-scale heater. The tests, materials, and related performances are the subject of this report.

2.0 GENERAL FUNCTION OF A STORAGE HEATER

The primary function of a storage heater is to heat a specified mass flow of air to within a specified temperature range for a specified period of time. A storage heater accomplishes this by slowly absorbing and storing thermal energy in a matrix during a heatup period, after which it is rapidly transferred to an air stream during a blowdown period. The salient features of the pilot heater are shown in Figure 1. It fundamentally consists of an insulated pressure vessel filled with a cored block heat storage matrix. The energy stored in the matrix is generated by the combustion of fuel with an oxidant which are both introduced at the top of the vessel through a premix burner. The combustion products heat the cored blocks as they pass through them and finally exhaust at the base of the vessel. When the desired temperature conditions are reached, the heater is switched from the heating cycle to the blowdown cycle. During the blowdown cycle, air is introduced at the base of the heater extracting the stored thermal energy from the cored block as it passes up through the matrix. Typically, the heatup period is measured in hours, and the blowdown period in seconds.

The temperature of the air after passing through the matrix, depends to a large degree on the temperature level near the top of the matrix. The maximum value is limited by the allowable service temperature of the matrix and insulation materials. A decrease in exhaust air temperature with time will occur which is generally referred to as the "temperature droop." For a given size heater the droop depends primarily on the mass flow rate and the vertical temperature distribution through the matrix. For any given mass flow, the droop would be the least if the entire matrix were initially heated to the air temperature level desired. Heating the entire matrix to a uniform temperature, however, is intolerable from other standpoints. First of all, the matrix is supported at its base by a metal grate support structure. The grate is designed to operate at maximum temperature of 1000°F. Secondly, the ceramic cored blocks are limited as to the maximum cooling rate they can tolerate without fracturing.

The cooling rates for the cored block are directly related to the vertical temperature profile (ramp) through the matrix. The thermal stresses in the cored block are in turn directly related to the cooling rates. As the ramp is made steeper, the cooling rates, and thus the thermal stresses, become greater for the same blowdown air mass flow. Therefore, the desired temperature profile is one in which the ramp portion is uniform and is the "steepest" consistent with the allowable cooling rate limitations of the cored block. As a result, the vertical temperature profiles in a storage heater for operation at different maximum temperatures will have the general shape of those shown in Figure 1.

In the specification of a heater, certain performance requirements are established relating to maximum temperatures, pressures and mass flows for which the storage heater must be capable of delivering. These requirements form the storage heater design criteria.

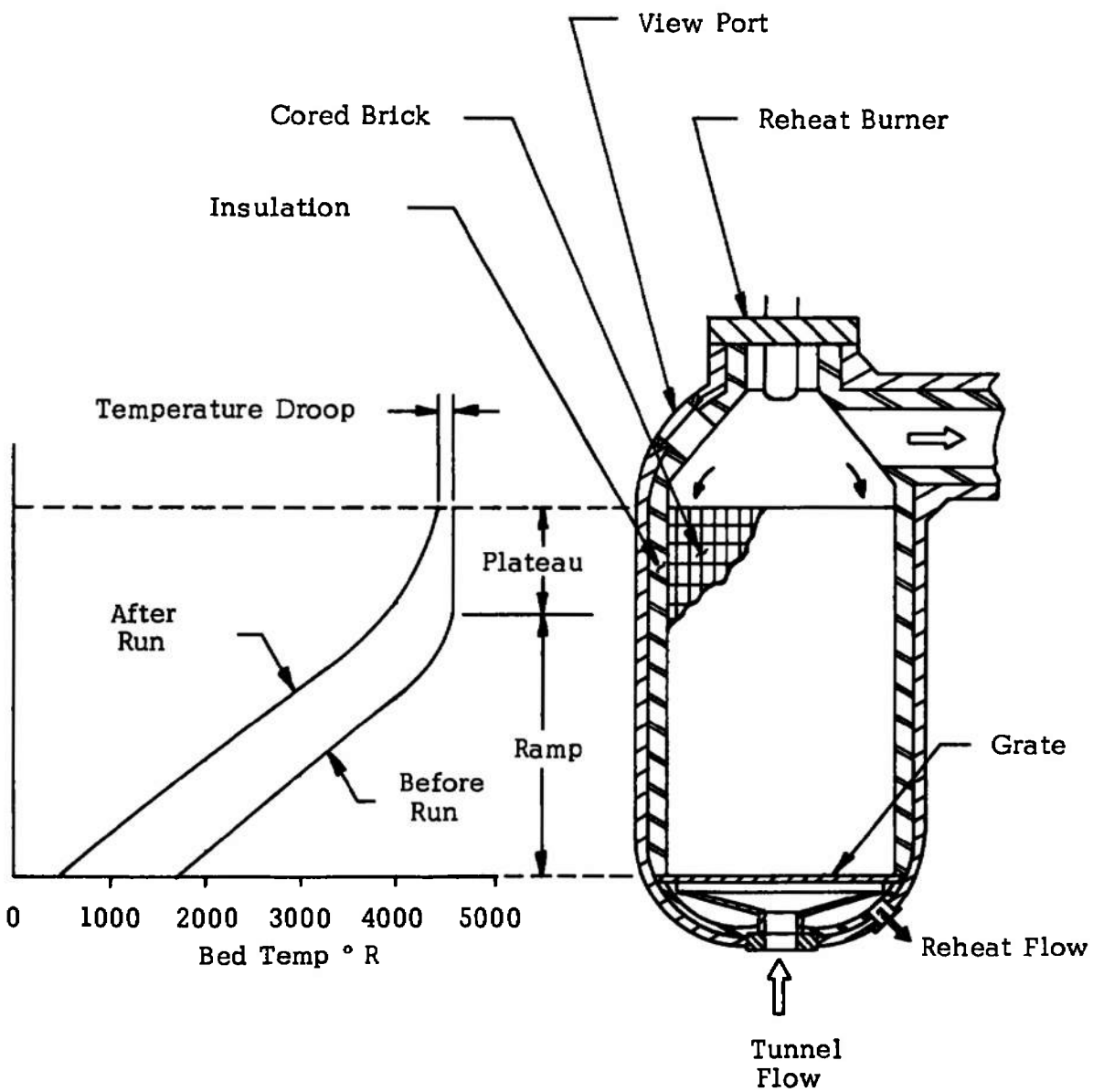

FIGURE 1. HEATER CONFIGURATION

3.0 DESIGN CRITERIA FOR THE FULL SCALE PROTOTYPE HEATER

As in any design project, before the initial design, material selection and subscale testing can begin the design criteria must be established. In the case of the prototype heater, this effort was undertaken on previous contracts and was fairly well formalized at the beginning of this effort in 1964.

As the material selection and subscale testing progressed and results were obtained and analyzed, there were periodic modifications to both the original work statement and the prototype heater design criteria. The final design criteria that evolved and within which the subject work was conducted included the design point performance requirements plus the following limitations:

1. The heater shell must be a single pressure vessel.
2. The vessel must be shop fabricated versus field fabrication.
3. The vessel shell temperature shall not exceed 500°F during steady state operation at the heater's design point.
4. Dusting from the ceramics must be negligible.

To meet the design point within the above limitations placed very narrow boundary conditions on the type of material that could be employed, its characteristics and the geometry it must assume.

The necessity for the heat storage media to be contained in one pressure vessel and that the vessel be shop fabricated, specified the volume available for heat transfer media. To satisfy the design requirements within the given volume, required that a high density material be used to store the required amount of thermal energy. Further, it was necessary that the material be fabricated into a geometry such that thermal energy could be extracted at a rate high enough to satisfy the design requirements without exceeding the thermal stress limitations for the matrix.

4.0 CANDIDATE MATERIALS

The requirement for heating air limited the selection of high temperature materials for the heat storage media and insulation to the refractory oxides.

The refractory oxides beryllia and thoria were dropped as candidates both due to cost and potential health hazards. Beryllia is stable to 3000°F in air, carbon monoxide and nitrogen, however, it is volatile in the presence of water vapor above 2450°F. Thoria on the other hand has the highest melting point of any oxide and is stable under most conditions. Thoria has the disadvantages, however, of high cost, radioactivity (thorium is one of the naturally occurring radioactive elements and is the parent of the thorium disintegration series) and is sensitive to thermal shock (due to its relatively high coefficient of thermal expansion and low thermal conductivity). Of the refractory oxides remaining only magnesia, zirconia and alumina met the requirements of having potentially useful properties at a reasonable cost. Magnesia was marginable, however, because of its high vapor pressure. Tests were performed to determine whether the resulting weight loss of magnesia would be detrimental in the operation of a storage heater. The results of these tests are discussed in Section 6.2.1.

The axial temperature profiles experienced in a storage heater are highest at the top and decrease to some lower temperature at the bottom of the heater. The temperature at the base of the heater cannot exceed the service temperature of the material from which the supporting grate structure is made (typically stainless steel with a useful maximum service temperature of about 1000-1500°F). With the lower temperature requirements in the bottom portion of the heater, materials with lower maximum temperature capabilities could be considered for these regions. Alumina was considered for this application both because of its favorable properties and favorable cost.

The two materials considered for the high temperature portion of the heater, zirconia and magnesia, possessed properties that would not allow their use without first verifying and qualifying their performance under subscale simulated operating conditions.

4.1 MAGNESIA

Magnesia, as mentioned previously, has the disadvantage of possessing a high vapor pressure. At the time of the subscale tests, however, magnesia had not been evaluated in an oxidizing combustion gas atmosphere at the temperatures and mass flow conditions under consideration for the storage heater. It was desirable, therefore, to evaluate magnesia and various doped magnesia compositions, on a subscale basis, to determine their performance under typical operating conditions.

4.2 ZIRCONIA

Zirconia is an unusual material in that it is polymorphic with a destructive volume change accompanying its crystalline phase change. Upon heating, pure zirconia transforms from monoclinic to a tetragonal crystalline form between 1890°F and 2200°F. This crystalline form is accompanied with a 7-8% reduction in volume. The volume change, however, occurs over a relatively small temperature range (2000-2200°F) and results in complete fragmentation of the material. The reverse transformation occurs upon cooling accompanied with a large increase in volume.

Zirconia can be forced into a stable cubic crystal structure by adding an adequate amount of so called stabilizers. Once in the cubic form, zirconia does not experience the phase and volume changes characteristics of pure monoclinic zirconia. The stabilizers consist of various oxides and have been the subject of several investigations, (References 1, 2, 3 and 4). Several oxides both singly and in various combinations have been used as stabilizers both in research studies and in commercial applications. These stabilizing oxides include calcia, magnesia and various rare earths. The rare earth used in this study involved a mixture of 90% yttria with the remaining 10% consisting of other heavy rare earths (primarily dysprosia).

As mentioned previously, an adequate amount of stabilizer will force the zirconia into a cubic crystalline structure. Any amount less than this will result in partial stabilization. The partially stabilized form is frequently used because of its lower overall thermal expansion. Figure 2 illustrates the thermal expansion characteristics of fully stabilized (cubic) and a typical, partially stabilized zirconia. The slight inversion zone of the partially stabilized material is due to the volume change associated with the remaining monoclinic portion present in the cubic zirconia material. The size of the inversion zone and the temperature range over which it occurs is dependent on the kind and amount of stabilizer. For materials evaluated in this program, the temperature range was approximately 800-2000°F.

The monoclinic content has been known to increase when partially stabilized zirconia is repeatedly cycled through its inversion zone. This phenomena is commonly termed "destabilization." Destabilization can continue until the monoclinic content reaches a level where destructive cracking and fracturing takes place. This has been commonly observed with calcia stabilized zirconia, especially when used as insulation in wind tunnel storage heaters (Reference 5). The phenomena is not restricted solely to partially stabilized material but has also been observed in zirconia that was initially stabilized (i.e., 97-99% cubic).

4.3 ALUMINA

Alumina is a material not plagued by the problems associated with either magnesia or zirconia. Alumina is a very stable material over its entire temperature range. The most serious disadvantage of alumina, relative to magnesia and zirconia, is its lower maximum service temperature. The maximum service temperature for alumina is 3300°F and slightly lower if used in contact with zirconia. Alumina's stability and lower cost, however, make it a very favorable candidate for the lower portion of the heater.

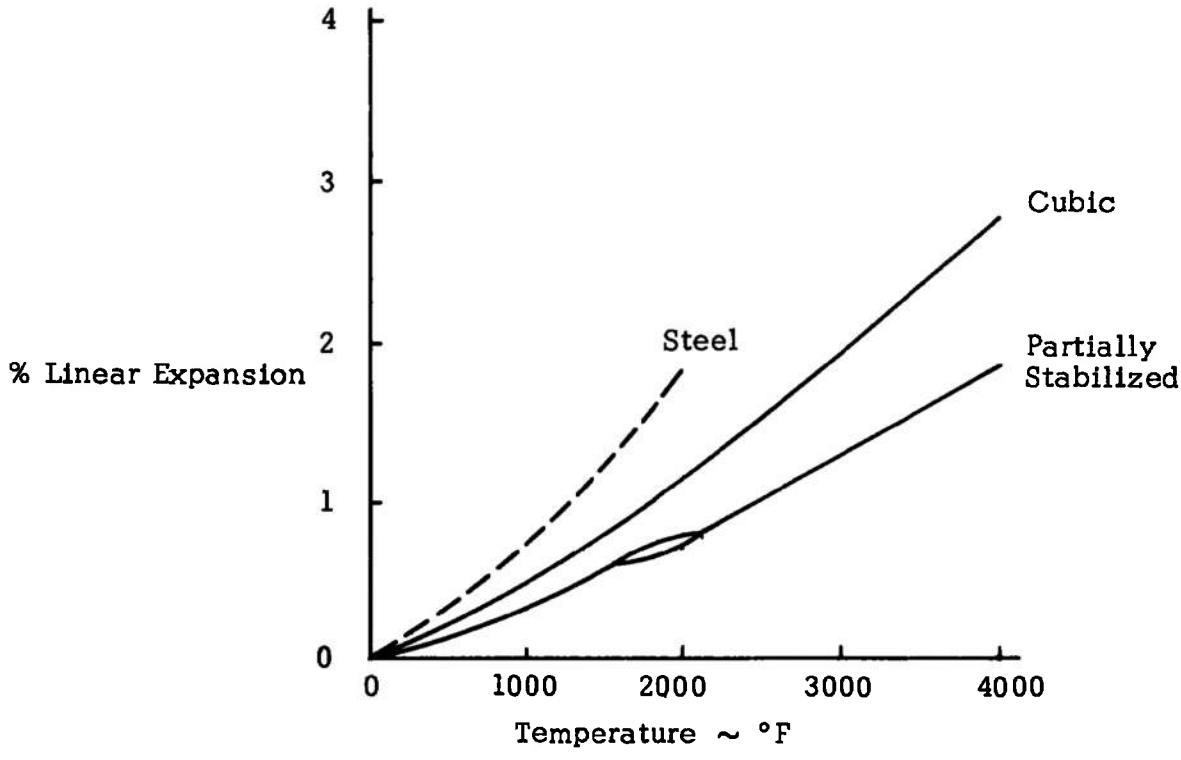

FIGURE 2. THERMAL EXPANSION OF ZIRCONIA

5.0 MATRIX ELEMENT SHAPE

Until 1964, all ceramic heaters for aerodynamic testing were designed using spherical pebbles for the heat storage matrix. These heaters employed alumina matrices for temperatures to 3000°F and calcia stabilized zirconia and magnesia for temperatures to 4000°F. Industrial heaters on the other hand have been operating at lower temperatures (up to 2000°F) and have employed a variety of shapes including checkers (rectangular blocks layed up in a basket weave fashion) and cored blocks.

Pebble heaters have typically been plagued with fairly severe dust problems. The pebble storage heater concept is prone to dust generation because of both the high point contact loading and the abrasion between adjacent pebbles. The point contact loading also leads to pebble deformation and matrix compaction. The deformation is in many instances associated with dusting and the resulting compaction leads to an increased pressure drop across the matrix. Both phenomena are undesirable in a storage heater.

One of the major performance differences between pebbles and cored blocks, outside of the dusting and deformation problems, is the large differences in pressure drop across the matrix. A cored block matrix has a much lower pressure drop at the same flow rate than a pebble matrix and therefore, the mass flow required to lift the matrix is much greater for a cored block versus a pebble heater. Lifting of the matrix, or flotation, occurs when the pressure drop per unit length begins to exceed the weight per unit length of the matrix ceramics. A comparison of flotation limited mass flow rates for spheres and cored block is shown in Figure 3. These curves are calculated for a pressure gradient equal to one-half that necessary to lift the matrix elements (specifically, one-half the bulk density). The equations used in calculating the pressure drop across a cored block matrix are developed in Reference 6.

As can be seen from Figure 3, the cored block flow rates are four to five times as great as the sphere values. The matrix diameter and consequently, the heater vessel diameter, can thus be reduced by using the cored block design. For high pressure heaters, where the vessel cost is large, smaller vessels can introduce substantial economics.

A storage heater matrix is made up of cored block shapes by stacking them in vertical columns. This forms a matrix containing many closely spaced, vertical, parallel holes. The blocks are held in alignment by a keying system on either end of the block. In the development effort covered by this report several cored block shapes were evaluated. A number of cored blocks, pebbles and insulation configurations are shown in Figure 4.

The cored block concept was selected for this development effort for the following reasons:

1. The reduced matrix pressure drop leads to a lower percentage of matrix flow to bypass through the surrounding cooler insulation. Consequently, the exit air temperature approaches, more closely, the top of the matrix temperature.

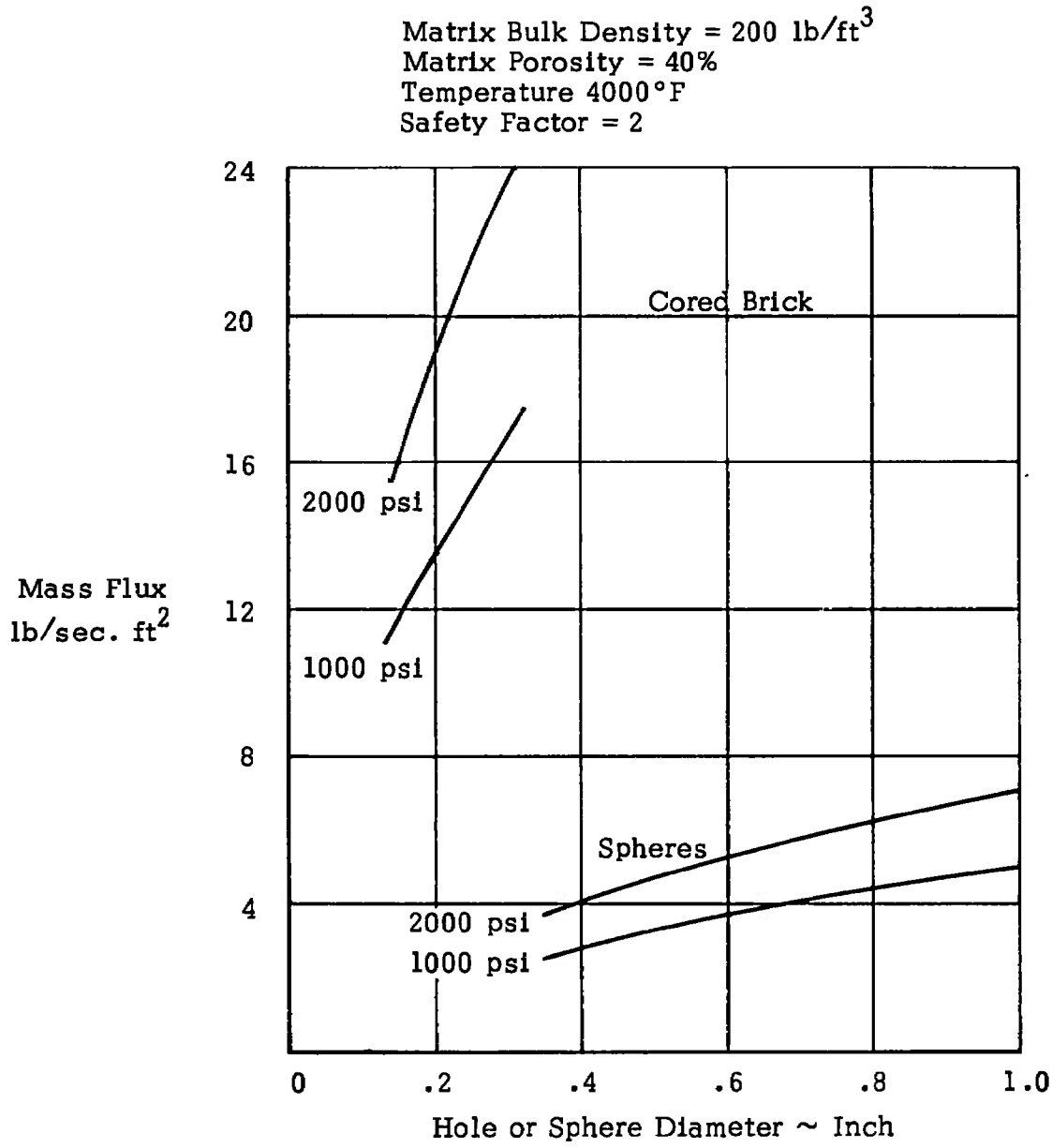

FIGURE 3. FLOTATION LIMITED MASS FLOW

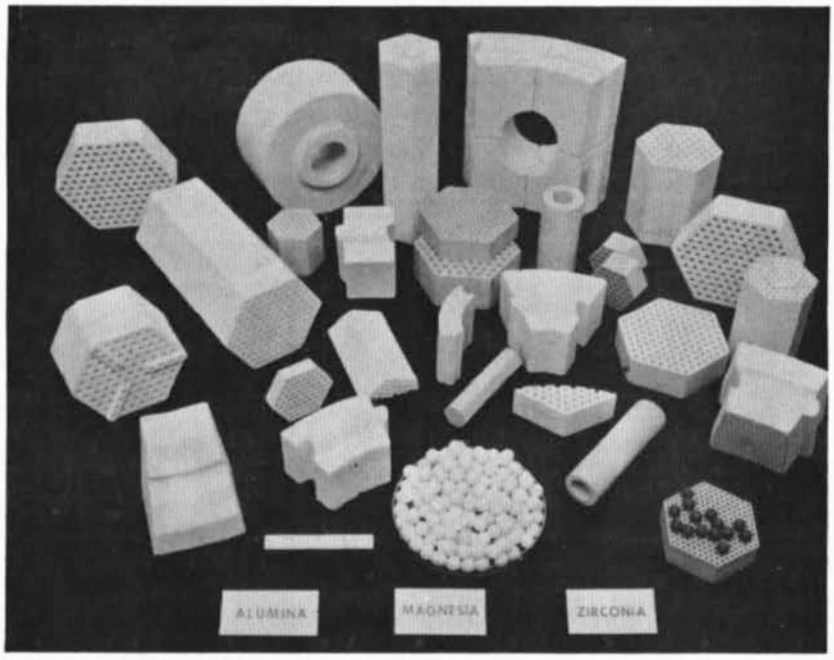

FIGURE 4. EXAMPLES OF CORED BLOCKS, PEBBLES AND HOT FACE INSULATION

2. The cored block matrix exerts a relatively small radial force on the vessel sidewall insulation compared to a pebble matrix of equal depth. This reduces the mechanical stresses experienced by the insulation.

3. The relative movement between adjacent matrix elements during heating and cooling is greatly reduced with a cored block design. As a result, the overall dust generation is reduced and also the life of matrix thermocouple installations are significantly increased.

4. The reduced bearing stresses between matrix elements in a cored block design essentially eliminates the matrix compaction experienced in pebble matrix heaters. Hence, performance remains essentially constant with time and matrix life is extended.

5. The reduced pressure drop through a cored block matrix permits pressurizing the heater at an increased rate such that the air storage and thermal capacity of the heater may be reduced or conversely remain the same and the useful run time increased.

6.0 MATERIALS EVALUATION - SUBSCALE TESTING

The principal requirements which a storage heater, and in particular the matrix material, must meet in wind tunnel applications are:

1. Have the capability of storing a specific quantity of thermal energy at a given temperature level.

2. Have the capability of releasing its stored thermal energy to a passing air stream at a given rate.

3. Remain essentially dust free during the heating and cooling process.

4. Remain geometrically stable other than for changes associated with typical thermal expansions.

Two alternate methods were available to determine whether a material would meet the requirements of a storage heater. First, the materials' performance could be calculated using the materials' thermo-physical and mechanical properties along with various theoretical and empirical relationships. Secondly, the materials' performance could be evaluated directly by an appropriate set of subscale tests designed to measure the materials' performance under simulated full scale storage heater conditions.

Calculation procedures would require both accurate assumption underlying the basic equations and accurate values for the material properties used in the equations. Slight variations in material compositions are often accompanied by large variations in material properties. Consequently, the properties of various materials are not always accurately known. Hence, under the subject contract the calculation procedures were used only to estimate the boundaries for the subsequent subscale testing. A procedure for estimating the stresses in a cored block during a heater blowdown cycle was used prior to testing under simulated conditions.

The testing was divided into two phases: subscale tests, where individual properties could be evaluated and pilot heater tests, where full scale heater operating conditions could be simulated.

6.1 TEST OBJECTIVES

The first major test phase involved subscale testing. The subscale tests were designed to evaluate the following material characteristics:

Thermal Stress Resistance

Permanence of Stability

Resistance to Rapid Changes in Pressure

The subscale, thermal stress resistance testing performed under the subject contract was directed toward determining the maximum cooling rates which the various materials would tolerate under simulated heater blowdown conditions.

The permanence of stability testing involved the stabilized zirconia materials only. This testing was broken into two phases; one concerned with the high temperature stability of the material and the second with the stability of the material when cycled repeatedly through the zirconia's inversion temperature zone.

A series of subscale tests were designed also to investigate the ability of the material to withstand the rapid pressure changes anticipated in the full scale heater. These tests were conducted at room temperature.

The second major test phase was concerned with evaluating all of the above mentioned material parameters concurrently in an operating pilot heater. A pilot heater was designed and fabricated with a matrix representing a section from the full scale heater. The pilot heater was designed to operate at temperatures and pressures duplicating those of the full scale heater and was also equipped with a reheat and blowdown system such that the reheat rates, cooling rates, temperature profiles and mass flows of the full scale heater could be simulated. The pilot heater proved to be a valuable tool for evaluating candidate ceramic material as well as the associated hardware (burner systems, blowdown systems, instrumentation, etc.). It also provided invaluable actual operating experience for the associated personnel. The design, operation and results of the pilot heater are discussed in Section 7.0.

6.1.1 Thermal Stress Resistance

The function of a storage heater matrix is to store thermal energy which is available for extraction at a relatively high rate. One of the first questions to be answered, therefore, is what is the maximum rate at which energy can be removed without fracturing the cored block.

Brittle ceramics, when exposed to thermal stress levels greater than their strength, may react in several ways. Cracks may be initiated but not propagated. Cracks may be initiated and propagate until fractures occur. Cracks may be initiated and propagate far enough to produce spalling. Thus, both crack initiation and crack propagation are important, and lead to two thermal stress resistance criteria.

The first criterion is the avoidance of crack initiation by limiting thermal stresses to values less than the strength of the material. This criterion has been applied to the bed design. The second criterion is to permit crack initiation but minimize damage. It applies especially in those cases where stresses greater than the strength cannot be avoided, and therefore applies to the insulation. Only the first of these criteria is amenable to analysis, but application of both relies heavily on test data.

6.1.1.1 Crack Initiation Criterion

The crack initiation criterion has been widely used in design applications and in determining the "thermal stress resistance" of various materials. The procedure is to calculate the stresses for the given geometry and heat transfer conditions. The criterion then requires that the maximum stresses do not exceed the material strength. Ceramics generally fail in tension, especially when cooled, which causes tensile stresses at the cooled surface. Heating may cause tensile or shear failures.

There exists a large body of literature, describing analytical and experimental applications, which demonstrate the validity of this approach. The primary conclusion is that the mechanical properties which characterize a material having high resistance to crack initiation are high strength, low thermal expansion coefficient, low Young's modulus, and low Poisson's ratio.

This criterion has been applied to the design of the matrix, and its influence is primarily to establish the web thicknesses between holes. As the bed is cooled during tunnel operation, tensile stresses develop at the surfaces of the holes in the cored block. The material around each hole can be treated as a tube. Elastic theory gives a particularly simple equation for the stress in this case.

$$S = \frac{\alpha \quad E}{1 - \nu} \quad (T_{average} - T_{surface}) \tag{1}$$

S is the maximum tensile stress, which occurs at the cooled surface, and $T_{average}$ is the average temperature in the cored block web. This equation also applies to other simple shapes having symmetrical temperature distributions. The average-to-surface temperature difference (ΔT) increases as the heat transfer rate increases. Thus the maximum allowable cooling rate is obtained by setting S equal to the tensile strength. In this way, $\Delta T = S(1-\nu)/\alpha E$ becomes a property value, one that is frequently used as a measure of thermal stress resistance. It is a function of temperature, inasmuch as the other properties are temperature dependent.

The temperature dependence of the modulus of rupture and Young's modulus is illustrated by the representative curves of Figure 5. These curves are based on the data of References 7 and 8, adjusted to a material porosity (void volume) of 10% using the following approximate relations (Reference 9).

$$S = S_o e^{-7p} \tag{2}$$

$$E = E_o e^{-4p} \tag{3}$$

Above 2000°F the strength and elasticity decrease rapidly. Calcia-zirconia appears to have a much higher modulus of elasticity than yttria-zirconia. However, the yttria-zirconia curve is the less reliable of the two. The data were

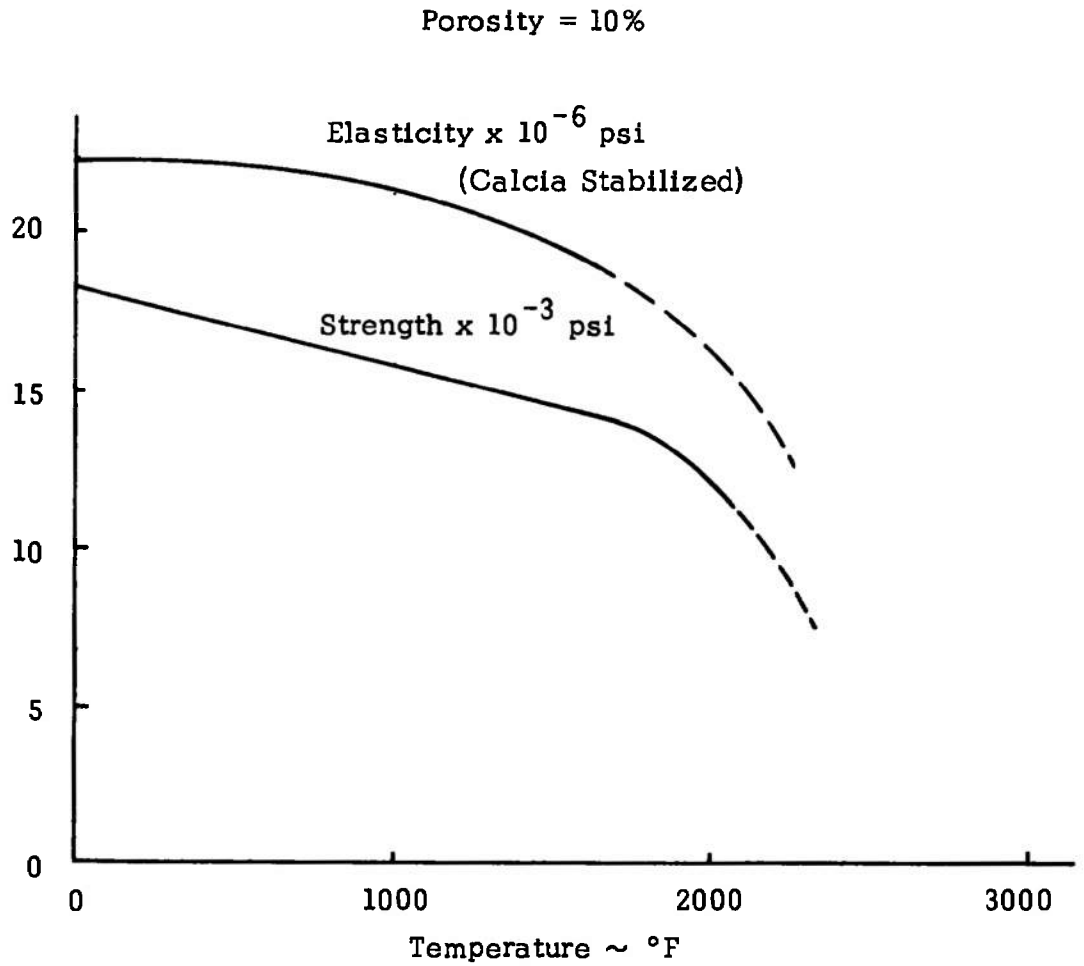

FIGURE 5. MECHANICAL PROPERTIES OF ZIRCONIA

taken with relatively porous specimens (20 to 30%) and consequently the extrapolation to 10% porosity may not be valid. For our purposes we have used the calcia-zirconia curve for all zirconia compositions, adjusting only for porosity level with Equation 3. More recent data shows that the modulus of 90% dense Y_2O_3-ZrO_2 specimens closely matches the CaO-ZrO_2 curve (personal communication, L. Fehrenbacher, ARL/WPAFB).

The crack initiation resistance, ΔT, is presented in Figure 6 for fully stabilized calcia-zirconia, using the curves in Figures 2 and 5, and with $\nu = 0.3$ assumed constant (Reference 7). As with Figure 5, these results are representative rather than definitive.

The effect of material porosity on crack initiation resistance is obtained by combining Equations 1, 2 and 3.

$$\Delta T = \Delta T_o e^{-3p} \tag{4}$$

Consequently, low porosity ceramics (i.e., a high percentage of theoretical density) have the greatest resistance to thermal stress crack initiation. This result has been demonstrated on a purely experimental basis (Reference 10).

Basing a design on the criterion of avoiding crack initiation does not mean that the structure will not tolerate some cracking. Allowance for a degree of cracking is particularly important with ceramic materials because of the variability in their strength. Thermal stress cracking, because of abnormally high local stresses or because of a localized weakness, will tend to relieve the condition. If the mechanical loads are not large and/or if there is a redundancy of support, structural failure will not occur.

Also important in determining the structural damage caused by cracking, is the nature of the crack propagation. This is the basis of the second thermal stress resistance criterion, namely the damage resistance criterion.

6.1.1.2 Damage Resistance Criterion

If thermal stresses exceed the material strength, cracks will develop, and the design approach is then to minimize the amount of damage. This is the situation for much of the heater insulation. Analytical methods of applying this criterion have not been developed. Hence, there is a complete reliance on performance tests. As an example, thermal stress damage of refractory blocks is frequently measured by the ASTM spalling test. In this test a panel of blocks is heated from one side in a kiln, removed and sprayed with an air-water mist. This is done for several cycles and the amount of weight loss is taken as the measure of damage. The test permits relative ranking of different blocks.

Thermal stress damage has been discussed on the basis of crack propagation by Hasselman (Reference 11). (Supporting data for this approach are given in References 12 and 13.) Cracks are propagated through the release of elastic energy stored at crack initiation. Continued propagation requires an energy release greater than the energy required to form new surfaces. Thus, once cracks have been initiated, they may propagate a certain distance and stop, or, they may continue until the piece is separated.

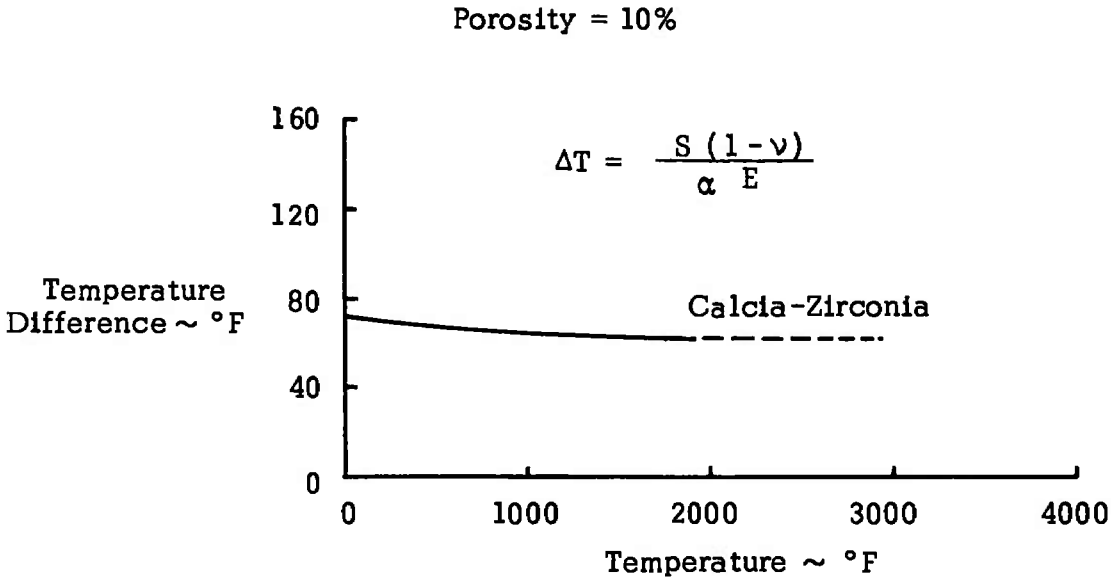

FIGURE 6. TEMPERATURE DIFFERENCE AT CRACK INITIATION

Greater thermal stress damage (e.g., spalling and loss of strength) will result from more extensive crack propagation. Crack propagation is increased by an increase in the elastic energy stored at the crack initiation. Mechanical property characteristics which decrease the stored elastic energy are: low strength, high Young's modulus, and high Poisson's ratio (Reference 11). These characteristics are the reverse of those desired for high resistance to crack initiation. The effect of porosity is also reversed. Porosity reduces the resistance to crack initiation but increased the resistance to thermal stress damage.

These results indicate trends only. There are other factors which influence crack propagation and the resulting damage. The most important of these may be the change in stress field (and stored elastic energy) after cracks have been initiated. These cracks tend to decrease stress levels, so that the influence of repeated temperature cycling is not additive.

The most important point of this discussion is that there are two separate kinds of thermal stress resistance. Furthermore, they have opposite dependencies on strength, elasticity and density.

In a cored block matrix thermal stresses are imposed on the individual elements due to rapid heating and cooling as well as from nonlinear axial and radial temperature gradients across the entire matrix. Associated with these temperature gradients are two types of stress fields which have been termed "web stresses" and "body stresses." The web stresses are generated during reheat and blowdown cycles in the web material separating the holes. Body stresses, conversely, exist across the entire block in both an axial and radial direction. During the first portion of this contract the body stresses existing across the individual blocks was thought to be small. As a result, the subscale thermal stress tests were concerned primarily with determining the maximum allowable web stresses and keeping the body stresses during these tests as low as possible.

6.1.2 Permanence of Stability

One of the characteristic properties, related only to zirconia among the candidate materials, is its tendency to change crystalline form during temperature cycling. As discussed in Section 4.2, zirconia material does undergo a reversible phase inversion below 2200°F. This phase inversion can be completely or partially suppressed by the incorporation of other specific oxide material into solid solution with the zirconia. During temperature cycling and during sustained periods at high temperature some of the stabilizing oxides have been observed to come out of solution with the zirconia. The decrease in stabilizer concentration is accompanied by an increase in monoclinic content. The appearance or increase in monoclinic content is commonly termed destabilization and appears to be the primary mode of failure for stabilized zirconia compositions.

It was necessary, therefore, to evaluate the candidate stabilized zirconia compositions under simulated heater conditions. Tests were designed to both expose the materials to repeated temperature cycling through their inversion zone and to maximum temperature conditions for several hundred hours.

6.1.3 Resistance to Rapid Changes in Pressure

The high flow rates permitted by a cored block matrix allow the heater to be pressurized in a very short period of time. In the case of the heater the time is less than one-half minute. Similarly, the heater can be depressurized rapidly should the need arise. One of the significant unknowns with respect to the design of the full scale heater was whether the refractory insulation materials possessed the ability to withstand such rapid pressurization and depressurization rates without structural failure or degradation. Performance of the material under these conditions was, therefore, one of the important parameters to be evaluated.

6.2 MATERIALS EVALUATED

As mentioned in Section 4.0, there were three basic materials selected for evaluation as possible candidate materials. These included zirconia and magnesia for the high temperature portion (i.e., above 3000°F) and alumina for the low temperature region (i.e., less than 3000°F). Within each of these basic material groups several different "alloys" or compositions were produced and evaluated.

6.2.1 Magnesia

Magnesia is commonly recognized as a material possessing the disadvantage of a high vapor pressure. However, in the literature, tests had not been conducted exposing magnesia to conditions similar to those experienced in a storage heater. Consequently, under the subject material's development program tests were conducted where the weight loss of various magnesia ceramics were measured under conditions simulating the reheat cycle in a stor - age heater. The specimens were held at constant temperature in a stream of flowing combustion products from a propane-oxygen burner. Tests were made at maximum temperatures of 3700°F. The weight loss rate at 3700°F was 4 mgm/cm^2-hr, corresponding to a surface recession rate of 1/2 mil per hour. This weight loss was considered too large for successful operation of a storage heater. A secondary disadvantage is that the vaporized magnesia condenses out as a solid in the lower temperature regions and attaches itself in a fine crystalline structure to the heat transfer surfaces. This magnesia condensate is very fragile and is easily expelled as dust during subsequent blowdown operations.

6.2.1.1 Test Equipment

A test facility was designed and fabricated, under the subject materials development contract, capable of simulating a full scale storage heater both in temperature and cycling operations (Figure 7, 8 and 9). The same facility was used for the subject magnesia weight loss tests. The test facility was designed for continuous 24 hour, high temperature operation. Magnesia tests typically consisted of a 26 hour heat up period, followed by steady state operating conditions held for 100 hours.

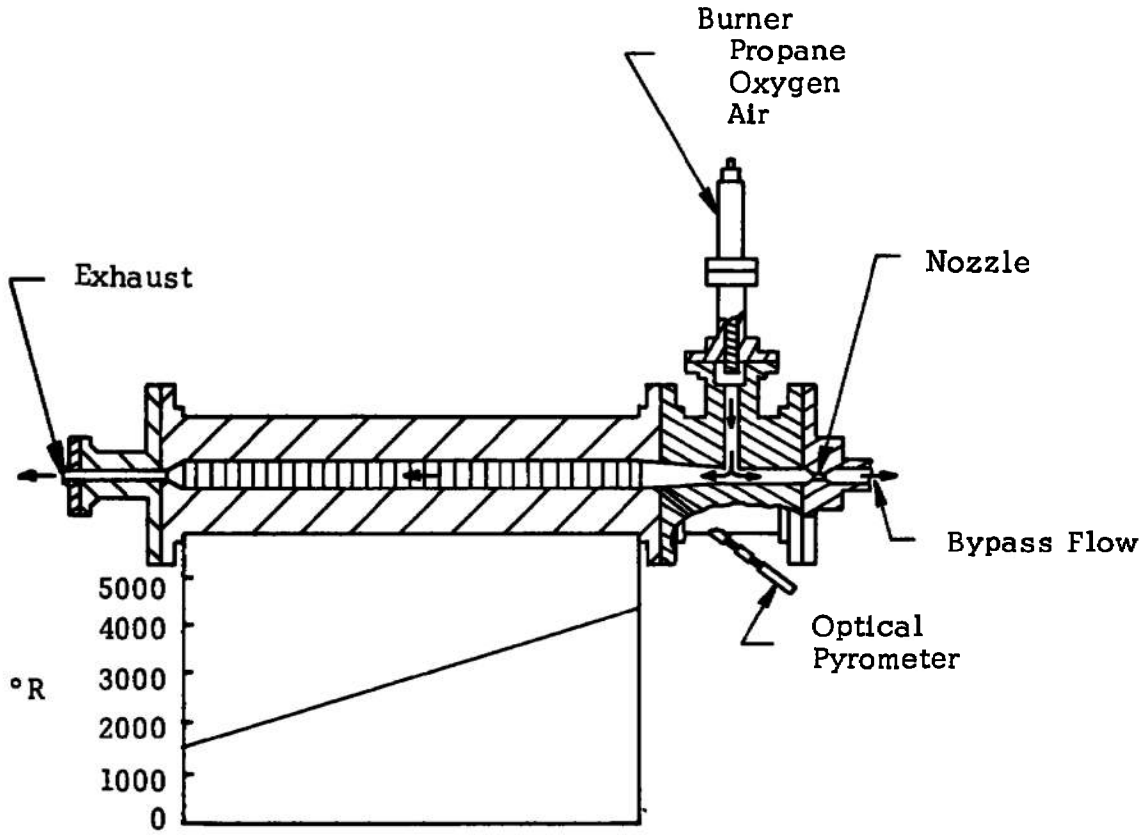

FIGURE 7. CERAMIC MATERIAL TEST SETUP

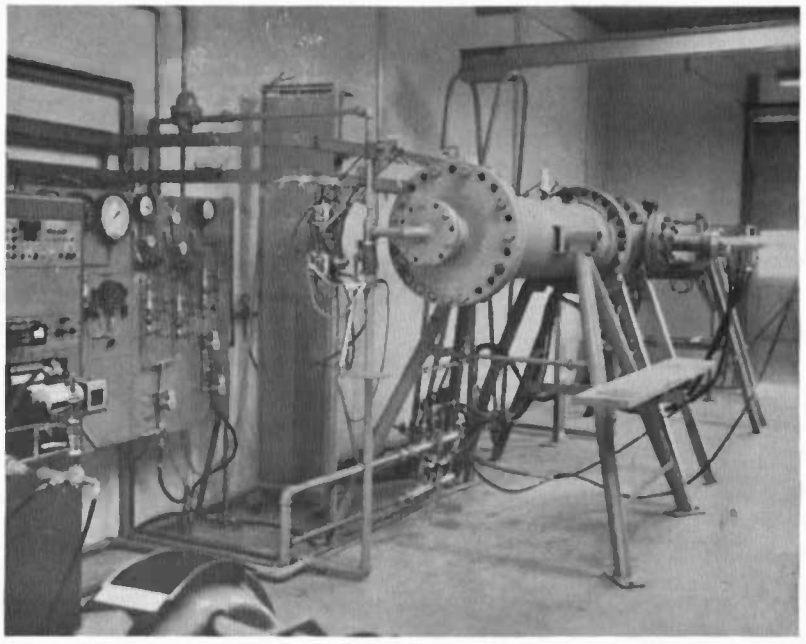

FIGURE 8. THERMAL CYCLING FACILITY VIEWING DOWNSTREAM

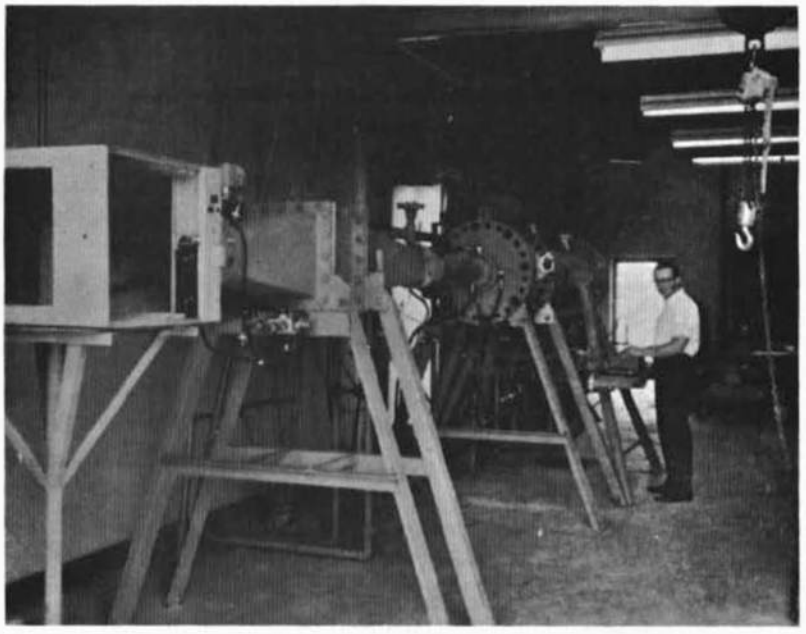

FIGURE 9. THERMAL CYCLING FACILITY VIEWING UPSTREAM

Temperatures below 3200°F were measured with thermocouples and above 3200°F with a Leeds and Northrup optical pyrometer and a Latronics single color automatic pyrometer.

Gas samples were taken periodically to check the atmospheres to which the test samples were being exposed. Samples were taken at the exit of the burner, the face of the test elements and at the exit of the test elements.

6.2.1.2 Design of Experiments

During the evaluation program several tests were performed on various magnesia materials. The first tests performed were conducted with a very high purity magnesia manufactured by Honeywell, Inc. These tests gave evidence that magnesia was susceptible to vaporization in a combustion gas atmosphere at high temperatures. The Honeywell tubes are shown before and after 100 hours at 3700°F in Figures 10 and 11, respectively. Suggestions were made by Honeywell that the vaporization may be partially due to carbonyl formation and reaction and/or reduction by carbon monoxide. It was hypothesized that metal ions may have lifted from the metal surfaces of the burner and been subsequently carried to the face of the matrix where they could act as a catalyst for some unexplained reaction. The second possibility was that magnesia is reduced directly by carbon monoxide, leaving magnesium which is extremely volatile at 3500°F.

$$MgO_{(s)} + CO_{(g)} \longrightarrow Mg_{(v)} + CO_{2\ (g)}$$

To eliminate the possibility of carbonyl formation, all exposed surfaces of the burner were plated with a two mil layer of gold. The CO problem could be reduced by operating with an increased level of excess oxygen.

Concurrently with this development effort NASA/Ames was interested in upgrading the performance of their storage heater facilities. One of the candidate materials in which they were interested was magnesia. After seeing the results of the magnesia tests under the subject Air Force contract, Ames was interested in pursuing the magnesia vaporization problem further to see if it could be reduced or eliminated within present technology. The following work on magnesia continued in Air Force test equipment with funding provided by NASA/Ames under Contract NAS2-2691.

One of the first items of concern was whether the large amount of weight loss experienced by the Honeywell material was characteristic of that material only or was representative of all magnesia compositions.

Samples of magnesia were procured from Coors Porcelain Company, National Beryllia Corporation, Honeywell, Inc. and a sample from the Ames pilot heater matrix. (Prior to these tests the Ames pilot heater had been operating with both a magnesia pebble matrix and a magnesia insulating hot liner.) The samples were mounted in a magnesia support structure (Harbison-Walker

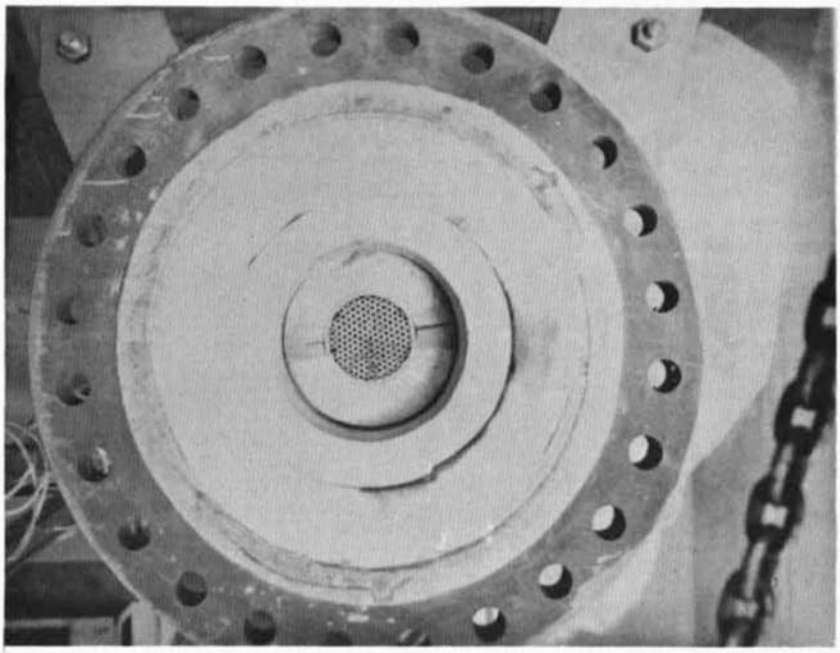

FIGURE 10. HONEYWELL HIGH PURITY MAGNESIA TUBES BEFORE FIRING

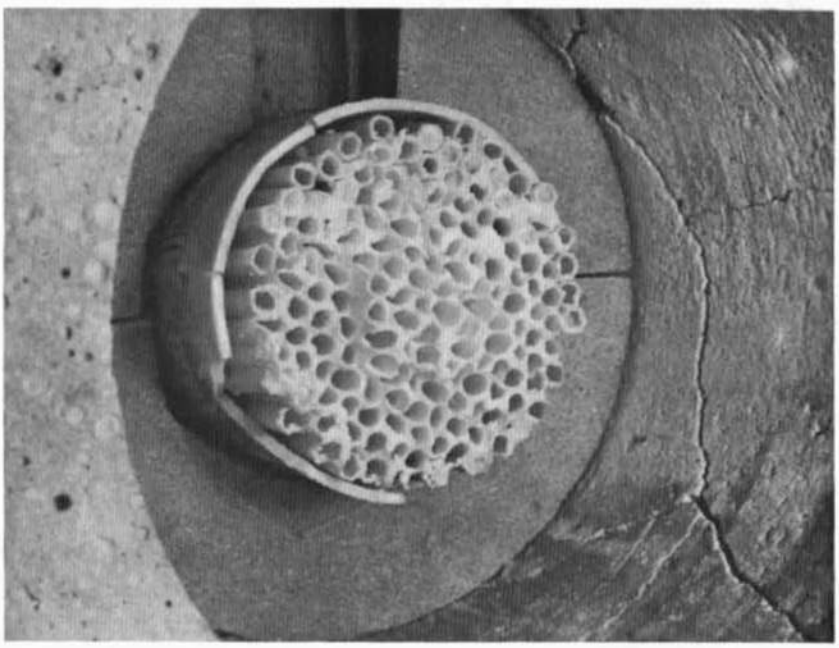

FIGURE 11. HONEYWELL HIGH PURITY MAGNESIA TUBES AFTER FIRING 100 HOURS AT 3700°F

97.5 % magnesia) as shown in Figure 12. The samples were exposed to flowing combustion products comprised of pure oxygen and propane. The upstream face of the samples was viewed with an optical pyrometer and maintained at a temperature of 4200°F.

The samples were held at 4200°F until excessive weight loss at the hot face and subsequent condensation in the cooler downstream region caused plugging of the flow passages. At this point, the test was terminated. Total run time was approximately 25 hours at 4200°F. Plugging of the downstream flow passages lead to nonuniform flow over the sample during the entire 25 hours of test. The nonuniformity made it impossible to compare the relative weight losses among the various samples. All of the magnesia samples did, however, suffer a very substantial loss of material as shown in Figure 13.

The next test series was designed with magnesia samples containing various additives in an attempt to reduce weight loss and/or control grain growth. The test setup was redesigned to minimize the possibility of plugging and assure uniform flow over all the test samples. The test configuration before test is shown in Figure 14. Two separate tests were planned because of the high weight loss found at 4200°F: the first at 3700°F, and the second at 4200°F using identical test sample configurations.

The 3700°F tests were terminated after 60 hours due to excessive weight loss and the necessity that enough sample material remain for analysis. The 4200°F tests were not conducted because of the high weight loss rate experienced at 3700°F.

Inspection revealed that the flow was fairly uniform over the samples during the test because of the uniform weight loss over all exposed surfaces of the support structure (Figure 15). Gas samples taken during operation indicated essentially no carbon monoxide present in the combustion gas atmosphere. Free oxygen made up about 25 to 30 percent of the atmosphere. According to gas equilibrium calculations for the test conditions there should be about 0.8% carbon monoxide present. This discrepancy may be due to a slower quenching rate than required to preserve the carbon monoxide.

6.2.1.3 Results and Discussion

The first test confirmed the fact that weight loss was not confined to any one particular manufactuer's magnesia. The second test investigated the possibility of reducing the material's weight loss rate by altering its structure through the use of various additives.

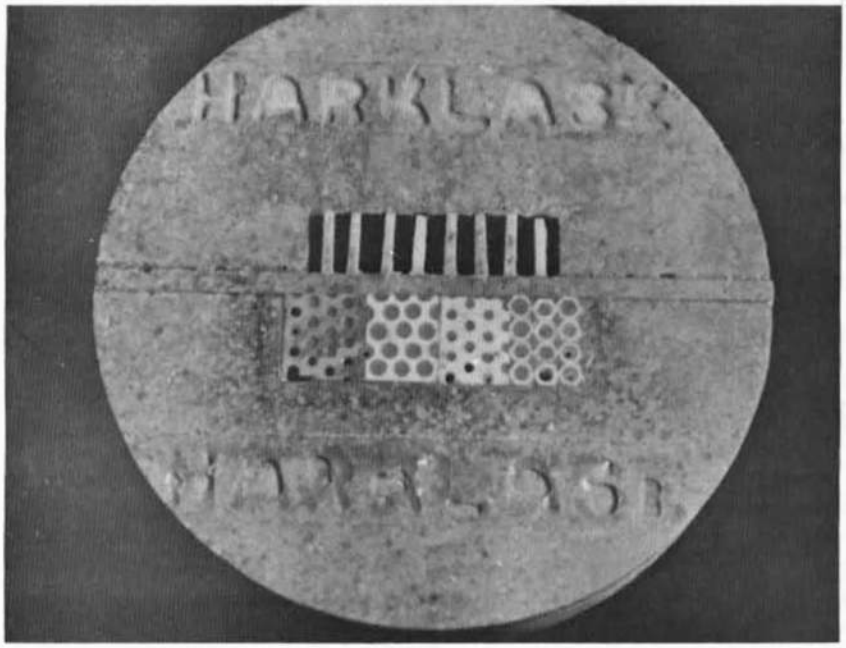

FIGURE 12. FIRST MAGNESIA WEIGHT LOSS TEST CONFIGURATION BEFORE FIRING

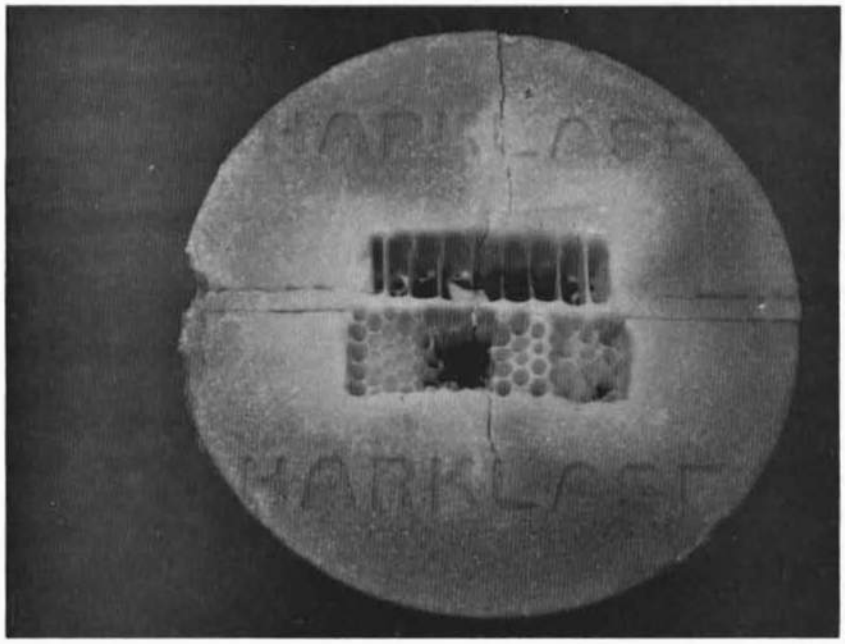

FIGURE 13. MAGNESIA TEST ELEMENTS AFTER 25 HOURS AT 4200°F

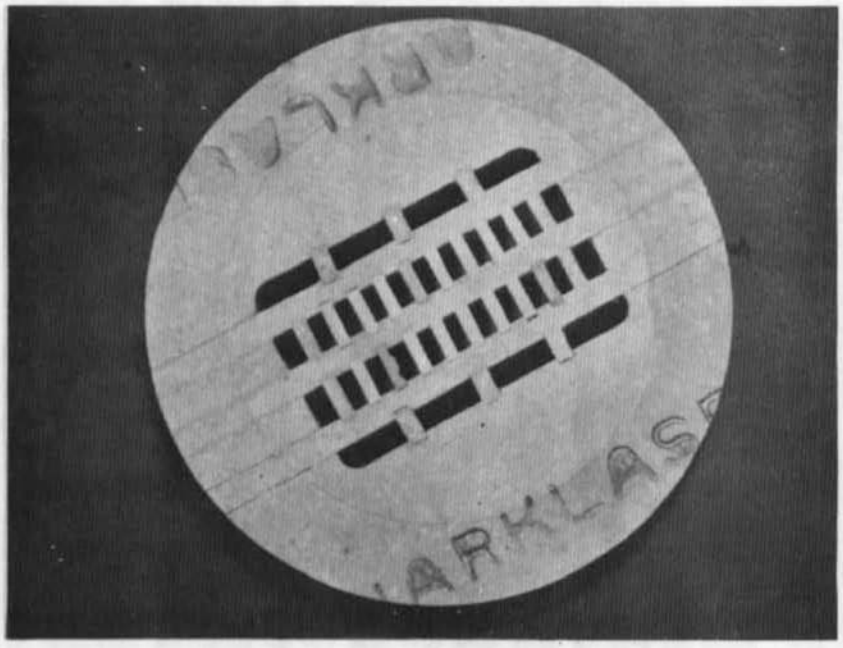

FIGURE 14. SECOND MAGNESIA WEIGHT LOSS TEST CONFIGURATION BEFORE FIRING

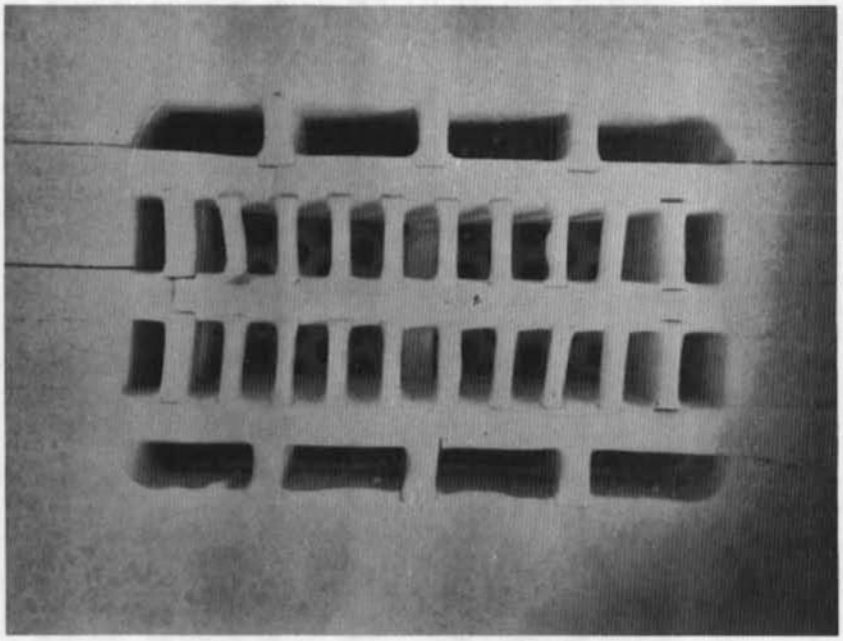

FIGURE 15. MAGNESIA TEST ELEMENTS AFTER 60 HOURS AT 3700°F

After 30 hours at 3700°F, the samples showed a weight loss rate of about 4 mgm/cm^2-hr. This is equivalent to a surface recession rate of 1/2 mil/hr. After 60 hours at 3700°F, the weight loss rate for each sample was about the same. The rates are based on the exposed area of the samples prior to firing.

These rates are more than can be tolerated in a full size heater. With a cored block hole diameter of 0.2-inch and a bed porosity of 0.4, a sustained weight loss rate of 4 mgm/cm^2-hr would "vaporize" the matrix in about seven days. Such massive losses would not occur because of saturation of the gas stream as it flows through the holes in the cored block. A lower limit to the weight loss would be a surface recession rate on the order of 1/2 mil per hour at the upper surface of the bed. Loss of material even at this lower rate would lead to a serious problem. That is, the contamination of the outlet air is a direct function of the weight loss rate because any material lost during reheat will condense in a colder region of the matrix and reappear as dustduring heater blowdown. Magnesia condensation was experienced in these tests and is shown in Figures 16 and 17. These are photos of cored block upon which magnesia has condensed. The condensed layer is a very open, weak structure, and therefore, easily removed.

The high weight loss rate experienced by the magnesia samples cannot be attributed to any one particular mechanism. Direct vaporization and chemical reaction with one or more components in the combustion gases may be responsible in varying degrees for the observed weight loss.

Reference 14 summarizes a Russian investigation of high temperature volatilization of various ceramic oxides. Two graphs are included in this article which gives vaporization of various oxides as a function of temperature for two different atmospheres: helium and a vacuum (Figures 18 and 19). The graphs give the material loss as a weight loss per unit area. However, in one section of the paper, various rates are listed in gm/cm^2-hr. which correspond to points on the graph; therefore, one can assume these graphs give vaporization rates versus temperature. As expected, the weight loss rates in a vacuum are greater by an order of magnitude as compared with the losses in helium. In both cases, the mechanism is vaporization since helium does not react with the ceramics.

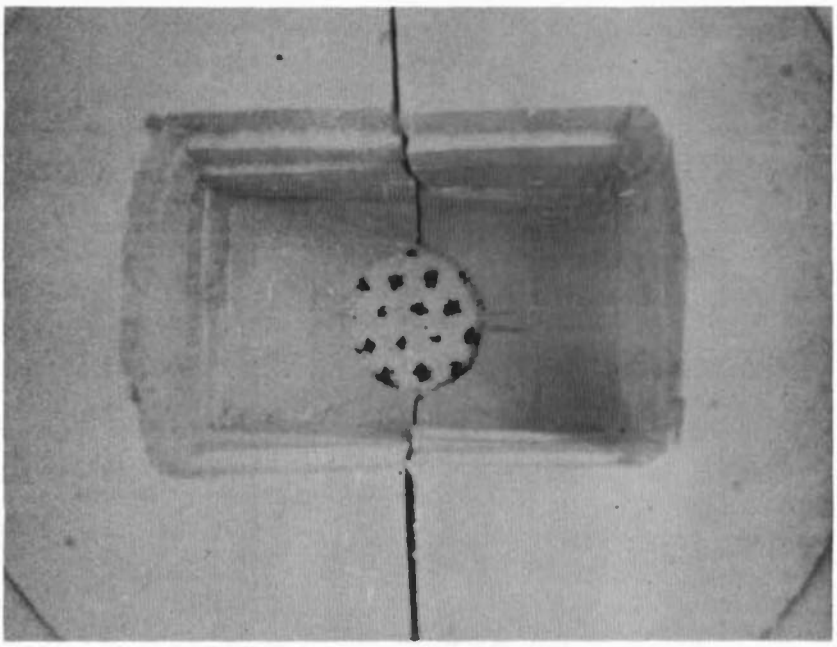

FIGURE 16. MAGNESIA CONDENSATION IN CORED BLOCK LOCATED DOWNSTREAM OF TEST CONFIGURATION

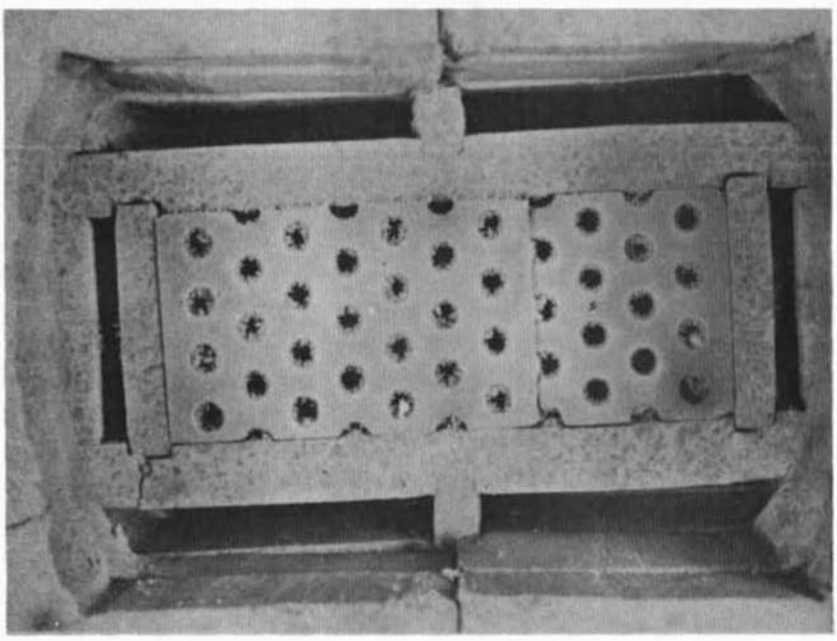

FIGURE 17. MAGNESIA CONDENSATION IN PRRESSURE DROP ELEMENT LOCATED BETWEEN TEST ELEMENTS AND CORED BLOCK SHOWN IN FIGURE 16

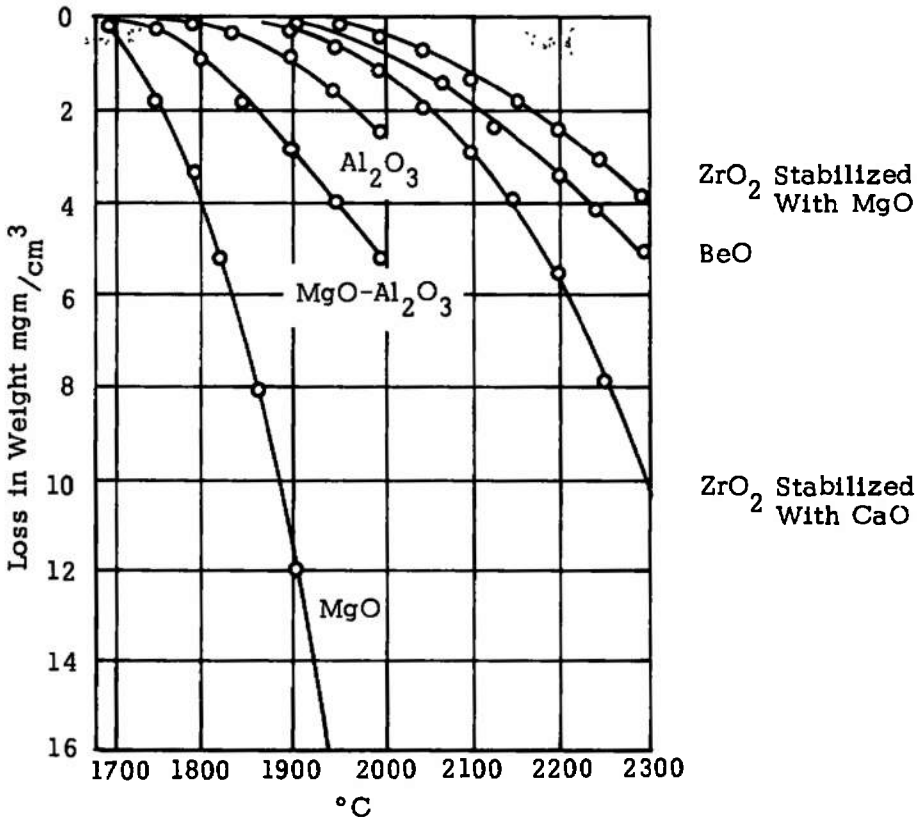

FIGURE 18. RELATIONSHIP BETWEEN VOLATILIZATION OF CERAMICS AND TEMPERATURE IN VACUUM OF 10^{-4} mm Hg

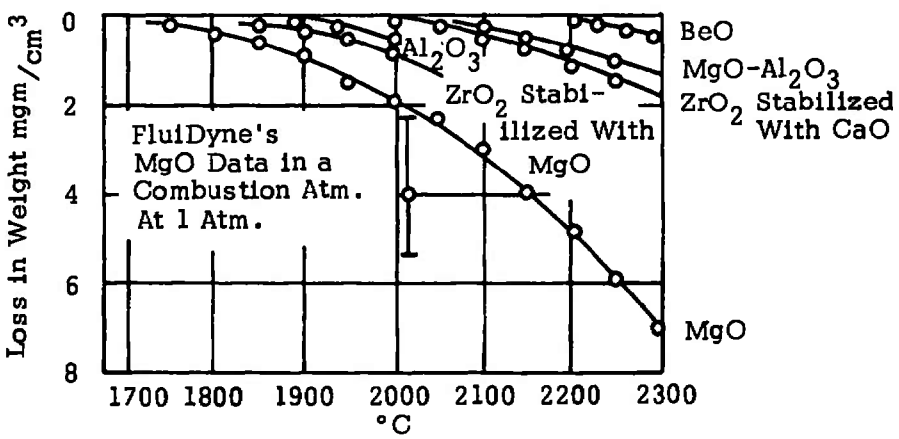

FIGURE 19. RELATIONSHIP BETWEEN VOLATILIZATION OF CERAMICS AND TEMPERATURE IN HELIUM AT 0.2 ATM

The data taken in helium (Figure 19) shows that magnesia experienced 2 mgm/cm^2-hr weight loss rate at 3700°F. The data from FluiDyne's test lies in the range from 2.3 - 5.0 mgm/cm^2-hr at 3700°F with an average weight loss rate of 4.0 mgm/cm^2-hr. This indicates that vaporization is playing a large role in the weight loss behavior. The increased loss in our test may be due to the removal of the vapors by the flowing stream and/or the influence of chemical reactions, such as the reduction by carbon monoxide mentioned earlier or reaction with water vapor to form the hydroxide. However, it is notable that the weight loss due to vaporization is large. This indicates that a change in the reheat gas, say, to air or nitrogen, would not reduce the weight loss of magnesia to acceptable values in this high temperature range.

As mentioned earlier, a weight loss rate of 4 mgm/cm^2-hr could not be tolerated in a wind tunnel heater. The loss rate from the top of the matrix would depend upon how rapidly the gas stream became saturated. However, it is certain that recondensation would create a serious dust problem. Establishment of a minimum acceptable weight loss rate would be difficult and arbitrary. However, it is obvious that it must be orders of magnitude less than the rates observed in our tests.

These results and the general problem of magnesia in this application have been discussed with ceramicists in industry, government, and university research organizations. The consensus of opinion is that magnesia is not applicable because of its high temperature weight loss characteristics. Furthermore, no hope is extended for reducing the weight loss to an acceptable level through a change in the reheat gases. These opinions are based on knowledge of the basic material from laboratory tests and operating experience with equipment such as furnaces and kilns.

6.2.2 Zirconia

Zirconia is a highly refractory material (melting temperature approximately 4700°F) that is chemically quite stable in the environments typically incurred in a storage heater. It becomes useful, however, only if its crystal structure is stabilized to avoid a monoclinic to tetragonal phase inversion that occurs within the material around 2000°F. The phase inversion is accompanied by a destructive 7-8% change in volume. Zirconia can be stabilized by

introducing a second oxide such as yttria, calcia or magnesia into the matrix engendering a solid solution and a stable cubic structure. Stabilizing oxides can be added in varying amounts such that the resulting zirconia structure is either all in the cubic form or the majority cubic and a small portion monoclinic. An all cubic zirconia body is commonly referred to as fully stabilized whereas a partially cubic body is partially stabilized. In some cases a partially stabilized body is preferred over a fully stabilized because of its slightly lower overall coefficient of expansion and the corresponding higher thermal shock resistance. The difference in thermal expansion is illustrated in Figure 2 where it is compared with a typical value for steel. One of the major disadvantages of zirconia, either partially or almost fully stabilized, has been its tendency to destabilize (i.e., increase in monoclinic) when exposed to typical storage heater operating conditions.

Storage heater operating experience confirmed two conditions which tend to promote zirconias tendency toward destabilization. These conditions are: (1) cycling the material through its temperature inversion zone and (2) exposing the material to high temperature for extended periods of time. Zirconia has proven itself a very useful but yet difficult and complicated material to understand. For example, during the course of this study it has been observed that some compositions of zirconia can tolerate very large amounts of monoclinic (~ 50%) and not suffer significant reductions in strength when temperature cycled through their inversion zone while other zirconia compositions have completely disintegrated when containing monoclinic contents as low as 5-15 %.

6.2.2.1 Test Objectives

Stabilized zirconia can be compared with the alloy steels in that slight changes in composition can make dramatic changes in the material properties. Consequently, the test objectives established for the subscale tests were to evaluate several zirconia compositions in terms of:

1. Permanence of stability at maximum heater temperature.
2. Permanence of stability when cycled through the material's temperature inversion zone.
3. Resistance to thermal stresses.
4. Maximum service temperatures.
5. Allowable interface temperatures.
6. Resistance to rapid changes in pressure.
7. Reheat shrinkage.

One of the most difficult problems with zirconia in the subscale tests was the identification of the type and amount of stabilizer which would provide adequate stabilization for the zirconia under storage heater operating conditions.

6.2.2.2 Types of Zirconia Materials Evaluated

Under a previous FluiDyne contract with the Air Force (AF40(600)-1039) a storage heater design study was conducted for a wind tunnel facility. This study concluded that a high density ceramic material would be necessary to satisfy the design requirements for the storage heater. At that time a letter was sent out to the various suppliers surveying their capabilities in manufacturing high density cored block. At the beginning of the subject contract small quantities (approximately 200 lbs.) of material were purchased from various suppliers in stabilized zirconia compositions. The material supplied was to represent production type materials and not isolated lot curiosities.

The initial design criteria established 3500°F as an outlet gas temperature for the full scale heater. It was estimated that to deliver 3500°F air, a temperature of 3700°F would be required in the upper portion of the bed. Initial subscale testing was conducted, therefore, at 3700°F. At a latter date the design requirements for the full scale heater were reviewed and the outlet air temperature requirement raised to 4000°F, thus raising the estimated maximum bed temperature to 4200°F.

The initial lots of zirconia materials procured for evaluation were stabilized with calcia. A few were special proprietary zirconia compositions with primary stabilizers of calcia and magnesia. During high temperature heat soak tests the problem of rapid destabilization associated with the vapor loss of both the calcia and magnesia stabilizer was identified. The result was an increase in monoclinic content plus a severe loss in strength upon subsequent cycling of the material through the inversion zone. The destabilization problem with calcia and magnesia stabilizers led to the consideration of yttria as an alternate.

From the subscale tests yttria, as a stabilizer, was found superior to both calcia and magnesia at temperatures above 3500°F. Because of the lower costs of calcia-zirconia and its adequate performance up to 3500°F, the use of calcia in the mid portion of the heater became attractive from an economic standpoint. The potential use of both calcia and yttria stabilized zirconias in the heater altered the test objectives of the subscale test program. With both materials as candidates it became necessary to determine the maximum service temperature for each material, their thermal stress resistance and the maximum interface temperatures which could be maintained between the adjacent compositions.

The cost of yttria in relation to calcia was quite high, as a result it was also necessary to determine the minimum amount of yttria required to stabilize the zirconia. Sample lots of zirconia material were procured for evaluation with both pure yttria (99%) and yttria plus rare earths (about 90% yttria) as the stabilizing agents.

6.2.2.3 Subscale Tests

Four test facilities were used in the evaluation of the zirconia materials. These included:

1. Thermal stress facility.

2. Thermal cycling/heat soak facility.

3. Cycling, 2000°F electric furnace.

4. Pressurization-depressurization facility.

The thermal stress facility was capable of holding a hex cored block sample about 2-inches across the flats and 3-6-inches in length. Samples installed in this facility were instrumented with thermocouples to determine directly the heating and cooling rates experienced by the test samples. The test facility was designed such that samples were heated from one end producing a ramp type temperature profile and cooled from the opposite end by an ambient temperature, low pressure air stream. The purpose of the test was to determine the maximum allowable cooling rate which the samples could withstand. The samples were heated by propane-oxygen-air combustion products directed axially through the holes of the cored block test samples. The test samples were protected from direct flame impingement and the associated thermal shock, by several buffer layers of the same material placed between the samples and the burner. A test program in this facility involved a series of slow heating and fast cooling cycles. A typical test program would begin with cooling rates of about one-fourth the maximum cooling rate predicted for failure of each particular sample. After five cycles the specimens were closely examined for cracks and fractures. If the specimens were in good condition the cooling rate was increased for the subsequent five cycles and so on until cracks and/or fractures appeared. These tests were carried out in the temperature range of 2000 to 2700°F.

To determine a zirconia material's permanence of stability at both high temperature and during exposure to temperature cycling in the temperature range anticipated in a storage heater, a second test facility was utilized. This facility was capable of holding a single column of cored blocks, six feet in length. The purpose of this test facility was twofold. First, it was capable of holding a number of zirconia samples in a combustion gas atmosphere at steady state temperatures as high as 4200°F for hundreds of hours to determine the materials' permanence of stability. Secondly, it could be used to simulate anticipated heating and cooling cycles automatically with maximum temperatures of 4200°F and pressures up to 300 psi. In this facility the column of samples were heated from one end and cooled from the other as would be experienced in a storage heater. The heating of the samples was accomplished with combustion products from a propane-oxygen-air, premix burner.

In addition to evaluating the permanence of stability of zirconia at high temperatures a test was also devised to expose the zirconia to repeated cycles through its inversion zone cycling at very low heating and cooling rates. The test equipment involved an electrically heated furnace capable of cycling samples through temperatures from ambient up to 2200°F in a static air environment. This test was intended to repeatedly cycle a number of zirconia samples through their inversion zone and determine their permanence of stability by measuring the monoclinic content of the samples both before and after a given test. The inner chamber of the furnace was lined with a high purity zirconia to minimize any impurity pick up by the test samples. Contact of each sample with the high purity liner was avoided by placing each of the test samples on a setter of the same material as the sample itself. A similar test was performed in a static combustion gas atmosphere (natural gas-air) at the NASA/Ames Research Center.

A fourth test facility was used during this program to evaluate the effect of high pressurization rates on the structural integrity of the samples. This facility was capable of accepting full size test specimens of both cored blocks and insulating material. Tests were performed with rapid pressurization and slow depressurization and with slow pressurization and rapid depressurization. The rapid pressurization and depressurization tests were conducted separately to allow for an inspection to determine during which period damage, if any, had occurred. Pressurization and depressurization rates as high as 1200 psi/sec were obtained at pressures up to 3500 psi.

6.2.2.3.1 Thermal Cycling and Heat Soak Tests With Calcia and Calcia/Magnesia-Zirconias

The permanence of stability and heat soak tests provided information on the effect of the heater environment on the microstructure and composition of candidate materials. The purpose of the thermal cycling tests was to determine the thermal stress resistance (resistance to crack initiation) of matrix materials. Furthermore, the method of simulating heater operation was chosen because it would yield data which could be applied to the design in the most direct fashion.

The maximum thermal stresses were thought to occur when the matrix was cooled during a run. These were tensile stresses which occurred at the surface of the holes in the cored blocks. Equating the increase in air enthalpy as it flows through the matrix to the decrease in energy stored in the matrix gives the following equations (Reference 15).

$$T_{average} - T_{surface} = \frac{R_3}{8} D^2 \frac{C_p}{k_s} \frac{\dot{m}}{A} \frac{dT}{dL} \qquad (5)$$

$$T_{average} - T_{surface} = \frac{R_1}{8} \frac{D^2}{a} \frac{dT}{d\theta} \qquad (6)$$

R_1 and R_3 are functions of the hole spacing-to-hole diameter ratio and T on the right hand side is the web temperature at any radial distance from the surface.

These equations are based solely on heat transfer and energy balance considerations. Note that the left hand side is proportional to the maximum tensile stress, according to Equation 1. Thus, the stress becomes proportional to the product of mass flux ($\dot{m}/A$) and temperature gradient (dT/dL) and also to the rate of cooling of the matrix ($dT/d\theta$). A measurement of the maximum allowable cooling rate of a given cored block material and hole pattern could then be used directly for heater design purposes. From the cooling rate, the quantity $(\dot{m}/A)(dT/dL)$ could be determined. This quantity was then used to determine the allowable mass flux and temperature ramp slope, both of which enter into the establishment of the required bed dimensions.

This procedure required knowledge of the thermal conductivity and specific heat of the ceramic, but not of the mechanical properties which entered into the thermal stress equations. Consequently, the need for measurements of mechanical properties at high temperatures was eliminated.

The test process involved two steps. Specimens were first evaluated in a small scale apparatus, having a test region 1-1/2 x 6-inches. The test pieces were first heated to about 2800°F, then cooled by flowing air. Temperatures were measured with thermocouples attached to the webs between holes. Runs were made in groups of five, each group at a successively greater cooling rate. The specimens were examined after each group of runs for cracks and for the general degree of crack propagation.

Thermocouples were cemented in shallow grooves sawed into the test pieces. It is noteworthy that these grooves have rarely been the origin of cracks.

The results of these tests were used to establish conditions for a larger scale test in the facility sketched in Figure 7. This apparatus provided space for a bed of 5-inch diameter by 6 feet long. It was operated as a small heater. The insulation was designed to provide a nearly linear temperature distribution, as shown in the figure. The test pieces were instrumented with thermocouples up to the 3000°F level. A time sequenced control system was provided, such that after an initial period of adjustment, the system cycles automatically through heating and blowdown periods. A complete cycle took about 30 minutes.

Calcia and magnesia-calcia stabilized zirconia cored blocks were evaluated in this way. In these tests it was found that at high temperatures (~ 3700°F) calcia and combinations of magnesia and calcia come out of solid solution with the zirconia thus leaving the zirconia high in monoclinic content. The thermal stress results from the tests were obscured by the destabilization suffered by the material. Additional tests were made during which the samples were not cycled but rather held at high temperature (3700°F) for long periods of time (in excess of 100 hours). During these tests the samples again experienced an increase in monoclinic content and a reduction in strength.

At this point in the test program, the design criteria for the wind tunnel facility was modified increasing the maximum temperature for the ceramics from 3700°F up to 4200°F.

The conclusion from this test series was that calcia would provide adequate stabilization for the zirconia material up to 3500°F. Above 3500°F and particularly above 3700°F calcia did not provide sufficient stabilization for periods over several hundred hours. From the results of this test it became necessary to consider other stabilizers, namely yttria.

6.2.2.3.2 Heat Soak Tests With Calcia, Calcia/Magnesia and Yttria Stabilized Zirconia Materials

The destabilization problems encountered with the calcia and calcia/magnesia-zirconia materials made it necessary to consider yttria as an alternate stabilizer. Yttria relative to calcia, however, is considerably more expensive. Therefore, it was necessary to determine the minimum amount of stabilizer required to adequately stabilize a zirconia body for use in a storage heater environment. A number of zirconia samples were procured with varying levels of yttria stabilizer. This provided samples of both partially and fully stabilized yttria-zirconia.

To evaluate and compare the performance of the yttria, calcia and calcia/magnesia-zirconia samples a special test setup was designed in which several samples could be evaluated simultaneously. The samples were machined and assembled in a compartmentalized array. The array was installed and tested in the thermal cycling facility at 4200°F for 240 hours. The samples after test are shown in Figure 20. This view looks at the upstream face upon which the hot combustion gases first impinged. The length of the array of test samples was 11-inches. Each sample was separated from the others by an array of shelves and spacers fabricated from 8 w/o high purity yttria-zirconia plates.

The test samples consisted of the following zirconia compositions:

1.	Magnesia/calcia:	2 compositions
2.	Calcia:	3.8 w/o 4.0 w/o 9.0 w/o 9.4 w/o
3.	Yttria plus 10% rare earths (10% principally dysprosia):	6.0 w/o 8.0 w/o
4.	Yttria:	6.0 w/o 8.0 w/o 10.0 w/o 12.0 w/o

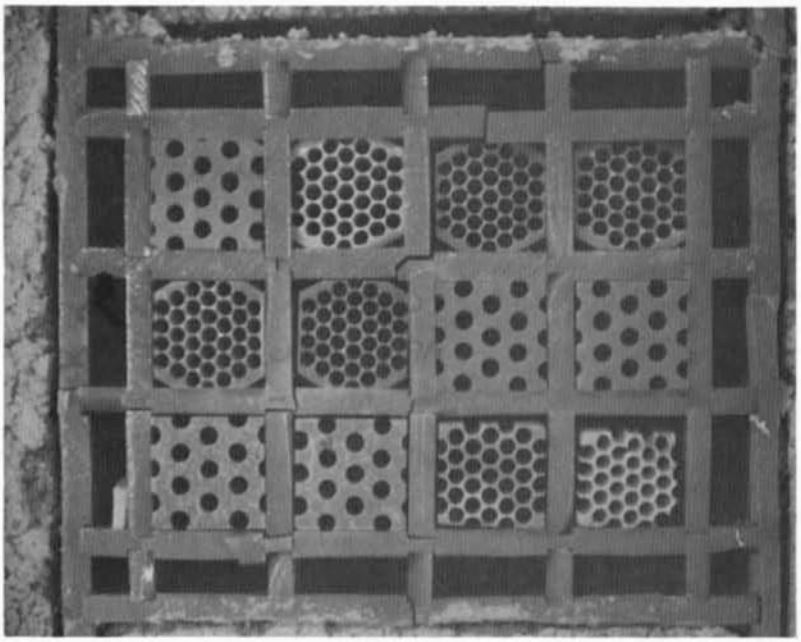

FIGURE 20. ZIRCONIA SPECIMENS AFTER 240 HOURS AT 4200°F

The upper two rows in Figure 20 contained the yttria-zirconia listed in Items 3 and 4 above. The two magnesia/calcia-zirconia samples (Item 1 above) are in the left hand spaces of the lower row. Two of the calcia samples (Item 2) are in the right hand side of the lower row. Visual examination of the samples after test showed a large difference between the yttria(with and without rare earths) stabilized materials and all others.

The magnesia/calcia-zirconia samples were completely fragmented. The calcia-zirconia samples all experienced severe reheat shrinkage with volume reductions ranging from 5 to 10%. In addition, two of the calcia-zirconia samples fractured into several pieces, one sample developed hairline cracks and one survived free of cracks.

Among the yttria-zirconia materials, tight hairline cracks were observed on the two yttria plus rare earth-zirconia samples (Item 3) and on the 6 w/o yttria-zirconia sample of Item 4. The remaining samples from Item 4 experienced no cracking during this test. All samples were checked for cracks using a dye penetrant inspection.

An extensive analysis of the before- and after- test specimens was made by the Air Force Materials Laboratory. The analyses included x-ray diffraction for phase determination and lattice parameter measurements, optical microscopy for microstructural comparison and grain size counts, and emission spectrographs for purity analysis. The following results were taken from this work.

1. An appreciable loss of Si, Mg, and Al occurred in all test samples. (These components are all impurities, except for Mg in the magnesia-calcia stabilized compositions.)

2. The chemical and structural stability of yttria and yttria-rare earth stabilized materials were found vastly superior to the calcia and magnesia stabilized zirconia specimens.

3. Destabilization of the calcia and magnesia stabilized materials occurred due to loss of the stabilizing agent.

4. Calcia readily diffuses at this temperature level. A fully stabilized (9.4% CaO) piece in contact with a partially stabilized (3.8% CaO) piece inhibited destabilization in the latter by diffusion of calcia.

5. The yttria and yttria-rare earth stabilized bodies exhibited uniformly sized, equiaxed grain structures with small spherical pores evenly distributed intragranularly. The calcia and magnesia-calcia stabilized bodies consisted of exaggerated "discontinuous" grains with large void areas distributed randomly.

The conclusion from this test series was that only the yttria and yttria-rare earth stabilized zirconias possess the long duration, high temperature stability required for the highest temperature portions of the heater.

6.2.2.3.3 Permanence of Stability Tests

Following the successful performance of the yttria-zirconia materials in the hightemperature heat soak tests, discussed above, it was next necessary to determine the performance of the material under low temperature cyclic conditions. The first cycling tests were performed in the range of 200 to 2200°F in both a static air and static combustion gas atmosphere. The static air atmosphere tests were conducted in an electrically heated furnace at the Flui-Dyne Engineering Corporation. The combustion atmosphere tests were performed in a natural gas-air fired furnace at the NASA/Ames Research Center. The number and types of samples used in both test set ups were identical. In both test set ups the samples were enclosed in a muffle fabricated from a high purity calcia-zirconia material to reduce the possibility for contamination of the samples from the furnace linings. Each sample was placed on a setter cut from the same material to prevent any interaction between the samples and the muffle. The samples were heated and cooled very slowly to both minimize the influence of thermal stress and to assure that adequate time was provided for any and all phase changes to occur. The electric furnace was cycled once every 12 hours and the combustion furnace once every 24 hours. The combustion products were at all times maintained oxygen rich to prevent reduction of the zirconia.

Specimens of each material were cut from a single block. The test specimens were compared visually with the "as received" material. Abrasion resistance was determined qualitatively by rubbing the corners of tested and untested specimens upon one another. The phase composition was measured by x-ray diffraction methods, with particular emphasis on the amount of monoclinic phase.

The results of these tests can be summarized as follows:

1. All specimens which were partially stabilized with calcia plus magnesia, experienced cubic phase destabilization (i.e., an increase in monoclinic content).

2. Fully stabilized calcia-zirconia experienced little or no destabilization (maximum monoclinic content less than 5%).

3. Specimens stabilized with yttria or with yttria plus rare earths showed little or no destabilization if the original monoclinic content was about 3% or less.

4. The monoclinic content of one yttria-zirconia specimen increased from 5% (as received) to about 15% with no apparent loss of abrasion resistance. Two other specimens, containing 20% monoclinic as received, disintegrated completely after less than 12 cycles.

5. The effect of destabilization on the structural integrity of the material was variable. In most cases it caused a loss of abrasion resistance (by the scratch test).

6. There were no significant differences detected between identical materials tested in air and in combustion products.

Additional information was obtained by examination of both insulation and cored block shapes in operating storage heaters (at the FluiDyne Engineering Corporation and at the Air Force Aerospace Research Laboratory, Dayton, Ohio). Information was also obtained by placing special test blocks in these heaters. The results with calcia-zirconia have confirmed the small scale test conclusions.

The full scale tests revealed a phenomenon that did not appear in the small scale tests. It was observed that lightweight (130-150 lb/ft^3) partially stabilized calcia-zirconia insulation developed a variation in monoclinic content across the width of the blocks. The hot face became fully cubic, but the center and back face contained monoclinic (up to 40%). These blocks had fractured and the failure was probably caused by the variation in thermal expansion coefficient created by the variation in crystalline composition. Dense blocks (260 lb/ft^3) in similar service conditions did not fracture.

The final conclusion from these investigations was that all of the zirconia used in the heater would be fully stabilized. Yttria-zirconia is used in the hottest regions, and with it there is no choice. The small scale tests demonstrated that only the fully stabilized version is useful. Calcia-zirconia in the fully stabilized form will have a longer life, without the hazard of severe deterioration from destabilization. Its greater thermal expansion, as compared with partially stabilized, requires some additional care in the design of the insulation.

6.2.2.3.4 Pressurization-Depressurization Tests

One of the significant unknowns with respect to the design of the full scale heater was the ability of the refractory insulation materials to withstand rapid pressurization and depressurization without structural failure or degradation. A preliminary design of the heater included a tunnel starting process in which the heater is pressurized in time periods on the order of 10 - 15 seconds. The depressurization rates anticipated were at a somewhat slower rate. Both the pressurization and depressurization rates, however, were at rates greater than those for which operating experience or experimental data existed. Consequently, a subscale test was necessary to determine if the candidate materials for use in the pilot heater would be capable of surviving the transient pressure environment.

The test hardware devised exposed samples to pressurization and depressurization rates of 1000 psi/sec and 1200 psi/sec and maximum pressures of 2000 and 3500 psi, respectively. The test facility was capable of operating at room temperature only.

Samples of all the refractory material, matrix as well as insulation, to be used in the pilot heater were subjected to the pressurization-depressurization tests. The results of these tests indicated that the samples were

unaffected by the high pressurization and depressurization rates. In all cases there were no indications of spalling or cracking evident to the naked eye. Abrasion resistance of the material was unaffected.

6.2.3 Alumina

Alumina is one of the most plentiful and one of the most widely used of the available oxide ceramics. As a result a large amount of data and fabrication experience exists for alumina material. Of the various suppliers contacted, however, the Coors Porcelain Company was the only supplier successful in fabricating high density, high purity cored blocks. Alumina compositions of both 94 and 99% purity were tested with densities of about 94 to 98% of theoretical, respectively (theoretical density is 4.0 gms/cc).

The alumina material was tested concurrently with the various zirconia compositions. The alumina cored blocks were installed in the downstream half of the thermal cycling test facility. This arrangement subjected the alumina material to reheat and blowdown conditions similar to those which were anticipated for the full scale heater. Temperatures of the alumina during test ranged from 1000°F at the grate region to 2600°F to 2800°F at the alumina-zirconia interface. Both the 94 and 99% purity alumina materials exhibited excellent performance during the thermal cycling tests.

Because of the phase stability of the alumina material in a storage heater environment it was not affected by the thermal cycling tests nor was it necessary to subject it to permanence of stability tests.

The alumina material possessed a high mechanical strength and a very low porosity and consequently was unaffected by the changing pressure environment of the pressurization-depressurization tests.

The lower density alumina insulation material fabricated by Norton and Harbison Walker and used extensively in existing operating heaters has shown excellent performance and therefore was not a subject of investigation during this test series.

6.3 MATERIAL SELECTION FOR THE PILOT HEATER

From the subscale tests, calcia was found to be a useful stabilizing agent for zirconia at temperatures up to 3500°F. Yttria was demonstrated to be useful as a stabilizer at temperatures as high as 4200°F. The performance of combined stabilizers consisting of calcia and magnesia did not exceed that of straight calcia.

Based on the subscale tests the pilot heater was designed with a graded matrix comprised of yttria-zirconia, calcia-zirconia and alumina cored blocks. Yttria-zirconia, being the most expensive material, was specified for the upper region (3500-4200°F) only; calcia-zirconia for the midregion (2600-3500°F) and alumina for the cooler region (1000-2600°F) of the heater. The same design philosophy was used for the sidewall insulation.

The pilot heater program was established to both evaluate candidate materials in prototype shapes and under prototype conditions as well as to develop multiple ceramic material suppliers for future prototype heaters. To evaluate several different materials a number of compositions were specified for both the calcia-zirconia and yttria-zirconia regions of the heater. The material specifications written and used for the pilot heater procurement included the following:

NUMBER	DESCRIPTION
7000-100	Yttria-rare earth oxide mixture
7000-101	6 w/o yttria-zirconia plus secondary stabilizer (matrix)
7000-102	8 w/o yttria-zirconia plus secondary stabilizers (matrix)
7000-104	8.2 w/o yttria-zirconia (matrix)
7000-105	9 w/o yttria-zirconia (matrix)
7000-106	8 w/o yttria-zirconia plus secondary stabilizers (light weight insulation)
7000-107	8 w/o yttria-zirconia plus secondary stabilizers (insulation)
7000-108	9 w/o yttria-zirconia plus secondary stabilizers (insulation)
7000-109	9 w/o yttria-zirconia (matrix)

The suppliers had considerable difficulty in producing both the yttria and calcia-zirconia cored blocks. Consequently, the actual materials which were installed in the heater are quite different from the variety originally specified. The procurement was handled by FluiDyne under a separate Air Force contract. The procurement is described in detail in Reference 16 and in part in Sections 7.1.3.1.8 and 7.1.3.2 of this report.

7.0 MATERIAL EVALUATION - PILOT HEATER

The purpose of the subscale tests, discussed in Section 6.0 was to evaluate small samples of material under simulated test conditions. The subscale tests consisted of several different set ups, each representing a different phase of the storage heater environment. In these tests a number of materials could be inexpensively evaluated. Before the materials could be used in the design of a prototype heater with any assurance it was necessary that they be evaluated in a pilot heater where the majority of the conditions of the prototype heater could be simulated simultaneously. A pilot heater was designed and fabricated by FluiDyne Engineering Corporation and installed at AEDC, Tullahoma, Tennessee.

The pilot heater was designed large enough to accommodate and test a typical vertical section of bed of the full scale heater. The reheat and blowdown systems for the pilot heater were designed such that the temperature gradients, thermal stress and mechanical loads anticipated in the full scale heater could be duplicated in the pilot heater. The pilot heater "as built" is shown in Figure 21. The heater vessel was designed for 2000 psi and was fitted with a 14-inch diameter matrix, 15.5 feet in length. The lower half (7.5 feet) of the matrix contained alumina and the upper portion (8 feet) contained yttria stabilized zirconia.

The pilot heater was completely instrumented both through the matrix and insulation such that the temperatures at various locations and times could be determined. Thermocouples were used in regions operating below 3000°F, and radiation pyrometry equipment in regions above 3000°F. In the upper portion of the matrix a pyrometer and special viewport slots were provided which allowed temperature measurements to be made, at the center of the matrix, at temperatures up to the maximum heater conditions of 4200°F. The pilot heater was one of the first storage heaters in which temperature measurements could be made within the matrix above 3000°F.

In addition to being an essential part of the materials evaluation program, the pilot heater has proven to be a valuable tool for providing basic storage heater operating experience for the operations personnel involved at ARO/AEDC.

7.1 PILOT HEATER DESIGN

The design of the pilot heater and support hardware was carried out by FluiDyne Engineering Corporation. The elements designed included the vessel, internal grate support structure, burner, burner control system, refractory insulation, cored block matrix and instrumentation systems.

7.1.1 Pressure Vessel

The pilot heater vessel was designed to accommodate an 18-inch diameter matrix, 16 feet long. The first ceramic internals, procured under Air Force Contract F40600-67-C-0004, were designed to provide a 14-inch diameter matrix, 16 feet long.

7.1.1.1 Vessel Design

The heater vessel internal dimensions are 3 feet inside diameter by 21-1/2 feet long with outlets located at the top, side and bottom. The top outlet was designed large enough to provide access to the vessel during refurbishment as well as an opening through which the burner can be inserted prior to operation. There are six side outlets; five of these are small outlets used as viewports in conjunction with the temperature measuring radiation pyrometry equipment. The sixth forms the outlet for the hot air during a blowdown cycle. There are two outlets located at the base of the vessel. The one centered in the base serves as an outlet for the exhaust gases during a reheat cycle and as an inlet for the high pressure air during a blowdown cycle. The outlet located to one side of the centerline would be used for annular reheat. This outlet remained blocked during the first pilot heater test program.

The heater vessel was designed by FluiDyne and fabricated by Northern Ordnance, Minneapolis, Minnesota. It was designed per Section VIII, ASME Boiler and Pressure Vessel Code to a working pressure of 2000 psi. It has been hydrotested to 3000 psi. The vessel is described in Figure 22. The vessel support structure was designed by ARO and is described on their drawings.

7.1.1.2 Vessel Cooling

Two cooling systems were designed for the vessel shell. One provided cooling air for the individual viewport glasses and the second provided a controlled air flow over the vessel's outer surface.

The heater vessel has five penetrations through the sidewalls that allow viewing of the ceramics as they are brought up to temperature during a reheat cycle. These viewports are all fitted with fused silica (quartz) windows which remain in place during both the reheat and blowdown cycles. During the reheat cycle, a slight trickle of cool air is passed over the inside of the glass to prevent condensation. The cooling air, after passing over the glass, exits into the heater matrix. Therefore, the amount of cooling flow is kept to a minimum to avoid introducing excessive stresses in the cored blocks adjacent to the viewport. During the blowdown cycle, low temperature, high pressure air is introduced into the viewport to purge the viewport passage and prevent the high temperature, high pressure air in the matrix from reaching the viewport glass and cooling system. This purge air is bled from the high pressure blowdown air line at the base of the heater, is metered by a small orifice inserted in the air line and has a driving potential equal to the pressure drop across the adjacent matrix.

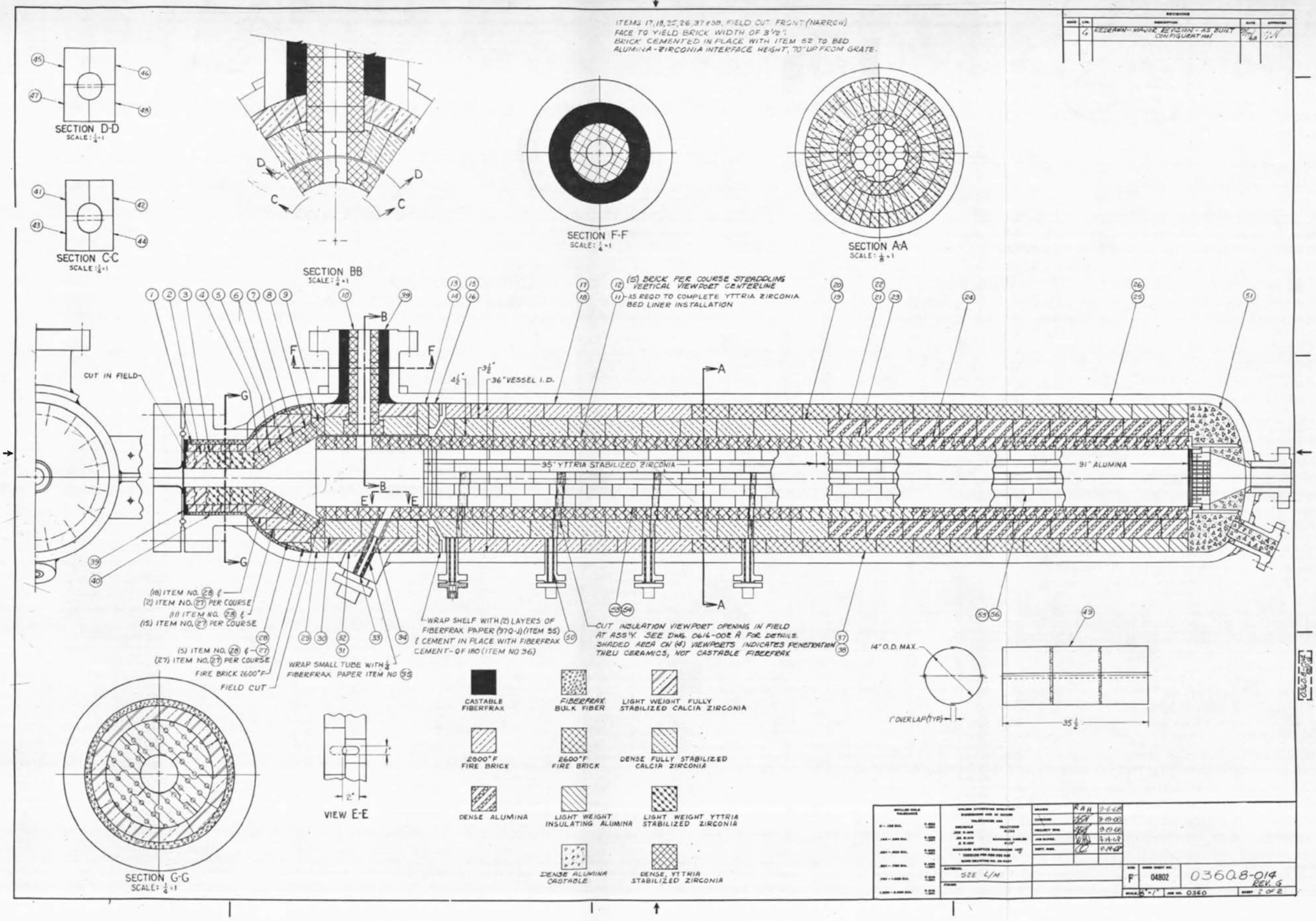

FIGURE 21. REFRACTORY ASSEMBLY - PILOT HEATER

ITEM NO.	QTY REQD	COURSES	NO IN COURSE	PART NUMBER	DESCRIPTION	DENSITY PCF	MATERIAL	STABILIZER	FLUIDYNE SPEC	MANUFACTURER AND DESCRIPTION
56	146 lbs/ft			7003 - 008B	CORED BRICK	3.8 g/cc	ALUMINA	NONE	AD99 OR EQUAL	COORS XAD99
55	97 lbs/ft			7003 - 604A	CORED BRICK SEGMENT	3.8 g/cc	ALUMINA	NONE	AD99 OR EQUAL	COORS XAD99
54	151 lbs/ft			7003 - 008C	CORED BRICK	5.8 g/cc	F.S. ZIRCONIA	YTTRIA	7000-105	COORS
53	98 lbs/ft			7003 - 604A	CORED BRICK SEGMENT	5.8 g/cc	F.S. ZIRCONIA	YTTRIA	7000-105	COORS
52	200 lbs			-	CERAMIC SET CEMENT	-	-	-	-	KAISER HILO SET
51	900 lbs			-	ALUMINA CASTABLE	-	ALUMINA	-	-	NORTON 33 HD
50	8			TUBE	7/8 I.D. x 1 3/8 O.D x 6 LG	250-280	P.S. ZIRCONIA	CALCIA	-	ZIRCOA - 1651
49	12	4	4	-	12" SQ. x .037 THK ROLLED TO 7" RAD.	-	INCONEL	-	-	-
48	1			7001 - 604	BACKUP OUTLET RIGHT BOTTOM	250-280	F.S. ZIRCONIA	YTTRIA	7000-107	ZIRCOA
47	1			7001 - 603	BACKUP OUTLET LEFT BOTTOM	250-280	F.S. ZIRCONIA	YTTRIA	7000-107	ZIRCOA
46	1			7001 - 605	BACKUP OUTLET RIGHT TOP	250-280	F.S. ZIRCONIA	YTTRIA	7000-107	ZIRCOA
45	1			7001 - 606	BACKUP OUTLET LEFT TOP	250-280	F.S. ZIRCONIA	YTTRIA	7000-107	ZIRCOA
44	1			7001 - 610	INNER OUTLET RIGHT BOTTOM	250-280	F.S. ZIRCONIA	YTTRIA	7000-107	ZIRCOA
43	1			7001 - 609	INNER OUTLET LEFT BOTTOM	250-280	F.S. ZIRCONIA	YTTRIA	7000-107	ZIRCOA
42	1			7001 - 608	INNER OUTLET RIGHT TOP	250-280	F.S. ZIRCONIA	YTTRIA	7000-107	ZIRCOA
41	1			7001 - 607	INNER OUTLET LEFT TOP	250-280	F.S. ZIRCONIA	YTTRIA	7000-107	ZIRCOA
40	30 lbs			-	FIBERFRAX BULK FIBER	-	-	-	-	CARBORUNDUM
39	10 GAL			-	CASTABLE FIBERFRAX FC-25	-	-	-	-	CARBORUNDUM
38	176	11	16	7002 - 625	#1 ARCH STD 9" SERIES	-	2600° FIRE BRICK	-	-	HARBISON WALKER
37	330	11	30	7002 - 627	#2 ARCH STD 9" SERIES	-	2600° FIRE BRICK	-	-	HARBISON WALKER
36	1 QT			-	FIBERFRAX CEMENT QF 180					CARBORUNDUM
35	25 lbs			-	FIBERFRAX PAPER, 970-J	-	-	-	-	CARBORUNDUM
34	1			TUBE	2" I.D. x 3" O.D. x 10" LG	250-280	P.S. ZIRCONIA	CALCIA	-	ZIRCOA 8D CASTABLE
33	1			TUBE	1" ID x 2" O.D. x 12" LG	250-280	P.S. ZIRCONIA	CALCIA	-	ZIRCOA 8D CASTABLE
32	78			7002 - 627	#2 ARCH STD 9" SERIES	150-180	F.S. ZIRCONIA	CALCIA	0360.8-014D	ZIRCOA
31	43			7002 - 625	#1 ARCH STD 9" SERIES	150-180	F.S. ZIRCONIA	CALCIA	0360.8-014D	ZIRCOA
30	95			7002 - 627	#2 ARCH STD 9" SERIES	250-280	F.S. ZIRCONIA	CALCIA	-	NORTON TZ5608
29	24	1	24	7001 - 635	DOME SUPPORT	250-280	F.S. ZIRCONIA	CALCIA	-	NORTON TZ5608
28	45			7002 - 633	DOME INSULATION	150-180	F.S. ZIRCONIA	CALCIA	0360.8-014D	ZIRCOA
27	55			7002 - 632	DOME INSULATION	150-180	F.S. ZIRCONIA	CALCIA	0360.8-014D	ZIRCOA
26	48	3	16	7002 - 625	#1 ARCH STD 9" SERIES	70-90	ALUMINA	NONE	-	NORTON RA 4058
25	90	3	30	7002 - 627	#2 ARCH STD 9" SERIES	70-90	ALUMINA	NONE	-	NORTON RA 4058
24	420	28	15	7001 - 626	24° BED LINER	185-200	ALUMINA	NONE	-	NORTON RA5190
23	150	10	15	7001 - 626	24° BED LINER	250-280	F.S. ZIRCONIA	CALCIA	0360.8-014D	ZIRCOA
22	20	10	2	7002 - 630	#3 ARCH STD 9" SERIES	185-200	ALUMINA	NONE	-	HARBISON WALKER KRUNDEL KD
21	350	10	35	7002 - 627	#2 ARCH STD 9" SERIES	185-200	ALUMINA	NONE	-	HARBISON WALKER KRUNDEL KD
20	22	11	2	7002 - 630	#3 ARCH STD 9" SERIES	250-280	F.S. ZIRCONIA	CALCIA	-	NORTON TZ5608
19	385	11	35	7002 - 627	#2 ARCH STD 9" SERIES	250-280	F.S. ZIRCONIA	CALCIA	-	NORTON TZ5608
18	112	7	16	7002 - 625	#1 ARCH STD 9" SERIES	-	2800° FIRE BRICK	NONE	-	HARBISON WALKER
17	210	7	30	7002 - 627	#2 ARCH STD 9" SERIES	-	2800° FIRE BRICK	NONE	-	HARBISON WALKER
16	13	1	13	7002 - 619	SHELF KEY BRICK	250-280	F.S. ZIRCONIA	CALCIA	-	NORTON TZ5608
15	17	1	17	7002 - 618	SHELF BRICK	250-280	F.S. ZIRCONIA	CALCIA	-	NORTON TZ5608
14	8	1	8	7002 - 617	UPPER SHELF KEY BRICK	250-280	F.S. ZIRCONIA	CALCIA	-	NORTON TZ5608
13	20	1	20	7002 - 616	UPPER SHELF BRICK	250-280	F.S. ZIRCONIA	CALCIA	-	NORTON TZ5608
12	240	16	15	7001 - 626	24° BED LINER	250-280	F.S. ZIRCONIA	YTTRIA	7000-108	ZIRCOA
11	435	29	15	7001 - 626	24° BED LINER	250-280	F.S. ZIRCONIA	YTTRIA	7000-107	ZIRCOA
10	8	8	1	7001 - 615	OUTLET RING	250-280	F.S. ZIRCONIA	YTTRIA	7000-107	ZIRCOA
9	24	1	24	7001 614	DOME SKEW	250-280	F.S. ZIRCONIA	YTTRIA	7000-107	ZIRCOA
8	18	1	18	7001 - 003	DOME BRICK #1	250-280	F.S. ZIRCONIA	YTTRIA	7000-107	ZIRCOA
7	16	1	16	7001 - 002	DOME BRICK #2	250-280	F.S. ZIRCONIA	YTTRIA	7000-107	ZIRCOA
6	12	1	12	7001 - 004	DOME BRICK #3	250-280	F.S. ZIRCONIA	YTTRIA	7000-107	ZIRCOA
5	12	1	12	7001 - 005	DOME BRICK #4	250-280	F.S. ZIRCONIA	YTTRIA	7000-107	ZIRCOA
4	10	1	10	7001 - 613	COMBUSTION CHAMBER EXIT	250-280	F.S. ZIRCONIA	YTTRIA	7000-107	ZIRCOA
3	32	4	8	7001 - 612	COMBUSTION CHAMBER	150-180	F.S. ZIRCONIA	YTTRIA	7000-106	ZIRCOA
2	16	2	8	7001 - 612	COMBUSTION CHAMBER	150-180	F.S. ZIRCONIA	CALCIA	0360.8-014D	ZIRCOA
1	84	7	12	7002 - 629	COMBUSTION CHAMBER INSULATION	150-180	F.S. ZIRCONIA	CALCIA	-	NORTON TZ5609

LIST OF MATERIALS

0360.8-014

DRILLED HOLE TOLERANCE

UNLESS OTHERWISE SPECIFIED: DIMENSIONS ARE IN INCHES. TOLERANCES ARE: DECIMALS .XX ±.010, .XXX ±.005; FRACTIONS ±1/32; MACHINED ANGLES ±1/2°. MACHINED SURFACE ROUGHNESS 125/. THREADS PER MIL-STD-8B. MARK DRAWING NO. ON PART.

DRAWN	OHH	9-6-68
CHECKED	[illegible]	9-18-68
PROJECT ENG.	[illegible]	9-19-68
JOB SUPER.	[illegible]	9-19-68
DEPT. MGR.	[illegible]	9-19-68

MATERIAL

FINISH

FIGURE 21. REFRACTORY ASSEMBLY - PILOT HEATER

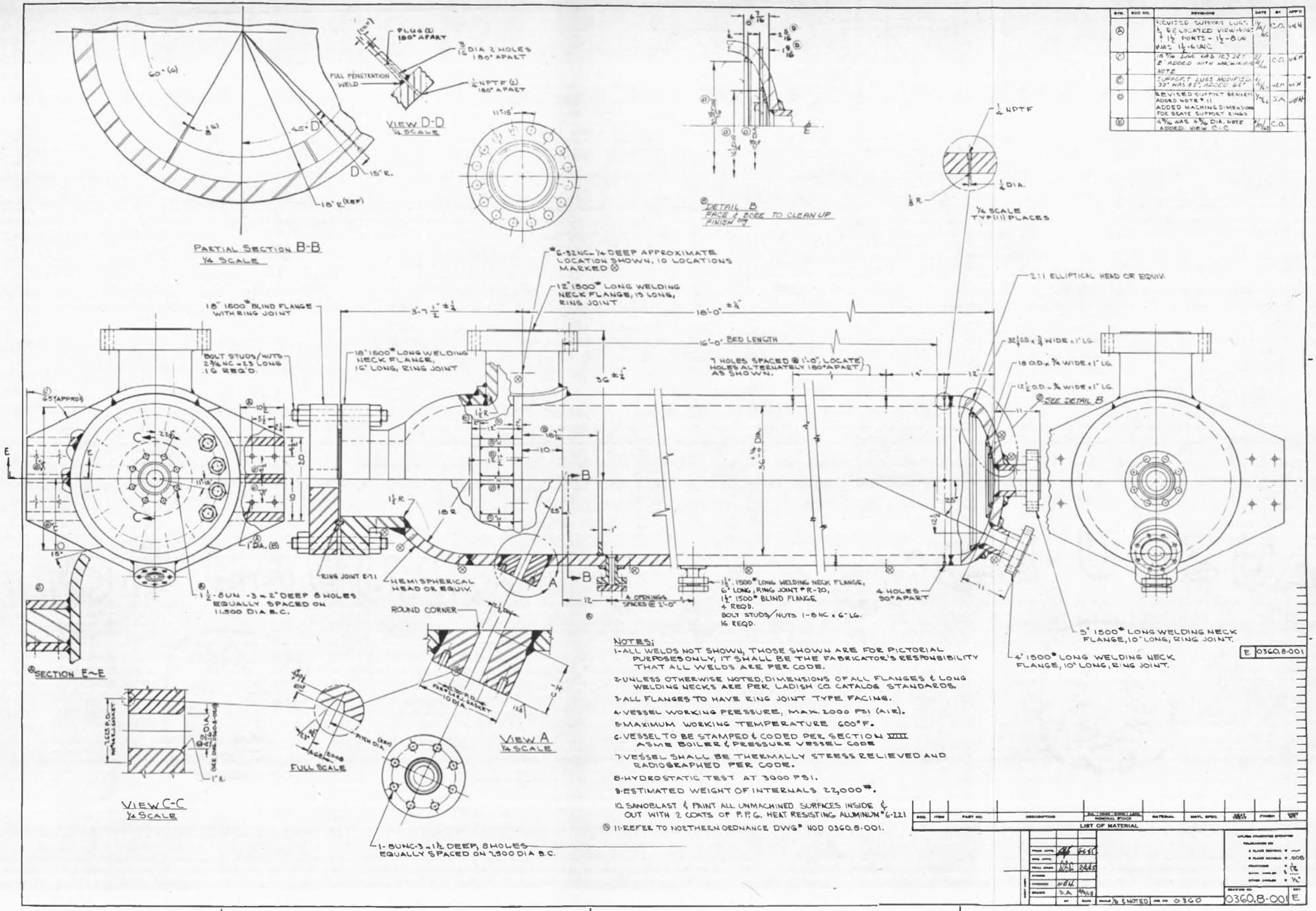

FIGURE 22. PRESSURE VESSEL - PILOT HEATER

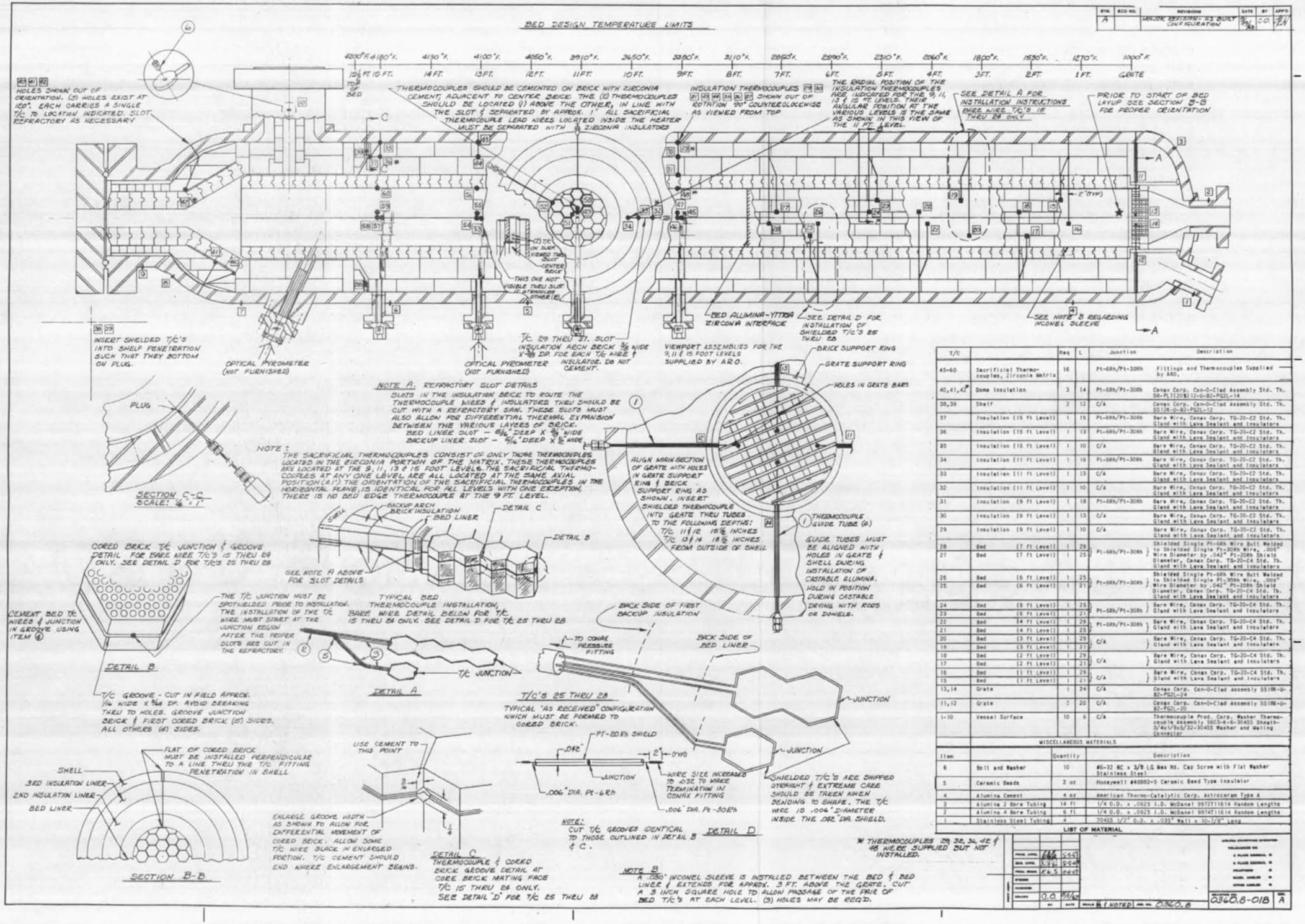

T/C		Req	L	Junction	Description
45-60	Sacrificial Thermocouples, Zirconia Matrix	16		Pt-6Rh/Pt-30Rh	Fittings and Thermocouples Supplied by ARO.
40,41,42	Dome Insulation	3	14	Pt-6Rh/Pt-30Rh	Conax Corp. Con-O-Clad Assembly Std. Th. SR-PLT120$ 12-U-82-PG2L-14
38,39	Shelf	2	12	C/A	Conax Corp. Con-O-Clad Assembly Std. Th. SS11K-U-82-PG2L-12
37	Insulation (15 ft Level)	1	15	Pt-6Rh/Pt-30Rh	Bare Wire, Conax Corp. TG-20-C2 Std. Th. Gland with Lava Sealant and Insulators
36	Insulation (13 ft Level)	1	13	Pt-6Rh/Pt-30Rh	Bare Wire, Conax Corp. TG-20-C2 Std. Th. Gland with Lava Sealant and Insulators
35	Insulation (13 ft Level)	1	10	C/A	Bare Wire, Conax Corp. TG-20-C2 Std. Th. Gland with Lava Sealant and Insulators
34	Insulation (11 ft Level)	1	16	Pt-6Rh/Pt-30Rh	Bare Wire, Conax Corp. TG-20-C2 Std. Th. Gland with Lava Sealant and Insulators
33	Insulation (11 ft Level)	1	13	C/A	Bare Wire, Conax Corp. TG-20-C2 Std. Th. Gland with Lava Sealant and Insulators
32	Insulation (11 ft Level)	1	10	C/A	Bare Wire, Conax Corp. TG-20-C2 Std. Th. Gland with Lava Sealant and Insulators
31	Insulation (9 ft Level)	1	18	Pt-6Rh/Pt-30Rh	Bare Wire, Conax Corp. TG-20-C2 Std. Th. Gland with Lava Sealant and Insulators
30	Insulation (9 ft Level)	1	13	C/A	Bare Wire, Conax Corp. TG-20-C2 Std. Th. Gland with Lava Sealant and Insulators
29	Insulation (9 ft Level)	1	10	C/A	Bare Wire, Conax Corp. TG-20-C2 Std. Th. Gland with Lava Sealant and Insulators
28	Bed (7 ft Level)	1	29	Pt-6Rh/Pt-30Rh	Shielded Single Pt-6Rh Wire Butt Welded to Shielded Single Pt-30Rh Wire, .005" Wire Diameter by .042" Pt-20Rh Shield Diameter, Conax Corp. TG-20-C4 Std. Th. Gland with Lava Sealant and Insulators
27	Bed (7 ft Level)	1	25		
26	Bed (6 ft Level)	1	25	Pt-6Rh/Pt-30Rh	Shielded Single Pt-6Rh Wire Butt Welded to Shielded Single Pt-30Rh Wire, .005" Wire Diameter by .042" Pt-20Rh Shield Diameter, Conax Corp. TG-20-C4 Std. Th. Gland with Lava Sealant and Insulators
25	Bed (6 ft Level)	1	21		
24	Bed (5 ft Level)	1	25	Pt-6Rh/Pt-30Rh	Bare Wire, Conax Corp. TG-20-C4 Std. Th. Gland with Lava Sealant and Insulators
23	Bed (5 ft Level)	1	21		
22	Bed (4 ft Level)	1	29	Pt-6Rh/Pt-30Rh	Bare Wire, Conax Corp. TG-20-C4 Std. Th. Gland with Lava Sealant and Insulators
21	Bed (4 ft Level)	1	25		
20	Bed (3 ft Level)	1	29	C/A	Bare Wire, Conax Corp. TG-20-C4 Std. Th. Gland with Lava Sealant and Insulators
19	Bed (3 ft Level)	1	21		
18	Bed (2 ft Level)	1	29	C/A	Bare Wire, Conax Corp. TG-20-C4 Std. Th. Gland with Lava Sealant and Insulators
17	Bed (2 ft Level)	1	21		
16	Bed (1 ft Level)	1	29	C/A	Bare Wire, Conax Corp. TG-20-C4 Std. Th. Gland with Lava Sealant and Insulators
15	Bed (1 ft Level)	1	21		
13,14	Grate	1	24	C/A	Conax Corp. Con-O-Clad Assembly SS18K-U-82-PG2L-24
11,12	Grate	2	20	C/A	Conax Corp. Con-O-Clad Assembly SS18K-U-82-PG2L-20
1-10	Vessel Surface	10	6	C/A	Thermocouple Prod. Corp. Washer Thermocouple Assembly 1603-K-6-30455 Sheath-3/4x1/8x5/32-30455 Washer and Mating Connector

MISCELLANEOUS MATERIALS

Item		Quantity	Description
6	Bolt and Washer	10	#6-32 NC x 3/8 LG Hex Hd. Cap Screw with Flat Washer Stainless Steel
5	Ceramic Beads	2 oz	Honeywell #40882-5 Ceramic Bead Type Insulator
4	Aluming Cement	4 oz	American Thermo-Catalytic Corp. Astroceram Type A
3	Aluming 2 Bore Tubing	14 ft	1/4 O.D. x .0625 I.D. McDanel 9972711614 Random Lengths
2	Aluming 4 Bore Tubing	6 ft	1/4 O.D. x .0625 I.D. McDanel 9974711614 Random Lengths
1	Stainless Steel Tubing	4	30455 1/2" O.D. x .035" Wall x 10-7/8" Long

LIST OF MATERIAL

* THERMOCOUPLES 29, 32, 34, 42 & 48 WERE SUPPLIED BUT NOT INSTALLED.

PROJ. ENGR.	[illegible]	5-5-67	
DES. ENGR.	[illegible]	5-5-67	
PROJ. MGR.	R.A.S.	5-6-67	
DRAWN			
CHECKED			
RELEASED	O.O.	5/11/67	

SCALE: AS NOTED | JOB NO. 0360.8 | 0360.8-018 | A

FIGURE 23. TEMPERATURE INSTRUMENTATION - PILOT HEATER

A cooling system which provides a uniform air flow over the outer surface of the pressure vessel was deemed necessary for two reasons. First, in the event vessel wall temperatures began to exceed the design limit of 600°F vessel wall cooling could be used to reduce it. Secondly, the heat loss from the vessel into the surrounding building would be quite large during periods of heater operation, hence, the vessel surface cooling could be used to vent this thermal energy from the building.

The vessel cooling was provided by enclosing the entire vessel with an aluminum shroud open at the base of the vessel and necking down at the top into a constant diameter pipe which terminated outside the building. The shroud provided a 6-8-inch gap surrounding the vessel. A variable speed fan, installed at the top of the vessel in the constant diameter pipe, provides some control of the air flow and corresponding heat transfer rate from the vessel wall.

The shell temperature is monitored by thermocouples attached at the various axial locations shown in Figure 23.

7.1.2 Heat Generation System

The thermal energy required to heat the ceramics is obtained by reacting a propane-oxygen-air mixture. The reactants are premixed and introduced into the heater through a water cooled burner positioned at the top of the heater vessel. The original burner and control system was sized for the maximum diameter matrix which could be installed in the heater vessel. The vessel is large enough to accept an 18-inch diameter matrix, thus the reheat system was designed accordingly. To heat an 18-inch diameter matrix to the desired conditions required a burner capable of delivering 1000 lb/hr.

The initial matrix installed in the heater was a 14-inch diameter requiring a maximum reheat mass flow of roughly half the burners total capability.

During the test program corrosion problems were encountered with the first generation burner which placed restrictions on its maximum operating conditions. Several repairs were made to the burner which proved to be temporary only. This led to the design of a second generation burner which was carried out by FluiDyne Engineering Corporation under a separate Air Force contract (AF Contract F40600-70-C-0009).

7.1.2.1 First Generation Burner

The first generation burner was a premix type burner capable of remaining in the heater during high pressure blowdown cycles. The burner was designed with a water cooled combustion chamber to avoid the problem of reacting combustion products washing across the refractory surfaces. The exit plane of the burner was tangent to the top surface of the dome which placed the burner exit about 40-inches above the matrix. A premix concept

was chosen over a diffusion type because of the inherently more complete and thus cleaner combustion that is typically obtained. From a refractory standpoint it is undesirable to have carbon or a reducing combustion atmosphere in contact with oxide refractories for prolonged periods because of their tendency to degrade the materials. Consequently, in addition to the premix design it was necessary during operation to always maintain an excess of oxygen in the fuel-oxygen mixture such that the resulting combustion products were oxidizing at all times.

The burner was designed to operate at maximum total flow rates of 1000 lb/hr with a corresponding heat rate of 2.4×10^6 btu/hr and a minimum mass flow of 40 lb/hr corresponding to 4.0×10^4 btu/hr.

The burner was fabricated by FluiDyne as shown in Figure 24. The primary materials used were zirconium-copper for the burner tube and nickel for the injector head. All of the surfaces exposed to combustion products were plated with gold to minimize corrosion. Unfortunately, operating experience in the pilot heater has demonstrated that the corrosion resistance of these materials to a combustion gas atmosphere is unacceptably low and as a result was the primary reason for discarding the burner.

7.1.2.2 Second Generation Burner

Based on the experienced gained with the first generation burner a set of design criteria were established for the design of a second generation burner. These criteria involved the following:

1. Minimize corrosion problems to the maximum extent possible.
2. Reduction of total mass flow capabilities.
3. Retain the original premix concept.
4. Retain the pressurized concept.
5. Design to generate useful information for the full scale heater.

These criteria evolved a design employing the original premix and high pressure concepts plus a modified mixer design and the use of a hot refractory combustion chamber. The end result has been a burner capable of remaining in the heater during a 2000 psi blowdown cycle and operating with a maximum flow capability of 550 lb/hr. The burner also possesses a decreased bypass flow requirement. The bypass flow requirement when operating with the second generation burner was decreased considerably over that of the first burner. In consideration of the mechanical and thermal loads the burners corrosion resistance was increased to the maximum extent possible by designing with a high grade stainless steel.

The second generation burner was fabricated by ARO/AEDC. The exit of the burner is shown in Figure 25.

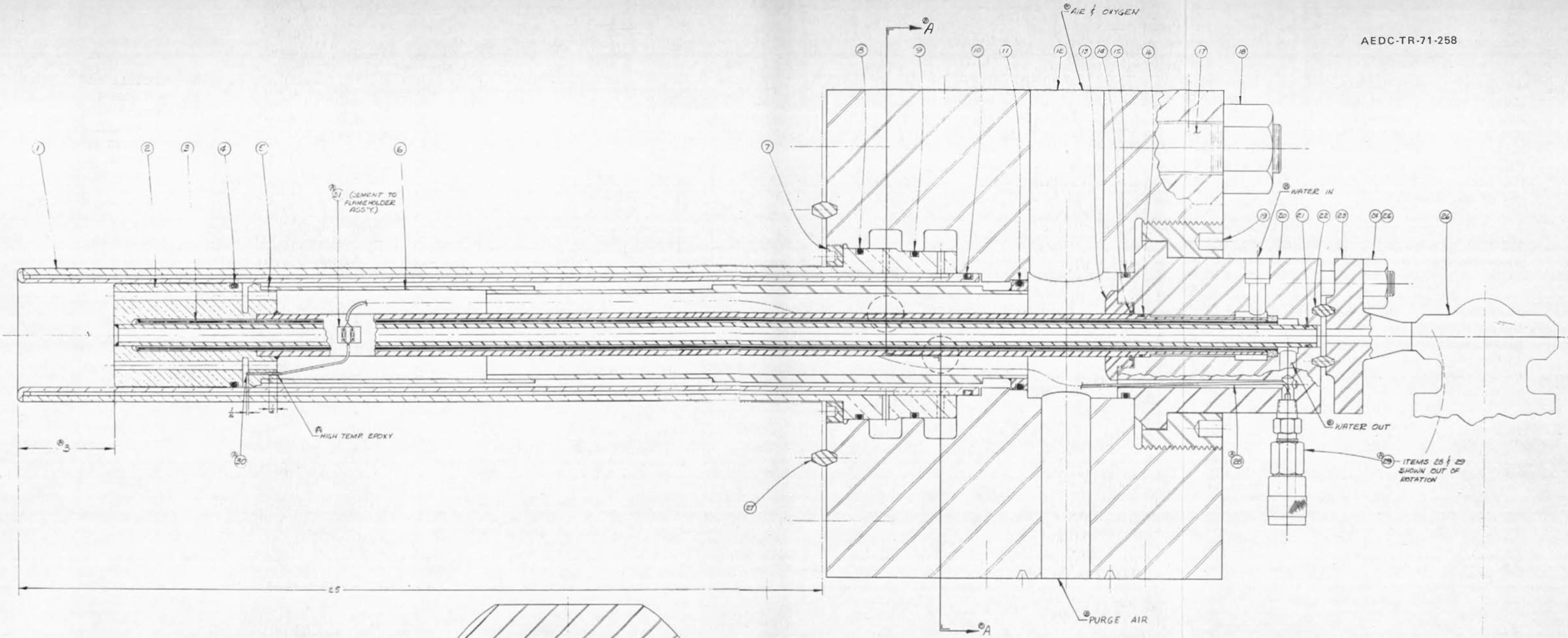

1	31		STRAIN GAGE TERMINAL
1	30		CHAM-CON-O-CLAD THERMOCOUPLE PLTG5-6-11-5
1	29		CONAX THERMOCOUPLE GLAND TG-20-CE (GALAND)
1	28		SERJ-RITE EXTENSION WIRE SXD-S-501
1	27		RING, JOINT GASKET (OCTAGONAL) LADISH # R24
1	26		3" -1500# PACIFIC VALVE FIG # 3155E
4	25		HEX NUT-1" O.N.C. HIGH STRENGTH STL
4	24		STUD BOLT-1" O.N.C. X 3½" LG. HIGH STRENGTH STL
1	23		8" DIA.-1500# RING JOINT WELD NECK FL FLANGE
1	22		RING JOINT GASKET (OCTAGONAL) LADISH # R16
1	21		"O" RING PEP # 016-4 VITON
1	20	-005	WATER MANIFOLD
1	19	-604	RING NUT-UPPER
8	18		HEX NUT-1½-8 THD. - HIGH STRENGTH STEEL
8	17		STUD BOLT-1½-8 THD. X 14½ LG. HIGH STRENGTH STEEL

B 0360-8-901

1	16		"O" RING PEP # 122 VITON
1	15		"O" RING PEP # 341 VITON
1	14		SNAP RING ST.STL TRU-ARC # 5100-131
1	13	-604	CLAMP NUT
1	12	-004	MAIN BODY
1	11		"O" RING PEP # 337 VITON
1	10		"O" RING PEP # 340 VITON
1	9		"O" RING PEP # 351 VITON
1	8		"O" RING PEP # 325 VITON
1	7	-606	RING NUT, LOWER
1	6	-004	PROPANE TUBE
4	5		#5-40 N.C. X ⅜ LG. FL HD. SOC. CAP SCR.
1	4		"O" RING PEP # 336 VITON
1	3	-604	BAFFLE
1	2	-004	FLAME HOLDER ASSEMBLY
1	1	0360-8-004	BURNER TUBE ASSEMBLY
REQ'D	ITEM NO.	DWG. NO.	NAME, DESCRIPTION, SIZE / MAT'L.

FIGURE 24. FIRST GENERATION BURNER - PILOT HEATER

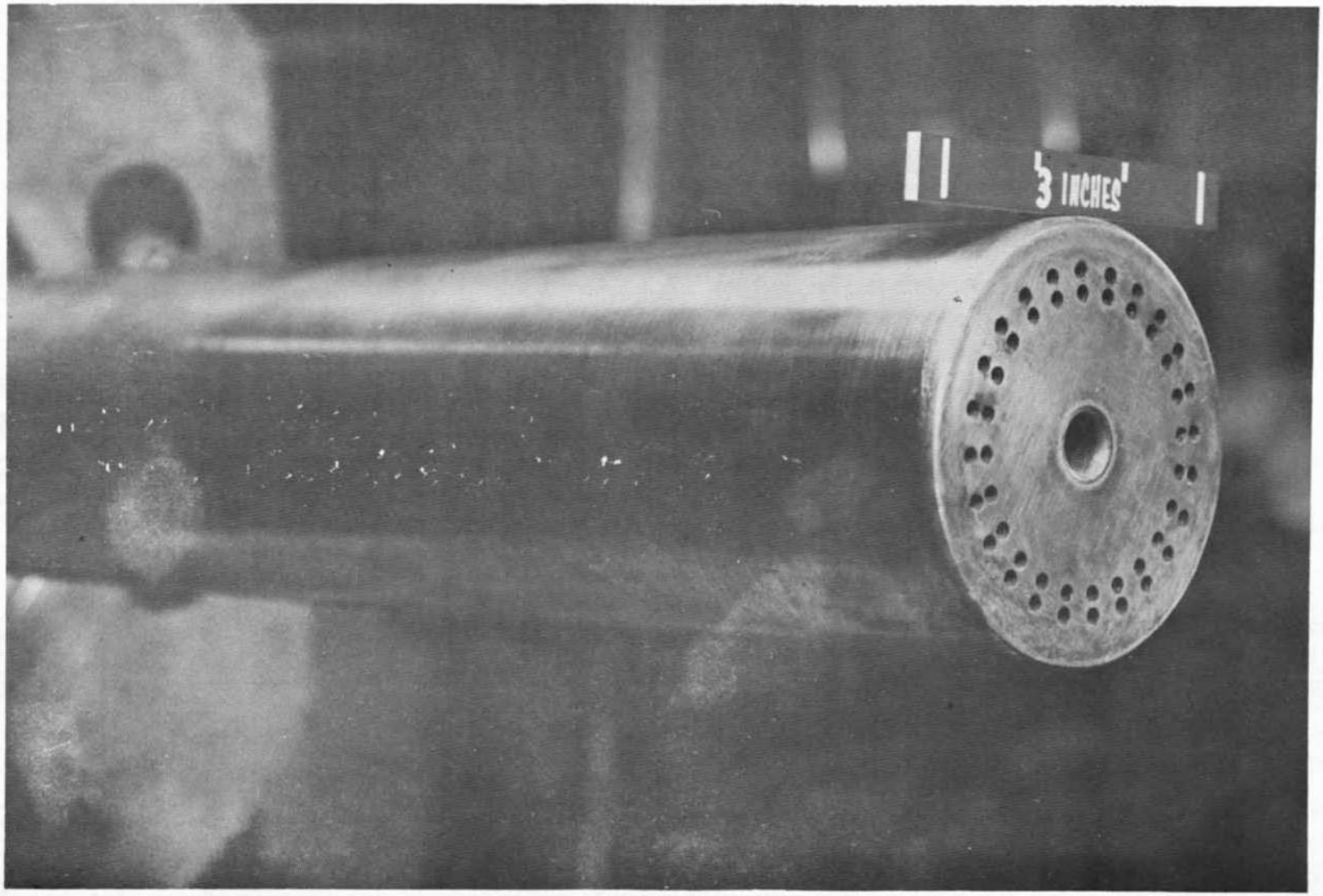

FIGURE 25. SECOND GENERATION BURNER - PILOT HEATER

7.1.2.3 Operating Characteristics

Premix burners have two operating characteristics, flashback and blowoff, which place upper and lower limits on their operating envelopes. The operating envelope for the first generation burner is shown in Figure 26 and for the second generation burner in Figure 27.

Flashback describes the phenomena whereby the flame moves upstream of the combustion chamber into the mixing portion of the burner. This phenomena limits burner operation in the low mass flow, high fuel-oxidant region. Figure 26 shows that increasing the fuel-oxidant ratio (f/ox) increases the total mass flow rate at which flashback occurs. For a specific fuel oxidant ratio (10% excess oxygen in the case shown) the fuel/oxidant ratio is increased by increasing the ratio of pure oxygen to air in the oxidant. Therefore, increasing the combustion temperature by reducing the air flow and increasing oxygen flow will eventually lead to the flashback limit for the burner. A flashback condition cannot be tolerated within the burner for other than a very short time because of local overheating which will occur within the burner mixing chamber. Consequently, a high temperature thermocouple has been placed in the mixing chamber to signal an interlock system and shutdown the flow of reactants in the event flashback occurs.

Blowoff describes the phenomena whereby the flame leaves its normal position in the combustion chamber and is either extinguished or becomes stabilized at some undesirable location downstream of the burner. This phenomena limits burner operation in the low fuel/oxidant region of the operating envelope. That is, blowoff places a limit on how lean the burner can be operated. Blowoff can be sensed only when the ceramics are below about 1500°F. When blowoff occurs below 1500°F the flame will be extinguished, whereas, above 1500°F the reactants will continue to burn because of ignition from the surrounding hot refractories and will stabilize some distance downstream of the combustion chamber. There are no viewports which allow viewing of the burner exit, therefore, blowoff at high temperatures cannot be detected.

7.1.2.4 Controls

The fuel and oxidant supplies to the burner are controlled through a system of regulators, valves and flowmeters. This system was designed by FluiDyne, detailed and fabricated by ARO. The system parts and details are described on ARO drawings.

7.1.3 Heat Storage System

The amount of heat that can be stored in a storage heater matrix and the rate at which it can be extracted depend on the type of heat storage material used, the materials' properties as well as the geometry into which the material is fabricated. The first ceramic internals purchased for the pilot heater, summarized in Reference 16, were designed to provide a 14-inch diameter bed 16

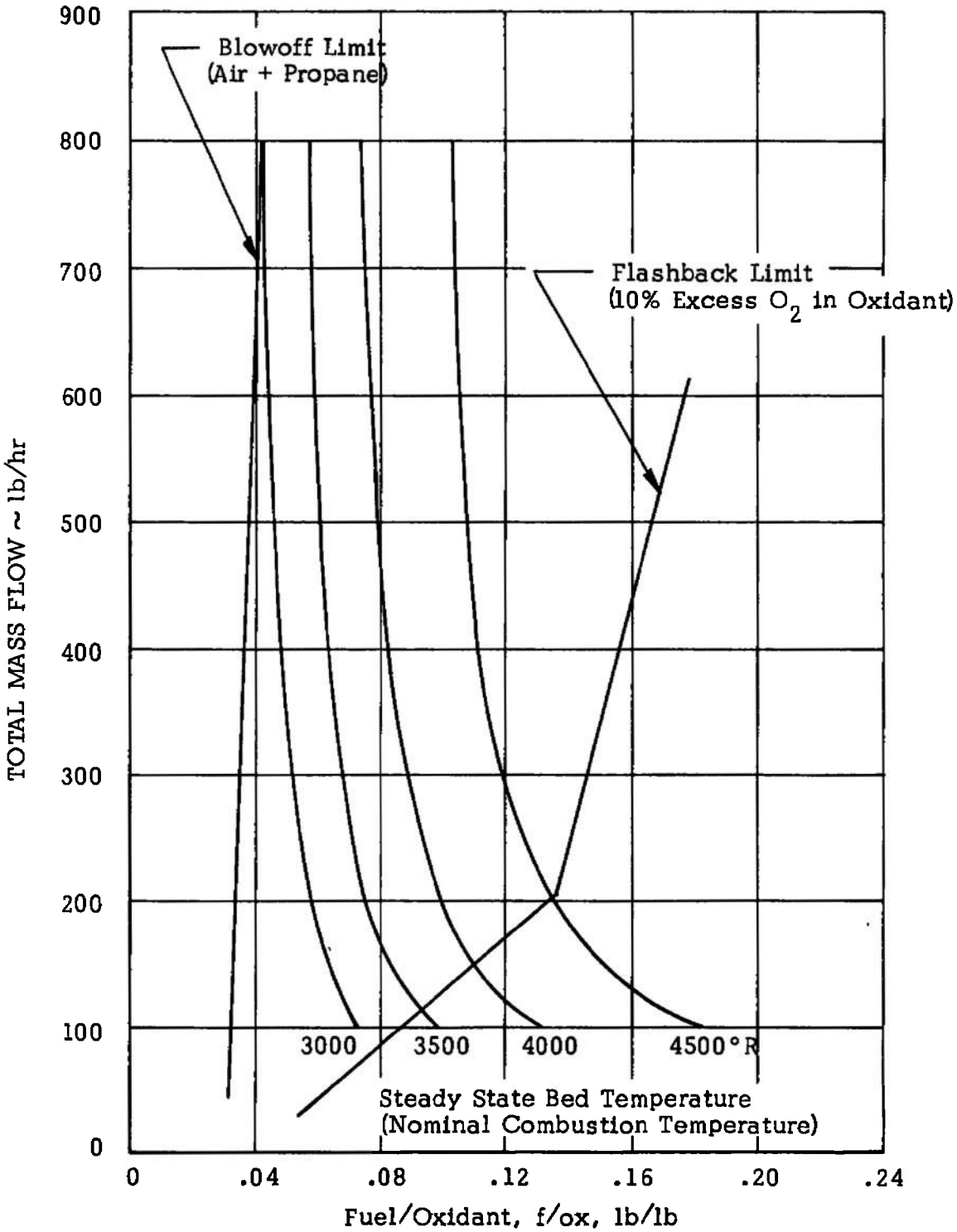

FIGURE 26. OPERATING ENVELOPE FOR FIRST GENERATION BURNER

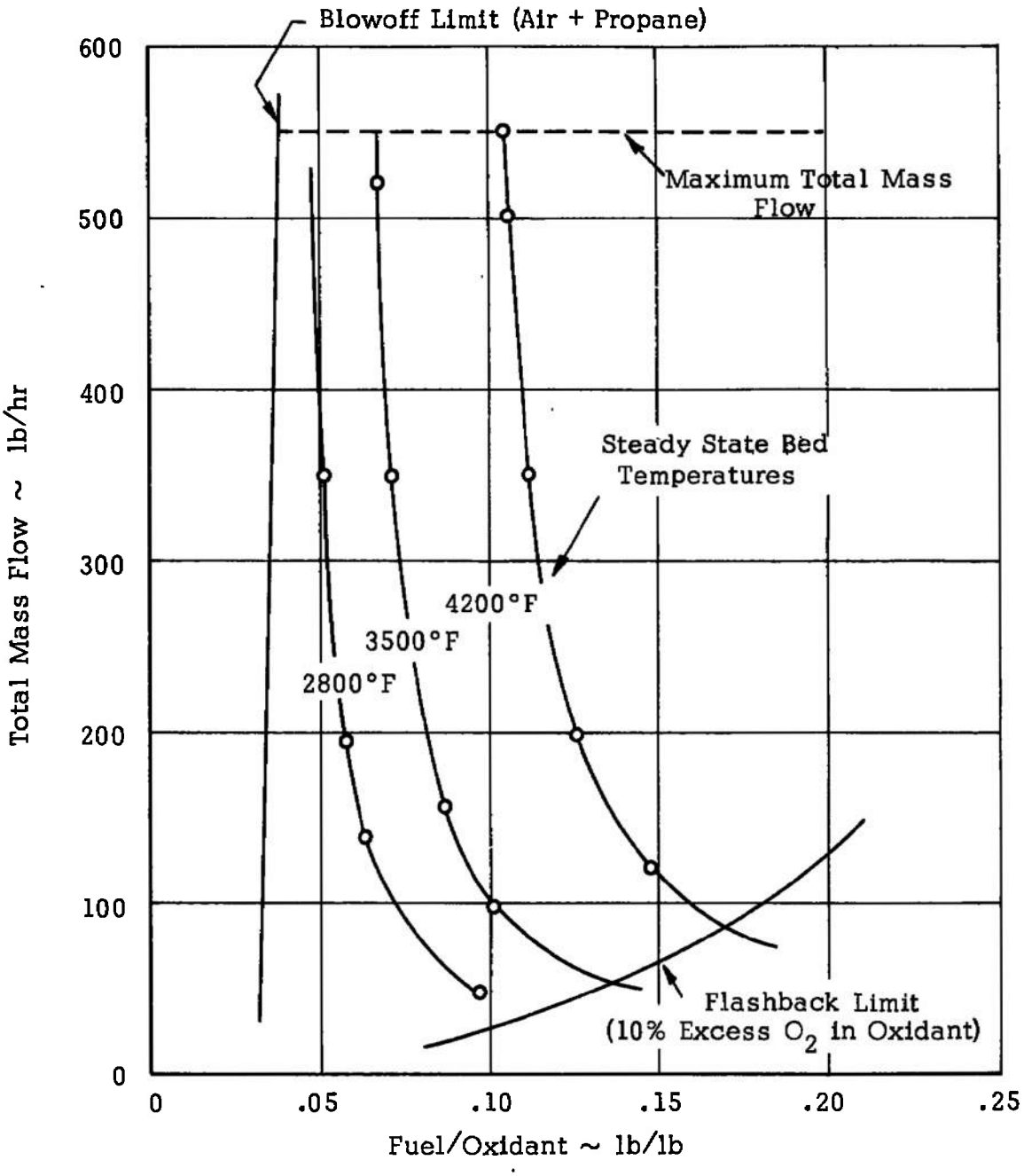

FIGURE 27. OPERATING ENVELOPE FOR SECOND GENERATION BURNER

feet long. This provided a bed somewhat shorter than the prototype bed of 20 feet. The design employed a graded bed consisting of three different materials: alumina, calcia-stabilized zirconia and yttria stabilized zirconia. The graded material concept was also carried into the insulation design.

7.1.3.1 Matrix

7.1.3.1.1 Matrix Length

The cost of a storage heater is proportional to its length. Consequently, for the pilot heater it was advantageous to employ the minimum length matrix that would still provide a reasonable simulation of the prototype heater. In the case of the pilot heater, the length of matrix selected was 16 feet.

It should be noted that as the length of matrix is reduced, the performance of the heater is similarly reduced. The reduced performance is measured in both lower mass flows for a given geometry and shorter run times for a given mass flow. For a given ceramic matrix, the maximum stress level allowable in the webs of a cored block, during the blowdown cycle, is related to the mass flow per unit area times the temperature gradient in the matrix in the axial direction ($\dot{m}/A \times dT/dZ$). For a given matrix material and geometry this product equals a constant which during operation is typically reduced from some maximum value by assigning a safety factor of at least two (Figure 28). The constant and how it was established, is discussed in Appendix C. When minimizing the matrix length, which was desirable for the pilot heater, dT/dZ will become larger if the temperatures at the top and bottom of the heater are held constant. The temperature gradient is further increased by lengthening the depth of temperature plateau in the upper portion of the heater while holding the bed length constant. Applying this to the pilot heater, as the bed length is decreased the mass flow per unit area ($\dot{m}/A$) must be reduced. Therefore, when prototype temperature plateau depths are simulated in the shorter matrix of the pilot heater, the allowable mass flows for the pilot relative to the prototype are less. Conversely tests at prototype mass flows with prototype ramp temperature gradients can be made in the pilot by reducing the temperature plateau.

7.1.3.1.2 Matrix Flotation

One of the major advantages of the cored block configuration over that of pebbles is the considerably lower pressure drop developed across a matrix of equal length. The pressure drop across a cored block matrix is caused by friction between the passing air stream and the adjacent hole surfaces and by hole misalignment between successive blocks in a given column. This net force across the bed, due to the pressure drop, tends to lift the matrix.

During the pressurization process, the maximum pressure drop occurs at the bottom of the heater, tending to lift the entire matrix. This occurs because air enters the heater at a greater rate than it leaves during pressurization. Consequently, the mass flow of air is greatest at the bottom and decreased as it continues up through the matrix.

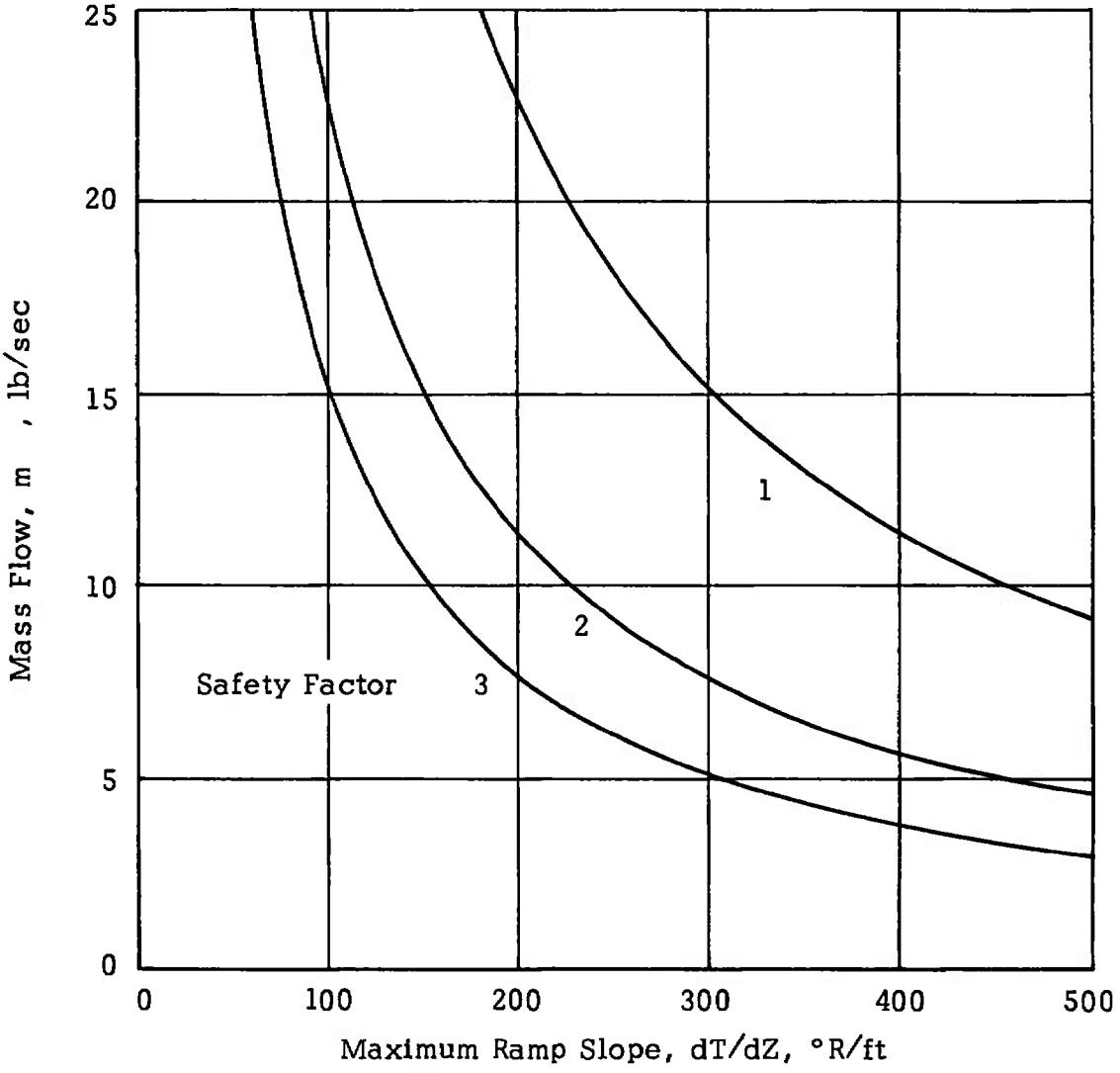

$$\frac{\dot{m}\,\frac{dT}{dZ}}{\text{Safety Factor}} = \frac{4230\,A_{BED}}{\text{Safety Factor}} = \frac{4530}{\text{Safety Factor}}$$

FIGURE 28. MAXIMUM THERMAL STRESS LIMITED MASS FLOW

Once steady state conditions are reached, the mass flow through the matrix becomes constant. The higher temperatures in the upper portion of the matrix expand the gas and as a result, a higher velocity is required to maintain the constant mass flow. During steady state conditions, therefore, the top portion of the matrix is the first to lift.

In a cored block heater it is found that flotation is not the limiting factor on the maximum mass flows because of the very low pressure drop. Rather, the maximum mass flow is limited by the allowable thermal stresses for the matrix. Pressure drop is a limiting factor only during the first few seconds of the pressurization process for a blowdown cycle.

7.1.3.1.3 Material Selection

The pilot heater, as originally designed, employed a graded bed with yttria-stabilized zirconia in the upper portion, calcia-zirconia in the middle, and alumina in the lower portion of the matrix. In general, the costs of ceramics decrease as the maximum service temperature decreases. Consequently, a substantial savings could be realized by employing a graded matrix design.

Candidate materials were evaluated in the subscale tests. Based on the test results calcia-zirconia was found to have a very limited life at temperatures above 3700°F. At these temperature levels, the calcia ion was believed to migrate from the zirconia lattice structure and be lost either to the flowing combustion products or to impurities concentrated at grain boundaries, resulting in a destabilized zirconia. X-ray fluorescence and emission spectrographic results indicated a decrease in total CaO concentration suggesting loss of stabilizer via a vaporization mechanism. The exact mechanism for calcia loss was never completely identified, however, the test results did provide adequate information to establish temperature design limitations.

Yttria-zirconia was also investigated in the subscale program and was found to be stable at temperatures up to 4200°F. Yttria, however, was found very expensive compared to calcia. The useful maximum temperature limit for calcia-zirconia in a storage heater was set at 3500°F based on subscale test data. The maximum service temperature of calcia-zirconia is considerably higher than 3500°F, however, as the operating temperature is increased the useful life of the fabricated shape is reduced due to destabilization.

To minimize matrix cost the pilot heater was designed with yttria-zirconia in the high temperature portion of the heater (3500-4200°F), calcia-zirconia in the midtemperature portion (2800-3500°F) and alumina in the low temperature portion (1000-2800°F).

7.1.3.1.4 Zirconia Stabilizers

The amount of stabilizer both for the yttria and calcia portions of the heater were investigated during the subscale tests. The results of these tests indicated that a fully stabilized zirconia should be utilized as the matrix of the pilot heater independent of the type of stabilizer.

Based on the results from the subscale tests a fully stabilized calcia-zirconia was specified for the mid-portion of the heater. This was specified by requiring essentially no monoclinic content in the fabricated shape.

The higher cost of yttria presented a more difficult problem in that it became necessary to keep the yttria content to a minimum and still retain a fully stabilized block. The subscale tests had shown 6 weight percent yttria to be inadequate to eliminate the monoclinic content. The results of the subscale tests indicated that 9.25 w/o yttria was adequate to fully stabilize the body, however, it was not felt to be the minimum. After extended discussions with both suppliers and consultants, zirconia materials with a number of different levels of yttria stabilization were specified. Purchase orders were placed with Coors Porcelain Company for materials with both 8 w/o yttria (Specification 7000-104) and 9 w/o yttria (Specification 7000-105).

The Zircoa Corporation felt strongly that the amount of yttria necessary could be reduced by providing the bulk of the stabilizer as yttria and a small portion as secondary stabilizers (i.e., calcia and magnesia). Compositions containing mixed stabilizers from Zircoa had been evaluated in the subscale tests and did exhibit satisfactory performance. Based on these subscale test results, purchase orders were placed with Zircoa for zirconia material stabilized with 6 w/o yttria plus 2 w/o secondary stabilizers (Specification 7000-101) and 8 w/o yttria plus 2 w/o secondary stabilizers (Specification 7000-102).

7.1.3.1.5 Interface Temperatures

The maximum temperature limitations placed on the interfaces between materials were considered in both the subscale tests and in the pilot heater design. The interface temperature limit between different materials is not simply the maximum service temperature limit of the lower melting point material, but rather the possible chemical reaction or eutectic that may occur between the adjacent two materials. Maximum interface temperatures of 2800°F were selected for the alumina/calcia-zirconia and 3500°F for the calcia-zirconia/yttria-zirconia interfaces based on subscale tests performed at both FluiDyne and Coors.

7.1.3.1.6 Cored Block Sizing

In the sizing of a cored block for a storage heater there exist certain restraints on both the maximum and minimum block size for a given matrix size. The maximum block size is usually governed by the following considerations:

1. Body thermal stresses.
2. Manufacturing capability.
3. Costs.

The minimum block size is dependent on several factors including the following:

1. Thermal expansion allowance.

2. Reheat shrinkage.

3. Pressure drop.

4. Block tipping.

Body thermal stresses are generated in a cored block as a result of the nonlinear temperature gradients existing across the entire block. The severity of these temperature gradients is strongly dependent on both the operating conditions and the size of the heater. For a given set of operating conditions and specified heater size the body stresses experienced by the individual cored blocks can be controlled, to some degree, by varying the size of the block. That is, the smaller the block, the smaller the body stresses for a given thermal environment.

The size of the block is also strongly influenced by the manufacturing capabilities of the suppliers. In the case of high density cored blocks the suppliers had essentially no background experience to draw from. This was especially true in the case of the pilot heater blocks because of the thin webs desired.

In the manufacturing of the cored blocks there are certain fixed costs related to the time and handling required to produce a single cored block. As the size is increased, within certain limits, the unit costs of the larger block are primarily a function of increased material costs. Therefore, matrix costs per unit volume appeared to decrease as the individual block size increased.

Thermal expansion and reheat shrinkage are also important parameters in the sizing of a cored block. It is important that the flat-to-flat dimensions of the cored block be larger than the possible gap that could accumulate in the upper portion of the bed from combination of thermal expansion and reheat shrinkage. Thermal expansion gaps are provided in the matrix during the installation to prevent crushing at the maximum temperature conditions. Reheat shrinkage is dependent on the material and may or may not occur after the material is operated for an adequate time at temperatures significantly above the materials' initial firing temperature.

Adjacent columns of cored blocks in the matrix are not keyed together in any fashion, consequently it is possible for the columns to intertwine in the event all the gaps accumulated at one location and the block width is less than the accumulated gap. A subsequent reheat with the blocks in this orientation would lead to crushing and fracturing.

From a pressure drop standpoint, it is desirable to keep the number of interfaces in the matrix to a minimum. If there is any significant amount of mismatch between adjacent blocks the mismatched holes act as orifices leading

to an increased pressure drop across the matrix. The keying of cored blocks holds both the mismatch and the pressure drop to a minimum.

Tipping of short blocks could occur if the adjacent columns of blocks expand and contract by different amounts. Differential movements can occur due to large radial temperature variations that do exist over a horizontal cross sectional plane through the heater. In a large heater, relative movements on the order of .5-inches have been estimated. In the event blocks were tipped they could produce large lateral forces within the heater.

After the subscale tests and review of the thermal conditions anticipated in the full scale heater, a block on the order of 4 to 5 inches across the flats and 12-inches in length was thought to be the optimum size for the heater. Manufacturing limitation decreased the flat-to-flat dimension to slightly under 3-inches. The length was specified as ranging from 4 to 12-inches (Figure 29). To minimize the thermal stress load from the burner to the cored blocks at the top of the matrix, three layers of 1-inch long blocks were specified. These short layers are commonly referred to as "buffer layers."

7.1.3.1.7 Cored Block Alignment

To assure that the hexagonal cored blocks would align with one another in a given column it was necessary to provide a keying mechanism between adjacent blocks. Keying is especially important when the heater is at temperature conditions less than maximum such that thermal expansion gaps exist between adjacent columns. Additional gap width may occur due to reheat shrinkage of all the refractories in the heater during the period they are exposed to high temperature operation.

Keying becomes more essential on a full scale heater due to the larger gaps that can accumulate. The pilot heater was designed with a 14-inch diameter matrix compared to the full scale 12 foot diameter matrix.

The key design adapted was a hexagonal shape about half the size of the outside cored block dimensions, depressed on one end of the block and raised on the other. The keying design and tolerances specified for the key as well as the whole block appear in Figure 29. A special shape was necessary to round out the hexagonal array to a round circle. A cored block segment was used for this purpose and is described in Figure 30.

7.1.3.1.8 Matrix Procurement

The cored block which form the matrix of the pilot heater were procured under a separate contract with the Air Force (F40600-67-C-0004). This procurement is covered in Reference 16. In summary, the matrix procurement encountered several difficulties which resulted in a matrix considerably different than originally designed. Purchase orders were originally placed with two suppliers for zirconia cored block. These two included the Coors Porcelain Company and the Zirconium Corporation of America. Each manufacturer was to supply a portion of calcia-zirconia and two compositions of yttria stabilized

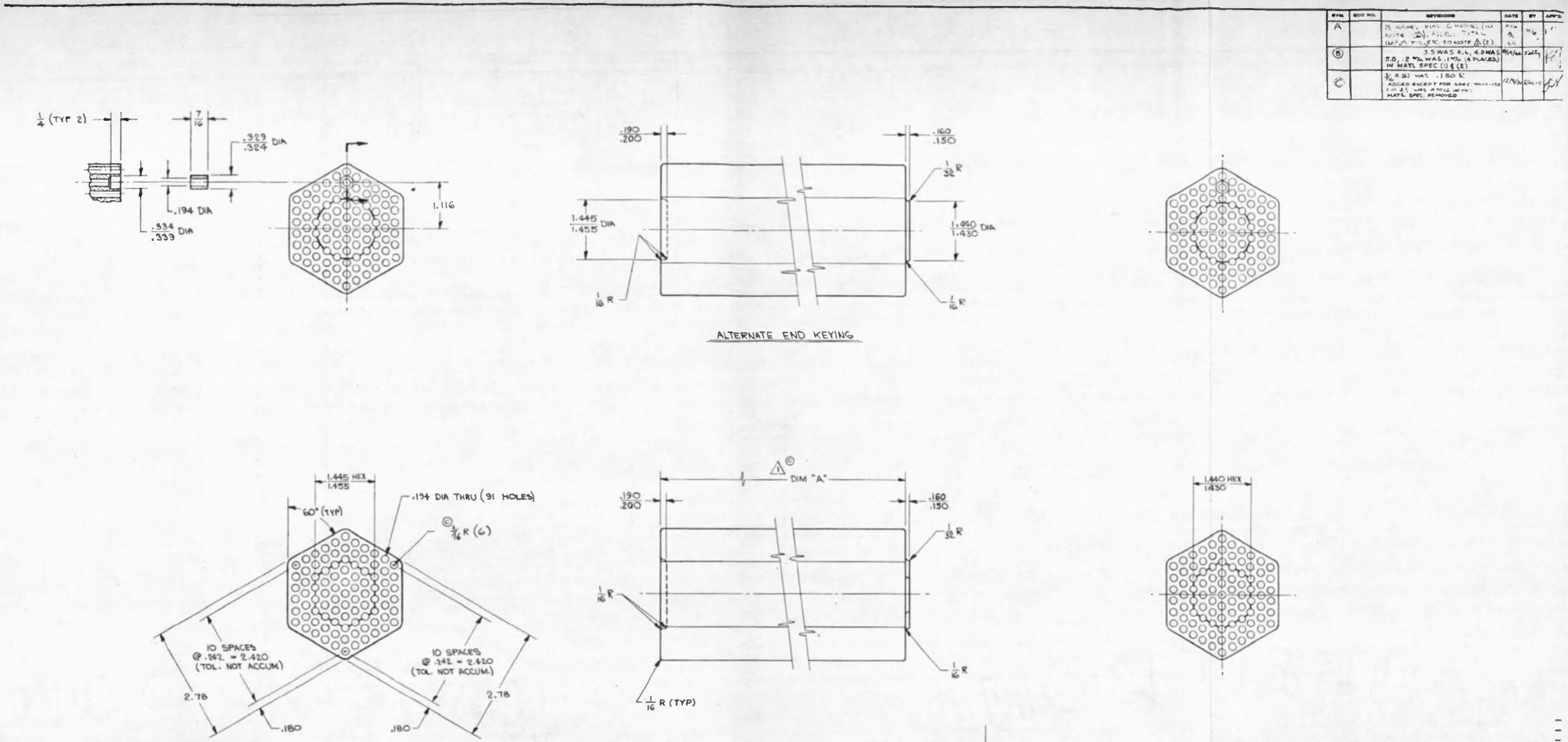

6 — BRICKS HAVING UP TO (3) HAIRLINE CRACKS NO GREATER THAN ½ IN. x ½ IN. WILL BE ACCEPTABLE (EXCEPT FOR SPEC. 7000-132)
5 — END FACES TO BE PERPENDICULAR TO SIDES WITHIN ± .030 IN 6 INCHES
4 — END FACES TO BE PARALLEL TO EACH OTHER WITHIN .030 T.I.R.
3 — END FACES TO BE FLAT TO WITHIN .010 T.I.R.
2 — SIDES TO BE FLAT & PARALLEL TO EACH OTHER WITHIN ± .030 IN 6 INCHES
1 — DIM. "A" TO BE 1 TO 2½ INCHES

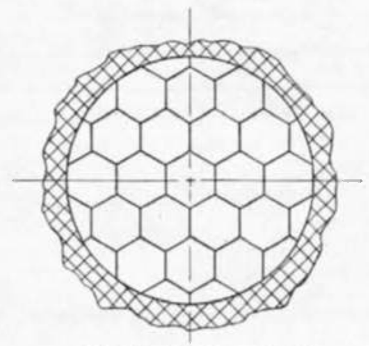

14" BED CROSS SECTION
SCALE 1/4 = 1

REFERENCE INFORMATION

HOLE DIAMETER	.194
WEB THICKNESS	.085
POROSITY	.40
TOTAL VOLUME / LINEAL FT.	80.3 IN.³
MATERIAL VOLUME / LINEAL FT.	48.0
BRICK WEIGHT / LINEAL FT.	6.8 LBS./FT. (ALUMINA)
BRICK WEIGHT / LINEAL FT.	9.5 LBS./FT. (ZIRCONIA)

FIGURE 29. CORED BLOCK CONFIGURATION

SYM.	ECO NO.	REVISIONS	DATE	BY	APP'D
A		12 WAS 6 (NOTE 2) ZIRCONIA WAS ALUMINA ALUMINA WAS ZIRCONIA ADDED (EACH SEGMENT) 4 PLACES	8-10-64	Kelly	[illegible]
B		4 TO 12 CHANGED TO 1 TO 2½ INCHES	12/9/70	RHOADS	[illegible]
C		.58 WAS .580	3/3/71	C.O.	[illegible]

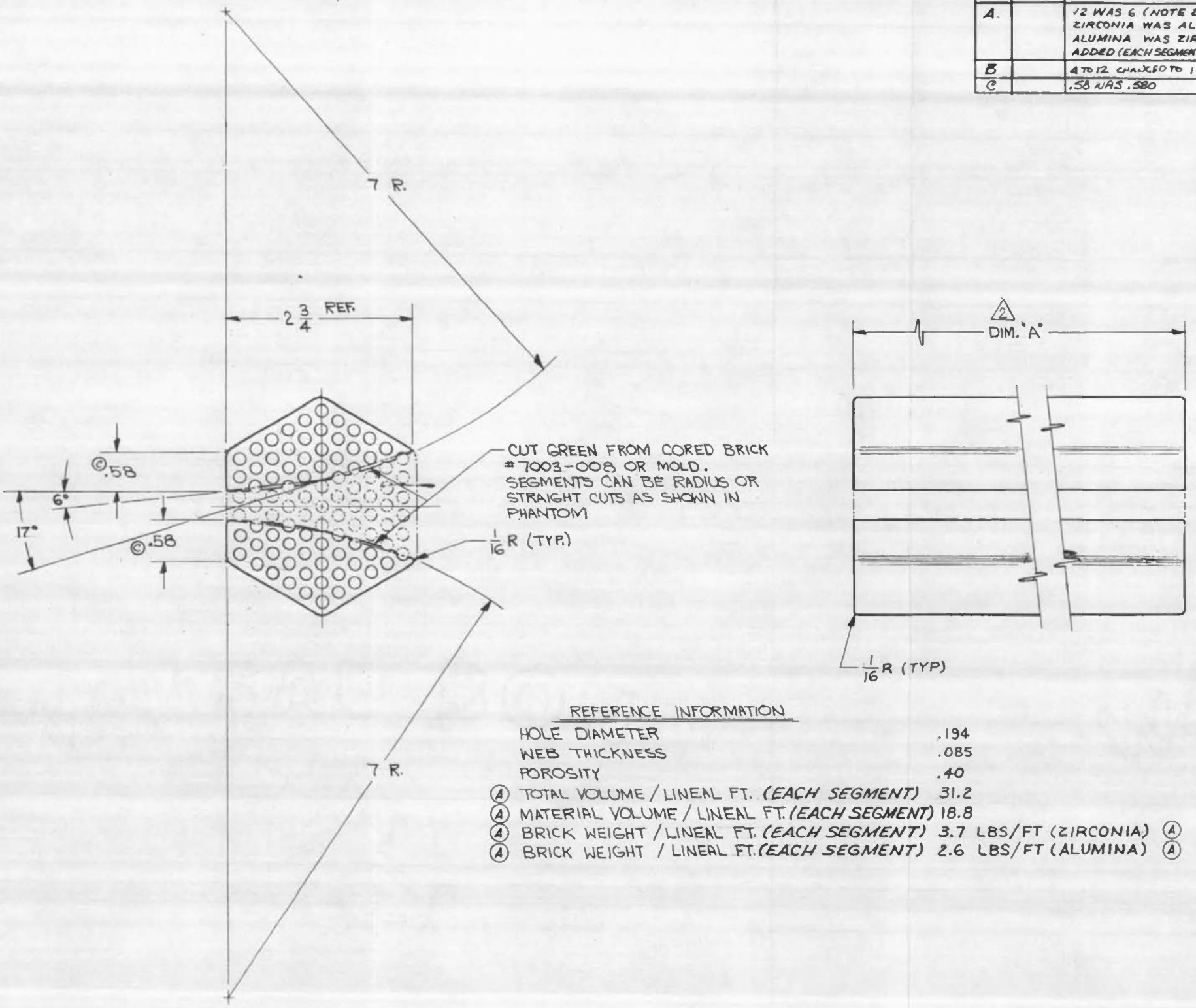

C 7003-604

REFERENCE INFORMATION

HOLE DIAMETER	.194
WEB THICKNESS	.085
POROSITY	.40
(A) TOTAL VOLUME / LINEAL FT. *(EACH SEGMENT)*	31.2
(A) MATERIAL VOLUME / LINEAL FT. *(EACH SEGMENT)*	18.8
(A) BRICK WEIGHT / LINEAL FT. *(EACH SEGMENT)*	3.7 LBS/FT (ZIRCONIA) (A)
(A) BRICK WEIGHT / LINEAL FT. *(EACH SEGMENT)*	2.6 LBS/FT (ALUMINA) (A)

(A) (B)

2 - RANDOM LENGTHS FROM 1 TO 2½ INCHES

1 - REFER TO DWG. # 7003-008 FOR BRICK DIMENSIONAL DETAILS & MATERIAL

FIGURE 30. CORED BLOCK SEGMENT

zirconia. The Zirconium Corporation was to supply a fully stabilized calcia-zirconia plus both 6 and 8 weight percent yttria-zirconia cored blocks (Specifications 7000-101 and 7000-102, respectively). The Coors Porcelain Company was to supply a fully stabilized calcia-zirconia plus both 8 and 9 weight percent yttria-zirconia cored blocks (Specifications 7000-104 and 7000-105, respectively).

A dual-supplier procurement was undertaken on the zirconia portion of the matrix to provide both a competitive market and a safeguard should one supplier be unable to produce a satisfactory cored block. Orders for the entire alumina matrix were placed with Coors Porcelain Company as the only established source.

The two manufacturers used different fabrication methods. Zircoa attempted to use the die pressing technique where a metal die is filled with powder and pressure is applied from two ends. Coors used the isopressing method. The die pressing technique did not prove successful primarily because of the length of block specified (minimum length of 4 inches). Die pressing would probably be useful in producing block on the order of one inch in length. Isopressing was successful and was the method used to produce the entire order.

Coors did, however, have difficulty in producing low monoclinic blocks in the 8 w/o yttria-zirconia and calcia-zirconia materials. As a result, they were given the option of substituting 9 w/o yttria-zirconia for the 8 w/o yttria- and calcia-stabilized materials. Coors exercised this option and supplied all of the bricks in the 9 w/o yttria material (FluiDyne Specification 7000-105). The blocks were supplied in lengths ranging from 4 up to 11 inches. Three layers of 1-inch blocks were fabricated for the top of the matrix to act as a buffer layer against any rapid changes in flame temperature which may occur during the reheat cycle.

A few deviations were allowed on the cored block that were delivered by Coors Porcelain Company. These included the following:

1. The hole spacing tolerance was increased from $2.420 \pm .010$ to $2.420 \pm .025$.

2. The allowable monoclinic content was increased from "essentially none" to less than or equal to 5%.

3. The crack specification was changed from three hairline cracks, 1/2 inch x 1/2 inch, and was left open to FluiDyne's judgment at the time of inspection. Cracked blocks were accepted where, in FluiDyne's opinion, they would not be detrimental to the heater's performance.

The matrix as finally installed in the pilot heater is shown in Figure 21. The final matrix configuration contained only one interface namely the alumina/yttria-zirconia interface. A shortage in the quantities of yttria blocks available at the time of installation resulted in the interface increasing from the 6 to the 7.5 foot level (Reference 16). To operate with the design temperature profiles required an increased alumina/zirconia interface temperature. Consultation with Dr. J. D. Plunkett, Materials Consultants, Inc.; Dr. L. L. Fehrenbacher, ARL/WPAFB; Dr. R. Ruh, AFML/WPAFB combined with inhouse test runs at Coors established 3000°F as the maximum temperature for the alumina/yttria-zirconia interface.

7.1.3.2 Insulation

In the design of high pressure, high temperature storage heaters, one of the costly items which must be considered is the pressure vessel itself. It is desirable, therfore, to provide the maximum matrix volume within a given pressure vessel. This is accomplished by optimizing the insulation design. The insulation is necessary to both protect the pressure vessel from overheating and simultaneously maintain the vessel at a near uniform temperature to avoid creating excessive thermal stresses in the pressure vessel itself. The insulation must not, however, be excessive such that water could condense from the reheat combustion gases. Condensation is undesirable in a storage heater for it would later appear as moisture in the blowdown air stream supplied to the wind tunnel nozzle. A vessel temperature near 500°F is a reasonable choice from both the insulation and vessel standpoints. This results in an insulation thickness of 11-inches.

Aside from the desirability of producing a uniform wall temperature to avoid excessive thermal stresses in the pressure vessel, it is also desirable for maintaining a uniform heat loss from the vessel. A uniform heat loss along the length of matrix helps produce a linear temperature distribution in the temperature ramp (Figure 1). The matrix design is thermal stress limited and, as discussed in Section 7.1.3.1.1, the thermal stresses are proportional to the slope of the temperature ramp, consequently, the linear ramp is the optimum choice.

Another point that was considered in the insulation design was the material's ability to withstand high pressure loads applied over a relatively short period of time. The high flow rates which a cored block matrix permit, allow the heater to be pressurized in less than half a minute. Conversely, the heater can be depressurized in similar time intervals should the need arise. To assure that the materials specified for the insulation design would withstand the high pressurization rates, all of the insulation material specified for the pilot heater was subjected to the pressurization-depressurization tests described in Section 6.1.3. All of the insulation blocks survived pressurization and depressurization rates up to 1200 psi/sec, with a maximum pressure of 3500 psi. These conditions represent the capability of the apparatus, consequently, failure rates were not determined.

Another important consideration in the design of the insulation is the potential for air, during the blowdown cycle, to bypass the hot matrix and pass up through the cooler insulation. Air flow through the insulation can have an important influence in reducing the air discharge temperature from the heater. The air in the insulation is at a lower temperature than in the matrix and is, therefore, at a higher density. If the bypass flow is large enough it can depress the final heater outlet temperature by a significant amount. The matrix and its surrounding insulation both experience the same pressure drop from inlet to outlet and in essence form parallel flow passages. The different pressure drops through the two passages, therefore, determine the amount of bypass flow that will flow through the insulation. In this situation cored blocks again have the advantage over pebbles because of their inherently lower pressure drop. Another important factor is the cross sectional area ratio of insulation to matrix. As the matrix area becomes large in relation to the insulation the effect of bypass flow is reduced. The relative amount of insulation is reduced as the heater diameter is increased and is also reduced as the allowable vessel wall temperature is increased.

In the pilot heater the tendency for the blowdown air to bypass the matrix was reduced by installing an inconel sheath between the matrix and insulation in the first three feet of matrix adjacent to the grate.

The insulation design for the pilot heater is illustrated in Figure 21. The upper portion of the heater insulation consists primarily of fully stabilized zirconia. All of the zirconia insulation directly exposed to combustion gases or adjacent to the cored block matrix were stabilized with yttria. All of the remaining zirconia was fully stabilized with calcia. The yttria-zirconia insulation was supplied by Zircoa Corporation in two levels of yttria; 8 w/o and 9 w/o (Specification 7000-107 and 7000-108, respectively). The 9 w/o material was supplied in bed liner material only and comprised about one-third of the zirconia bed liner insulation (Figure 21).

The insulation shapes varied from standard arch brick shapes for the backup liner to custom tongue and groove shapes for the hot liner. The insulation in the lower portion of the heater employs alumina tongue and groove shapes in the hot liner, plus a combination of alumina, 2600°F and 2800°F firebrick in standard shapes in the remaining backup insulation.

7.1.4 Heat Removal System

Thermal energy is stored in the matrix during the reheat cycle by allowing hot combustion gases to pass down through the cored block matrix. During the blowdown cycle a portion of this energy is extracted by flowing air in the reverse direction. As described in Section 7.1.3.1 there are relationships between the matrix thermal stresses and matrix flotation which are related to and limit the mass flow of blowdown air. Consequently, both adequate contols and pressure sensing equipment have been provided to both control and monitor the blowdown air flow rates.

The blowdown system concept was designed by FluiDyne and the system details were designed by ARO. The system as fabricated is covered on ARO drawings.

7.1.5 Temperature Instrumentation

The temperature instrumentation in the pilot heater consisted of both thermocouples, used in the regions operating below 3000°F, and optical pyrometers, used in the regions operating above 3000°F. Temperature measurements were made in the matrix, insulation and at various locations on the metal support hardware and vessel.

7.1.5.1 Matrix Instrumentation

To extract a certain level of performance from the storage heater, it is necessary that both the temperature level and profile through the heater be known. Thus, thermocouples were located at one foot intervals beginning at the base of the matrix and continuing up to the 7-foot level (Figure 23). The matrix thermocouples at the one, two and three foot levels are chromel/alumel and those at the 4-7 foot levels are Pt-30Rh/Pt-6Rh. Platinum-rhodium thermocouples have a melting temperature of about 3250°F, therefore, above the seven foot level a different method of temperature measurement was employed.

In the zirconia portion of the pilot heater matrix, special slots were designed and machined into the cored block at two foot intervals. These viewports were located at each of the following axial locations: 9, 11, 13 and 15 foot levels (Figure 21). The slots were cut through both the matrix brick and insulation such that they would all align at temperatures above 2000°F thus making it possible to view the center of the matrix with an optical pyrometer. The dimensions of the slots as well as their orientation in the heater are described in Figure 31. The slot in the cored block adjacent to the center cored block is considerably narrower than the others. In a storage heater the temperature from the center of the bed to the side can vary as much as several hundred degrees. The narrower slot is intended, therefore, to reduce the heat loss by radiation from the center block to the side which should result in a more accurate temperature measurement.

Thermocouples were also installed on each of the slotted center cored blocks such that the pyrometer measurements could be compared with thermocouple measurements at temperatures below 3200°F. Once above 3200°F these thermocouples would be lost. A special pyrometer of the disappearing filament type was provided which was especially suited for viewing small targets. The viewport design along with the pyrometer and calibration stand was supplied to the Air Force by FluiDyne under a separate Air Force contract (F400600-68-C-0002).

REVISIONS				
SYM	LTR	DESCRIPTION	DATE	APPROVED
	A	KEY SLOT DIMS & HISTORICAL CHG	7/1/62	[illegible]

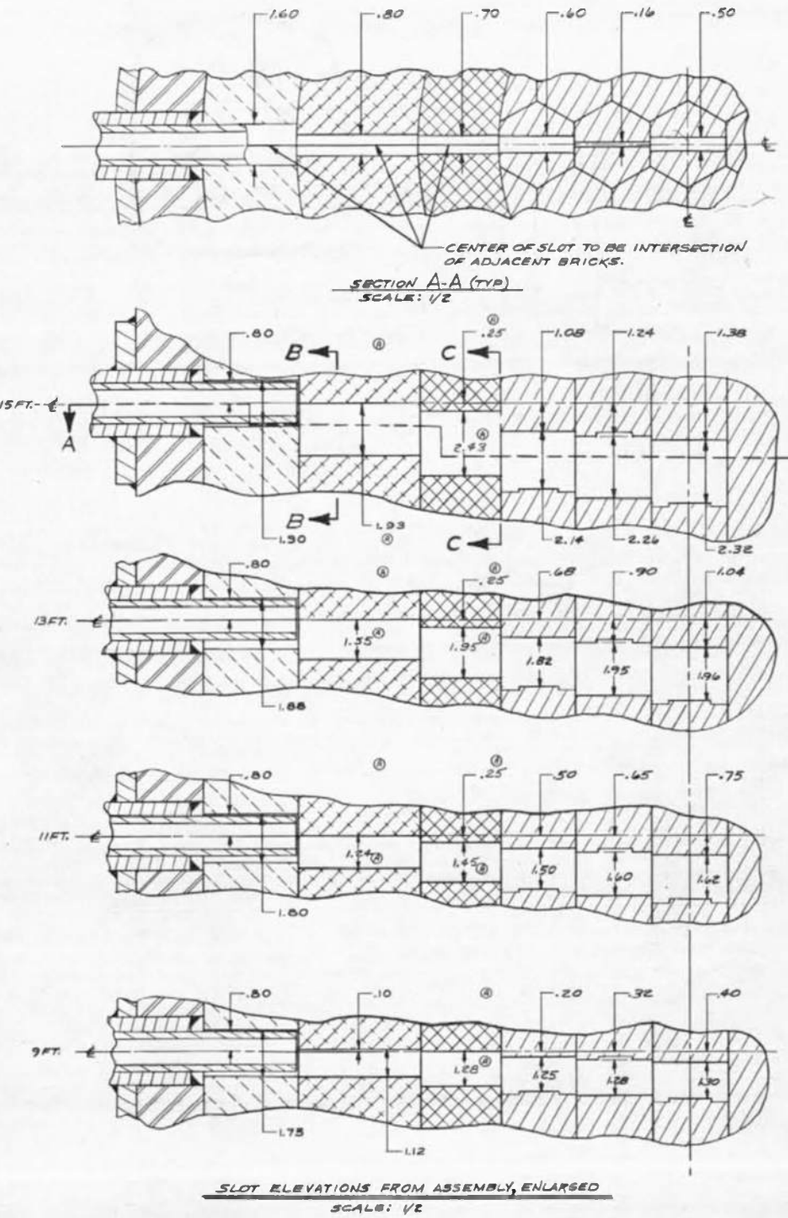

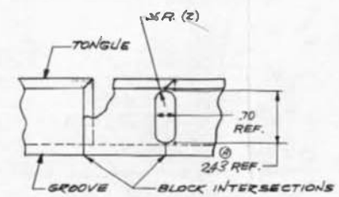

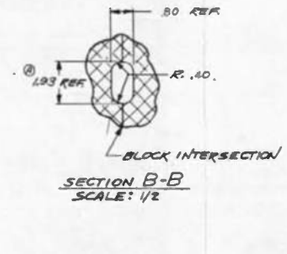

±.05 ON SLOT WIDTHS SECTION A-A
± 1/8" ON ALL OTHER DIM.

FIGURE 31. PYROMETER SIGHT HOLE ASSEMBLY - PILOT HEATER

7.1.5.2 Insulation Instrumentation

Temperature instrumentation was provided in the insulation to both detect overheating, in the event it should occur and to gather data on the performance of the insulation design. The bulk of the insulation instrumentation was located in the high temperature regions of the heater. The insulation areas containing temperature instrumentation included: the 9, 11, 13 and 15 foot levels, the insulation in the vicinity of the shelf and the dome region of the heater. The insulation instrumentation is described in Figure 23.

7.1.5.3 Vessel and Support Grate Instrumentation

The outside of the heater vessel was instrumented with ten chromel/alumel thermocouples (Figure 23). The thermocouples were of the washer type which could be attached directly to the vessel wall. The thermocouples were located on the various outlets of the heater as well as the main portion of the vessel shell itself.

The grate is located at the base of the heater and is the structural member which supports the entire matrix. The grate was fabricated from stainless steel and has been assigned a maximum service temperature limit of 1000°F. To monitor the grate's temperature, four shielded chromel/alumel thermocouples were installed. Two located near the center of the grate and two near the edge (Figure 23).

7.2 PILOT HEATER INSTALLATION

The pilot heater is located at the Arnold Engineering Development Center, Tullahoma, Tennessee. The heater vessel and ceramic installation was completed during June 1968. FluiDyne was responsible, under the subject contract, for providing technical supervision on site during the ceramic installation. The actual installation was performed by ARO personnel.

The first items to be installed in the pressure vessel were the grate and ceramic support hardware at the base of the vessel. The alundum castable was then cast in position to form a flat surface on which the insulation columns would rest. Figure 32 is a cutaway illustration showing the ceramics and support hardware at the base of the heater. A stainless steel multilayer perforated plate, with a hole pattern matching the cored block, was placed over the grate support bars to both avoid concentrated loads and reduce the thermal shock during a blowdown cycle on the bottom row of cored blocks.

During operation of the heater, the matrix as well as the insulation will experience an increase in volume as its temperature is increased, consequently, gaps must be allowed during installation to accommodate for this change in volume. The matrix was designed such that it is not restrained in the vertical direction and as a result vertical expansion is not a problem. Horizontal (diametral) expansion of the matrix, however, would be restrained by the

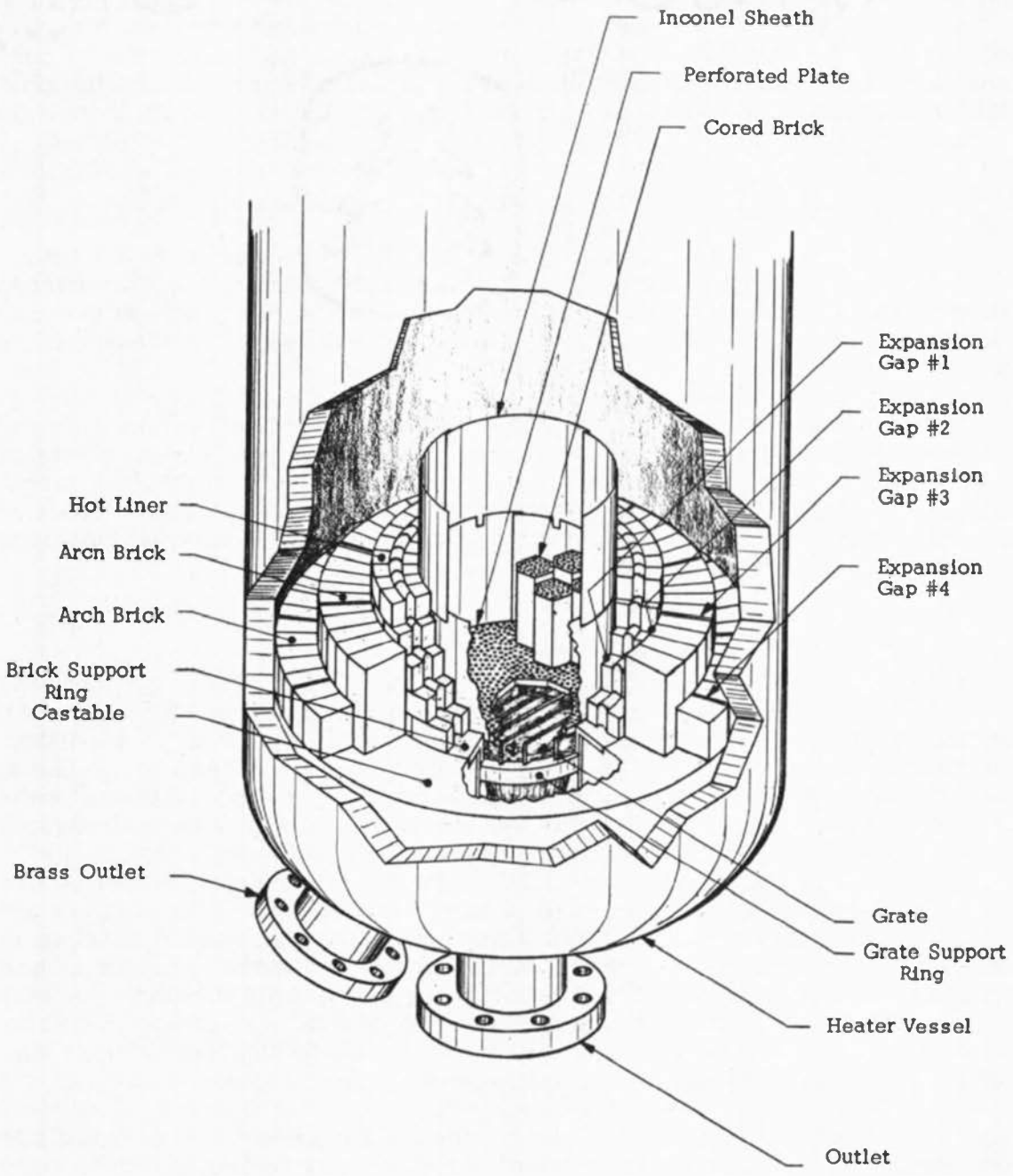

FIGURE 32. CUTAWAY VIEW AT BASE OF HEATER-PILOT HEATER

insulation and, therefore, gaps to accommodate this expansion were provided. The diametral expansion of the pilot heater matrix is quite small, even at 4200°F, because of the small diameter of the matrix (14-inches). Consequently, the matrix was installed with a single circumferential gap between it and the insulation.

The thermal expansion of the insulation had to be considered in addition to the matrix. The insulation in the pilot heater was made up of discrete rings of material: the bed liner plus two rows of arch brick. The expansion of the insulation was considered as three separate problems: first, the increase in thickness of the ring (diametral expansion); second, the increase in circumference (circumferential expansion) and third, the increase in height (vertical expansion).

The diametral expansion is quite small relative to the circumferential expansion because of the large difference in dimensions between the ring's thickness and circumference. Expansion from both sources was accommodated by providing gaps between the bed liner and first row of arch blocks (Gap 2, Figure 32), between some of the blocks in the first row of arch blocks (Gap 3), and between some of the blocks in the second row of arch blocks (Gap 4).

The vertical expansion was accommodated by designing the heater ceramics in columns which could move independently in the vertical direction. The matrix consists of 31 independent columns and the insulation consists of three concentric columns.

The appropriate gaps were maintained in the upper regions of the heater to accommodate the vertical expansion. All of the gap requirements were calculated based on the maximum operating temperature of the heater (4200°F). At 4200°F all of the gaps should theoretically be closed. During installation it was important that the gaps provided were not larger than required. If the gaps were too small, crushing of the ceramics would occur, introducing a source of dust. In the dome region gaps were allowed between the backup insulation and the pressure vessel. Gaps in the dome region were loosely packed with an alumina-silica ceramic fiber.

Thermocouples were installed to monitor the temperatures in the matrix, insulation as well as the pressure vessel and the grate support hardware located at the base of the heater. The thermocouples monitoring the matrix temperatures were installed along a line extending radially out from the thermocouple junction location through the pressure vessel wall. The thermocouple junctions were cemented in slots cut in the sides of the cored blocks as shown in Figure 23. Insulation thermocouples were installed in slots cut through the insulation (Figure 23). Optical pyrometer viewport slots were also provided for temperature measurement in the upper portion of the matrix. The temperature measurement instrumentation is discussed in detail in Section 7.1.5.

7.3 PILOT HEATER OPERATION

Operation of the pilot heater was initiated on 18 February 1969. Prior to operation an operations manual, general set of operating guidelines and a proposed test program was submitted to the Air Force by FluiDyne Engineering. During the course of operation several problems were encountered which included operational upsets as well as the material problems described in Section 7.3.3 and the burner problems described in Section 7.3.5. These problems resulted in the actual test program being somewhat different from that originally proposed.

7.3.1 Proposed Test Program

A test program for evaluating the pilot heater system was formulated and proposed to the Air Force as a partial requirement under the subject contract. The intent of the program was to test and evaluate the pilot heater ceramics, in conjunction with the system, to provide design information for the full scale heater as well as other storage heaters. Design information was sought on the entire system's performance together with the performance of individual components.

The pilot heater is a high temperature, high pressure, high performance type of device. As a result, errors in operation have potential for serious results. Therefore, the test program and procedures formulated and submitted were designed to develop information in a progressive fashion without assuming an excessive level of risk for either the personnel or to the system. Furthermore, because the results of individual tests could not be predicted in advance the test plan remained flexible.

The information generated by the test program would be primarily of a qualitative nature. Furthermore, identification of particular problems in the heater during operation (such as block cracking, dusting, plugged holes, etc.) would be very difficult. Identification of these types of problems would require the removal of a large portion of the ceramics. This represents a very expensive, difficult and time consuming task. Hence, the proposed program involved a minimum amount of ceramic removal. In lieu of extensive ceramic inspections, the program was written on the basis of an alert operating crew performing minor inspections at random intervals. These inspections would consist principally of visual examinations.

The test program specified an initial checkout with cold flow before the burner was ignited to ascertain that all systems were operational. The proposed heater test program provided for a stepwise increase in temperatures and pressures over a total of 50 runs with visual inspection recommended at specified intervals. The proposed test program is presented in Table 1.

TABLE I

TEST PROGRAM PROPOSED BY FLUIDYNE FOR THE PILOT HEATER

Run	Conditions and Purpose
1	Cold bed. Final check of air system.
2	Slow heat to low temperature. Final check of reheat system. Blowdown at low pressure. Examine top of bed.
3	Reheat and repeat Run 2.
4	Reheat to intermediate temperature. Blowdown at low pressure.
5	Repeat Run 4. Examine top of bed.
6	Reheat to 2800°F. Blowdown at low pressure.
7	Repeat Run 6. Examine top of bed.
8-12	2800°F - 500 psi.
	Cooldown for Examination of Ceramics
13-17	2800°F - 1300 psi
18-22	2800°F - 1600 psi
23-27	2800°F - 2000 psi
28-29	3500°F - 500 psi
30	3500°F - 1500 psi
31	3500°F - 2000 psi
32-33	4000°F - 500 psi
34	4000°F - 1500 psi
35-36	4000°F - 2000 psi
	Cooldown for Examination of Ceramics
37-38	4000°F - 500 psi
39-40	4000°F - 2000 psi
41-42	4200°F - 500 psi
43-44	4200°F - 1500 psi
45-50	4200°F - 2000 psi
	Cooldown for Examination of Ceramics

TABLE II. ACTUAL TEST PROGRAM FOLLOWED IN THE PILOT HEATER

TEST NO.	TEST DATE	DESIRED PRESSURE (psi)	ACTUAL PRESSURE (psi)	TEMPERATURE (°F)	COMMENTS
1					Cold matrix low pressure shakedown
2	2/21/69		430	1850	Blowdown to room temperature
3	3/14/69		400	1850	Blowdown to room temperature
4	3/27/69			2450	Blowdown to room temperature
5	4/4/69		700	2450	
6	4/6/69		-	2860	No blowdown-burner off due to electrical difficulty
7	4/7/69		800	3000	
8	4/8/69		650	2950	
9	4/9/69		550	2900	
10	4/10/69		700	2910	
11	4/10/69		-	2900	Steady pressure not obtained
12	4/11/69		450	2920	
VISUAL INSPECTION OF HEATER					
13A	4/30/69		-	3000	Steady pressure not obtained
13B	4/30/69		1380	3000	
14	5/1/69		1440	3000	
15	5/1/69		1300	2950	
16	5/2/69		1260	2980	
17	5/2/69		1270	3000	
18A	5/2/69		300	2820	Blowdown to room temperature
18B	5/10/69		1180	3000	
18C	5/10/69		1650	2980	
19	5/11/69		1600	2990	
20	5/12/69		1550	3000	
21	5/12/69		1670	3000	
22A	5/13/69		-	3000	No blowdown-equipment malfunction
22B	5/13/69		1600	3000	
23	5/14/69		1990	2970	
24	5/14/69		1920	2980	
25	5/15/69		2000	3010	

TEST NO.	TEST DATE	DESIRED PRESSURE (psi)	ACTUAL PRESSURE (psi)	TEMPERATURE (°F)	COMMENTS
26	5/15/69		2390	3000	
27	5/16/69		2080	3000	
VISUAL INSPECTION OF HEATER					Destabilization identified in 9.25 w/o yttria-zirconia matrix
4000°F FOR 96 HOURS --- HEAT SOAK TEST					
VISUAL INSPECTION OF HEATER					1. Restabilized 9.25 w/o yttria-zirconia matrix. 2. Installed Coors 12, 14, 16 w/o yttria-zirconia blocks on top of matrix.
28	12/11/69	500	500	3000	During Runs 28-32 operational upsets with the equipment did occur. During one run the propane flow to the burner dropped off resulting in a reduced bed temperature. Problems were also encountered with the oxidizer valves.
29	12/11/69	500	500	3000	
30	12/11/69	1000	1000	3000	
31	12/12/69	1000	1000	3000	
32	12/12/69	1000	1000	3000	
VISUAL INSPECTION OF HEATER					1. Bricks showed no signs of destabilization. 2. New blocks plus many buffer layers were severely cracked. Upset with propane flow suspected cause. 3. Additional Coors blocks installed prior to Run 33.
33	1/15/70	500	550	3700	
34	1/15/70	500	600	3700	
35	1/15/70	1000	1000	3700	
36	1/15/70	1000	1000	3700	
37	1/16/70	1000	1050	3700	

TEST NO.	TEST DATE	DESIRED PRESSURE (psi)	ACTUAL PRESSURE (psi)	TEMPERATURE (°F)	COMMENTS
VISUAL INSPECTION OF HEATER					1. Top foot of matrix removed and analyzed-no monoclinic identified. 2. Burner surfaces repaired. 3. Replaced top foot of matrix with Coors and Zircoa high density blocks plus Zircoa low density blocks.
45	8/5/70	1000	900	3000	
46	8/5/70	1000	800	3000	
47	8/5/70	1000	1100	3000	
48	8/6/70	1000	1150	3000	
49	8/6/70	1000	1050	3000	
50	8/6/70	1000	1000	3000	
51	8/6/70	1000	1000	3000	
52	8/6/70	1000	1050	3000	
53	8/6/70	1000	1050	3000	
54	8/6/70	1000	1000	3000	
VISUAL INSPECTION OF HEATER					1. Burner in good condition. 2. Condition of ceramics unchanged.
55	8/26/70	1500	300	3000	Run terminated during pressurization. Hand valve left open leading to excessive matrix ΔP
56	8/26/70	1500	1300	3000	
57	8/26/70	1500	1350	3000	
58	8/26/70	1500	1150	3000	
59	8/27/70	1500	1500	3000	
60	8/27/70	1500	1600	3000	
61	8/27/70	1500	1550	3000	
62	8/27/70	1500	1400	3000	
63	8/27/70	1500	1500	3000	
64	8/27/70	1500	1100	3000	

TEST NO.	TEST DATE	DESIRED PRESSURE (psi)	ACTUAL PRESSURE (psi)	TEMPERATURE (°F)	COMMENTS
VISUAL INSPECTION OF HEATER					1. Blocks showed no signs of destabilization. 2. Blocks showed a few hairline cracks. Cracking not as severe as last test series. 3. Low density combustion chamber blocks replaced. 4. Burner severely pitted. 5. Gold-plating removed from burner to check for possible galvanic corrosion.
38	2/27/70			3500	Maintained high temperature to evaluate performance of burner without protective gold-plating
VISUAL INSPECTION OF BURNER					1. Severe corrosion observed on burner. Corrosion attributed primarily to nitric acid formed in combustion products. 2. Initiated design of second generation burner.
39	5/14/70	1000	100	3500	1. Blowdown cycle terminated-leak in control valve. 2. Run series terminated-suspected water leak in burner.
VISUAL INSPECTION OF HEATER					1. Hydrotest of burner revealed no water leak. 2. Burner surfaces repaired.
40	6/25/70	1000	1000	3500	
41	6/25/70	1000	1050	3500	
42	6/25/70	1000	650	3500	
43	6/25/70	1000	1000	3500	
44	6/26/70	1000	1000	3500	

TEST NO.	TEST DATE	DESIRED PRESSURE (psi)	ACTUAL PRESSURE (psi)	TEMPERATURE (°F)	COMMENTS
VISUAL INSPECTION OF HEATER					1. Few hairline cracks visible in Zircoa high density blocks. 2. No cracks visible in Coors high density blocks. 3. No cracks visible in Zircoa low density blocks. 4. Burner in good condition. No repairs required.
65	9/17/70	1000	900	3500	
66	9/17/70	1000	950	3500	
67	9/17/70	1000	1000	3500	
68	9/17/70	1000	1000	3500	
69	9/17/70	1000	1150	3500	
VISUAL INSPECTION OF HEATER					1. Water leak identified on burner. 2. Ceramics located below burner were severely cracked and fractured into several pieces. 3. No cracking or fracturing observed in low density ceramics. 4. Severely cracked blocks replaced.
SECOND GENERATION BURNER INSTALLED (burner installation included new combustion chamber ceramics)					
70	2/11/70	500	500	3500	
71	2/12/70	500	500	3500	
72	2/12/70	1000	1000	3500	
73	2/12/70	1000	1050	3500	
74	2/12/70	1000	1050	3500	
VISUAL INSPECTION OF HEATER					1. Burner in excellent condition. 2. No significant change in the condition of the ceramics.

TEST NO.	TEST DATE	DESIRED PRESSURE (psi)	ACTUAL PRESSURE (psi)	TEMPERATURE (°F)	COMMENTS
75	3/17/71	500	500	4000	1. Pressures were decreased during this run series because of high ΔP encountered.
76	3/17/71	500	500	4000	
77	3/18/71	1000	900	4000	
78	3/18/71	1000	850	4000	
79	3/18/71	1000	550	4000	
VISUAL INSPECTION OF HEATER					1. High ΔP attributed to instrumentation difficulties. 2. No significant change in the condition of the ceramics. 3. Burner in excellent condition.
80	4/7/71	500	500	4000	1. Desired pressures were not obtained on the last three runs of this test series because of overtemperatures occurring in the flow restrictor. Safety interlocks shut system down.
81	4/7/71	1000	1000	4000	
82	4/7/71	1500	1450	4000	
83	4/7/71	2000	1750	4000	
84	4/8/71	2000	1600	4000	
85	4/8/71	2000	1850	4000	
VISUAL INSPECTION OF HEATER					1. Ceramics removed from heater down to the alumina/zirconia interface. 2. Details of this inspection are covered in the text of subject report.

7.3.2 Actual Test Program

The actual run program differed from that initially proposed owing to problems encountered with both the ceramics and burner reheat system. The actual test program comprised a total of 85 runs. The proposed and actual test program were similar in that both provided for test conditions beginning at some minimum run conditions and gradually increasing to the maximum conditions of 4000°F and 2000 psi. The run program was periodically interrupted during which time the heater was cooled and inspected. The extent of the inspection was dependent on the condition of the heater ceramics.

A typical inspection involved removing the burner and closely examining the exposed ceramics through the combustion chamber with the aid of lights, mirrors and telescopes. A number of cored block were usually removed from the bed top for a closer examination. The number of blocks removed was dependent on their condition. Samples were then selected and sent to the Aerospace Research Laboratory, Wright-Patterson Air Force Base, for analysis. During each inspection a photographic record was made of the exposed ceramics, wherever possible, and of all the ceramics removed from the heater. A very detailed record was maintained as to where each block was located in the heater, the number of runs and run conditions to which it was exposed along with an identification number that could be traced back to the manufacturers' records as to fabrication batch, kiln firing, etc. These records are being brought together by ARO/AEDC in an inhouse report.

The test program is outlined in Table II. This table lists the individual runs, run conditions and pertinent comments relating to each particular run series.

7.3.3 Performance of Matrix Material

The pilot heater test program was designed to provide a means of identifying and monitoring the performance of various materials when subjected to actual operating conditions. The general performance of the material was broken into specific classifications relating to the type of material, the shape and the combined class of material and shape. These classifications comprised the following detail items:

Material Related Factors

1. Phase changes and destabilization.
2. Chemical composition stability.
3. Stability to a combustion product environment.
4. Loss of strength.
5. Surface abrasion - tendency to dust.

6. Interface compatibility

7. Reheat shrinkage.

Shape Related Factors

1. Influence of dimensional tolerances on installation and assembly.

2. Cored block alignment.

3. Thermal expansion allowances.

Material and Shape Related Factors

1. Thermal stress effects resulting from reheat.

2. Thermal stress effects resulting from heat loss.

3. Thermal stress effects resulting from blowdown.

4. Effects of mechanical loads.

5. High temperature deformation.

The matrix material evaluated in the pilot heater to date has included both alumina and zirconia compositions. In the matrix, one alumina along with several zirconia compositions were evaluated. As discussed in Section 7.3.2, the initial test program, consisting of 85 runs, has been completed. The inspection following Run 85 has involved the removal of all the zirconia materials plus about one foot of the alumina cored block matrix. Analyses have been performed by the Aerospace Research Laboratory, WPAFB on a number of samples selected from the material removed.

7.3.3.1 High Density Zirconia - 9 Weight Percent Yttria

The first zirconia cored block material to be installed in the AEDC pilot heater was a 9 weight percent yttria stabilized zirconia supplied by the Coors Porcelain Company. This material was installed in the upper portion of of the heater and formed the matrix from the 7.5 to the 15.5 foot level. The material was very high in density (nominally 5.7 gms/cc or about 94% of theoretical). It was supplied per FluiDyne Drawings 7000-008 and 7003-604 (Figures 29 and 30) in lengths ranging from about 5 to 11-inches. The top surface of the matrix was covered with at least three layers of one inch long buffer layer blocks of the same composition. It was found during subscale tests and tests in other storage heaters that several layers of thin cored blocks would protect the longer cored block from sudden temperature changes

imposed by the burner both during ignition and minor operational upsets. These blocks form sacrificial layers which may require replacement more frequently than the entire matrix itself.

7.3.3.1.1 Material Related Factors

During the first 27 runs of the initial pilot heater test program the maximum conditions reached were 3000°F and 2000 psi. Normally a zirconia storage heater is not blown down to temperatures below 1500°F. As discussed in Section 7.3.2, the pilot heater was blown down to room temperature a total of four times during the first 27 runs of the test program. These first 27 runs did result in having a very significant effect on the structural integrity of the zirconia cored block material. Visual inspection of the cored blocks following this run sequence indicated the cored blocks in the upper portion of the bed had experienced extensive cracking. In some cases a change in color was observed from the original grey appearance to a spotted white and in some cases total white appearance. The white areas were accompanied by a substantial reduction in mechanical strength and an increase in monoclinic content. The monoclinic content was measured by x-ray diffraction analysis performed by the Aerospace Research Laboratories (ARL), Wright Patterson Air Force Base, Ohio. In general the white areas were typically weaker than the grey, however, both had suffered a loss in strength. The white areas were also typically higher in monoclinic content than the grey. The monoclinic content of the white areas ranged from 10 to 15 percent while that of the grey areas ranged from 2 to 5 percent. It was unnecessary to make quantitative measures of the materials' strength for qualitative measures indicated it was much too low to be useful as matrix material in a storage heater. Qualitative measures involve simply crushing the material with one's hand.

Photomicrographs of the material were prepared by Material Consultants, Inc. Observation under a 200X binocular microscope revealed that the sample's microstructure resembled more nearly a pile of powder than a fired dense ceramic.

Initial attempts to polish the mounted samples were unsuccessful. Due to the extremely low strength of the material, a procedure to cement the specimen fragments together was used in order to obtain a useful polished section. A technique published by Mr. A. King of the Zirconium Corporation of America was followed and did produce excellent results. The procedure involves placing pieces of the zirconia on the surface of a molten low melting, high lead glass (Ferrofrit No. 85 held in a mullite crucible) for about two minutes. During this period zirconium samples would become fully impregnated with glass and sink to the bottom of the crucible. The impregnated pieces were then mounted in plastic and polished in the usual manner without any difficulty. There was no tendency for grains to be pulled out during the polishing process and, consequently, no surface scratching from displaced grains. The samples were next etched by submerging the samples in cold dilute hydrofluoric acid ($1HF:5H_2O$) for three minutes such that the microcracks could be observed. This same process was performed onseveral pieces of yttria-zirconia of similar composition with no observed grain boundary etching. Hence it was possible to observe differences between the microcracks and the grain boundaries.

The microstructure of the destabilized samples under 200X magnifications are shown in Figure 33, 34 and 35. These photomicrographs indicate how almost every grain is separated from adjacent grains by a fine hairline crack. The material appeared to be held together by loose mechanical interlocking between adjacent grains. The photomicrographs justified the low strength of the material which was comparable to that of ordinary blackboard chalk. The fine network of microcracks was also believed to be the cause for the color change from a grey shiny to a white chalky surface appearance exhibited by the cored blocks. The alteration of the optical characteristics of the surface due to the microcracks would be adequate to change the color and surface texture of the samples.

Typically, cracks in ceramic will not heal upon refiring, but instead continue to propagate. During the close petrographic examination, described above, however, it was noted that the destabilized material was quite different from the typical cracked ceramic in that the cracked structure resembled a very dense green body comprising grains approximately ten times the size of the original zirconia powder used. Porosity measurements of the destabilized samples indicated that 2 to 4 percent of the total volume were voids due to microcracks. This indicated that the amount of material transport required for resintering the material was unusually small. In comparison, the porosity found in green pressed ceramic pieces (i.e., fabricated ceramic shapes before they are fired) is typically ten times that due to the microcracks which existed in the subject destabilized material.

To determine whether the destabilized material could in fact be restabilized, a number of samples were refired in laboratory type kilns at both the Air Force Materials Laboratory (AFML), Wright Patterson Air Force Base, Ohio and at the Coors Porcelain Company.

The Air Force Materials Laboratory/WPAFB fired a number of the destabilized samples in a combustion gas fired kiln at 3600°F for four hours. Examination following these thermal treatments found the material to be very hard and strong. The materials' surface texture had changed from the chalky porous appearance back to a dense shiny appearance. Every sample fired experienced a drop in monoclinic content. The actual data is summarized in Table III.

TABLE III

MONOCLINIC CONTENT OF SAMPLES REMOVED FROM PILOT HEATER AFTER RUN 27, BEFORE AND AFTER 4 HOUR HEAT SOAK AT 3600°F, COMBUSTION GAS ATMOSPHERE

SAMPLE NUMBER	COLOR (after Run 27)	% MONOCLINIC (after Run 27)	% MONOCLINIC (after Run 27 plus 4 hours at 3600°F)
6 - 5	Grey	2.2	<0.5
8 - 5	White	14.4	<0.5
11 - 7	White	13.6	<0.5
14 - 4	White	14.0	<0.5
15 - 4	White	14.9	<0.5

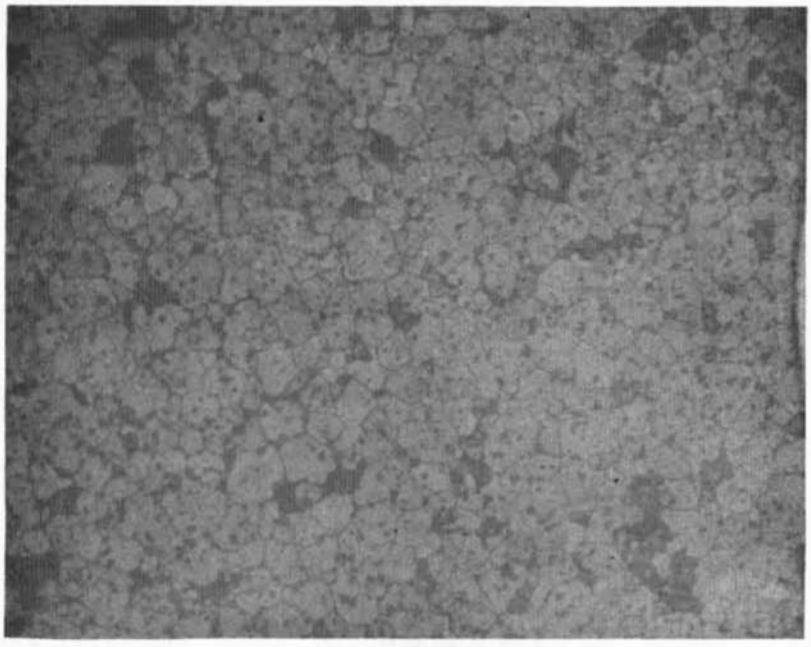

FIGURE 33. SAMPLE 14-1 (9.25 W/O YTTRIA-ZIRCONIA CORED BLOCK) REMOVED FROM THE PILOT HEATER AFTER RUN 27 - MAGNIFICATION 200X

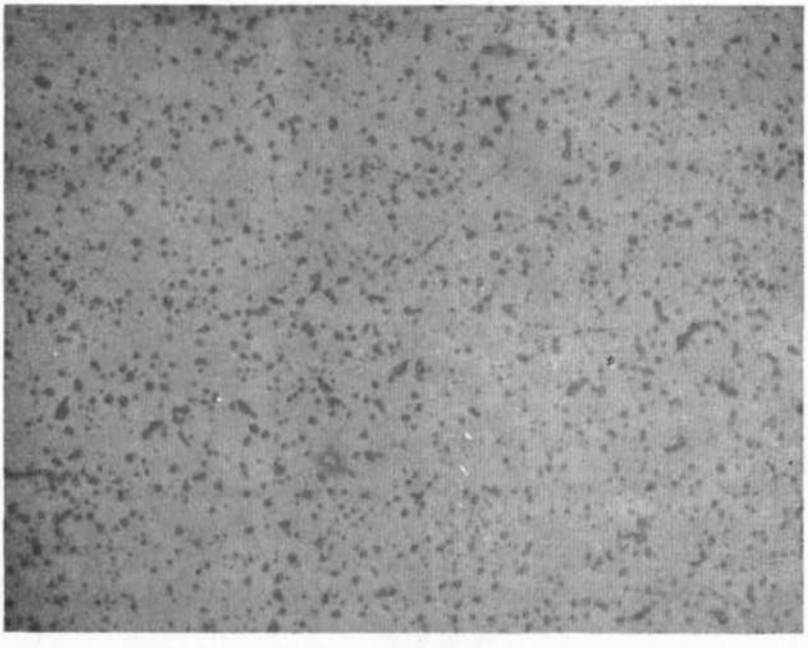

FIGURE 36. SAMPLE 14-1 (9.25 W/O YTTRIA-ZIRCONIA) AFTER RUN 27 IN THE PILOT HEATER AND SUBSEQUENT 8 HOURS AT 3450°F IN A HYDROGEN ATMOSPHERE - MAGNIFICATION 200X

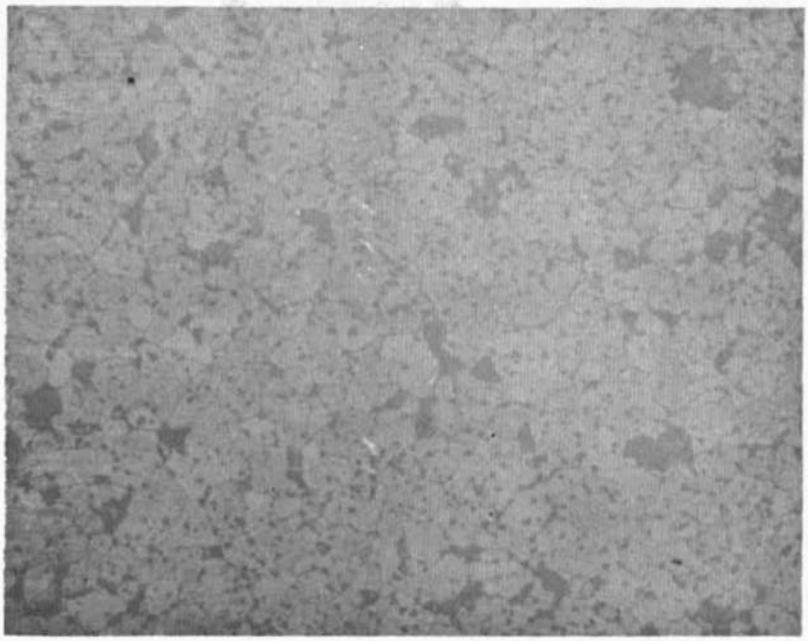

FIGURE 34. SAMPLE 15-1 (9.25 W/O YTTRIA-ZIRCONIA CORED BLOCK) REMOVED FROM THE PILOT HEATER AFTER RUN 27 - MAGNIFICATION 200X

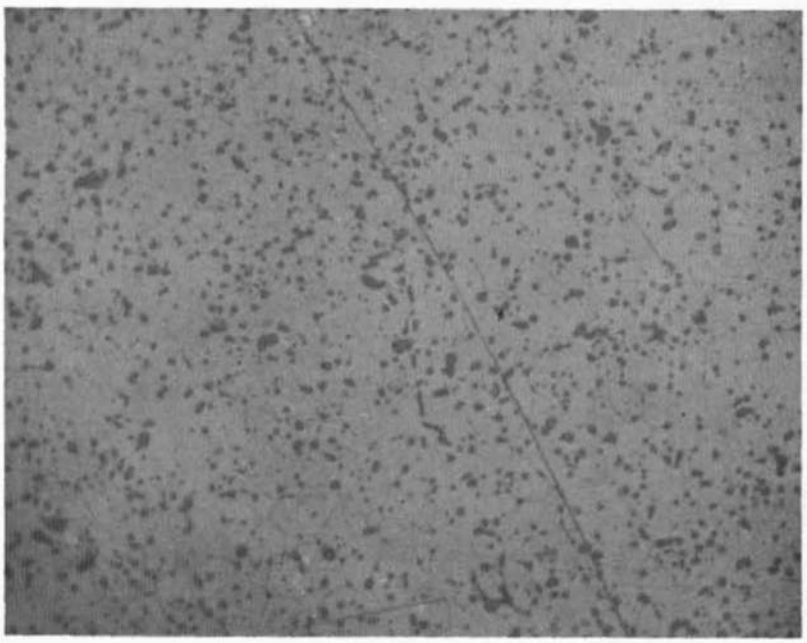

FIGURE 37. SAMPLE 15-1 (9.25 W/O YTTRIA-ZIRCONIA) AFTER RUN 27 IN THE PILOT HEATER AND SUBSEQUENT 8 HOURS AT 3450°F IN A HYDROGEN ATMOSPHERE - MAGNIFICATION 200X

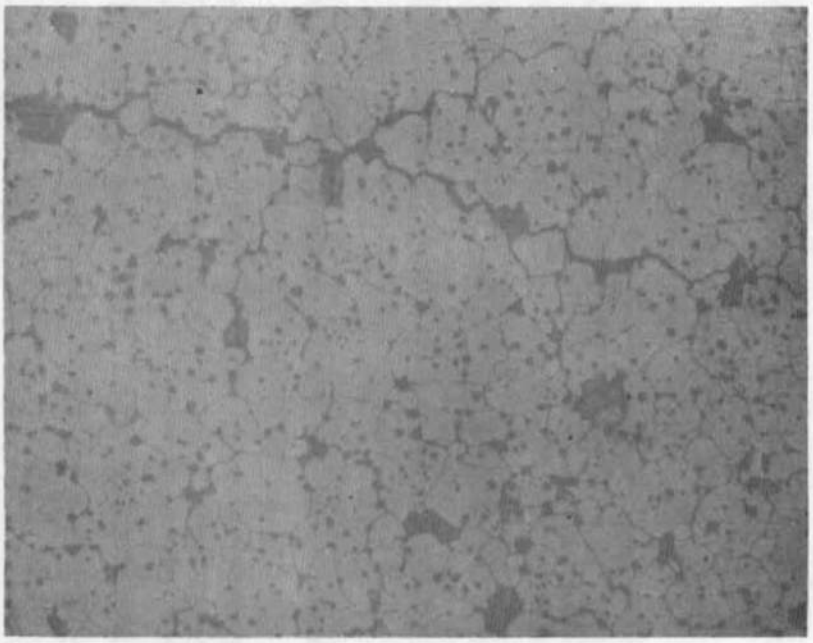

FIGURE 35. SAMPLE 3-1 (9.25 W/O YTTRIA-ZIRCONIA CORED BLOCK) REMOVED FROM THE PILOT HEATER AFTER RUN 27 - MAGNIFICATION 200X

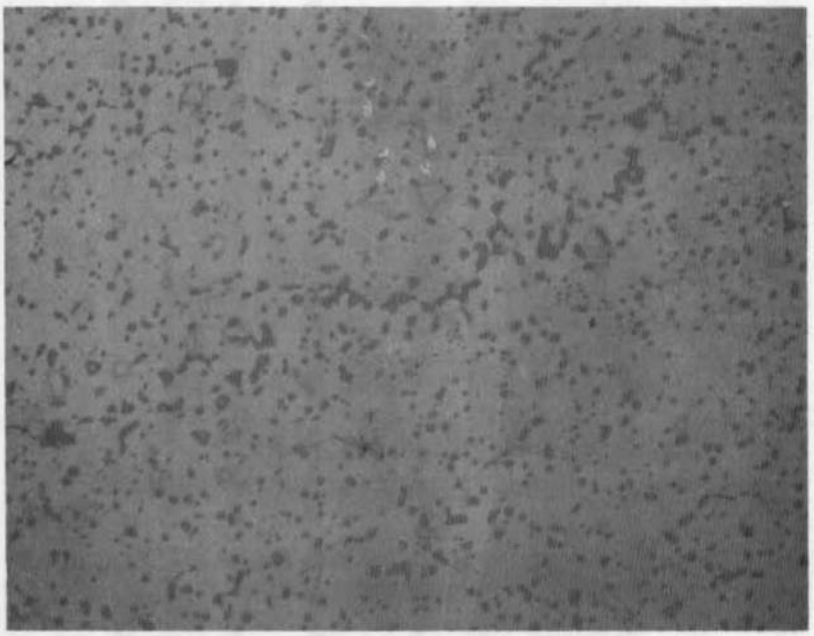

FIGURE 38. SAMPLE 3-1 (9.25 W/O YTTRIA-ZIRCONIA) AFTER RUN 27 IN THE PILOT HEATER AND SUBSEQUENT 8 HOURS AT 3450°F IN A HYDROGEN ATMOSPHERE - MAGNIFICATION 200X

Coors Porcelain Company also fired several samples under the direction of Materials Consultants, Inc. in a hydrogen atmosphere at 3450°F for a period of eight hours. A hydrogen atmosphere, in general, enhances the ceramic sintering process over that of a combustion atmosphere. It was estimated that a hydrogen atmosphere would reduce the required firing time by a factor of 5 to10 compared with that of a combustion gas atmosphere. On that basis, the eight hours in hydrogen at 3450°F was equivalent to about 40-80 hours in a combustion gas atmosphere. After the hydrogen firing, the samples exhibited the same properties as those fired by AFML at 3600°F with the exception of a color change. When fired in hydrogen all the samples became black in color. The surfaces, however, became dense, hard and shiny in appearance. X-ray analysis indicated the monoclinic content was reduced to undetectable levels. The x-ray analysis data for the hydrogen fired samples are summarized in Table IV.

TABLE IV

MONOCLINIC CONTENT OF SAMPLES REMOVED FROM PILOT HEATER AFTER RUN 27, BEFORE AND AFTER 8 HOURS HEAT SOAK AT 3450°F, HYDROGEN ATMOSPHERE

SAMPLE NUMBER	% MONOCLINIC (after Run 27)	% MONOCLINIC (after Run 27 plus 8 hours at 3450°F)
3 - 1	8.0	<0.5
14 - 1	6.5	<0.5
14 - 2	8.4 - 10.1	<0.5
14 - 3	13.2	<0.5
14 - 4	14.0	<0.5
15 - 1	9.8	<0.5

A petrographic examination was also made of the hydrogen fired samples. The photomicrographs prepared for this examination are shown in Figures 36, 37 and 28. These photomicrographs clearly indicate how the microcracks were resintered. Figure 38 also shows what was believed to be a larger hairline crack which initially would probably have been visible to the unaided eye. In this case, the high temperature heat soak reduced what was believed to be a thermal stress hairline crack to a string of voids, as sintered grains bridged the crack. The limit as to what size crack could be resintered was not revealed, however, it did appear that the friable material containing a multitude of microscopic cracks could be resintered into a dense, hard, strong, useable material.

A complete inspection of the ceramic matrix in the pilot heater would have involved removing all of the zirconia material. Subsequent reinstallation of the cored blocks would be impossible because of their friable condition.

In lieu of a complete inspection only the few blocks discussed above were removed from the top 18-inches of the matrix. The lower portion of the matrix was not inspected except for what limited information could be obtained by viewing and probing through the side viewports.

Based on the limited inspection performed, the conservative assumption was made that the entire matrix experienced destabilization. Subscale tests, however, indicated the destabilized material could be restabilized by refiring. The limiting temperature condition for the refiring of the pilot heater was the interface between the alumina and yttria-zirconia. From the literature and from experience generated at Coors it was concluded that the interface would be safe to about 3200°F. However, due to control limitations and possible instrumentation inaccuracies , the interface maximum temperature was set at 3000°F.

To determine if 3000°F would be adequate to restabilize and resinter the yttria-zirconia material, tests were conducted on samples of the destabilized material in laboratory kilns at the Coors Porcelain Company. These tests were also designed to establish the time period required at 3000°F. Thetest involved inserting 10 sets of samples into a kiln, firing the kiln to 3000°F, removing a sample set every 24 hours and analyzing the samples for monoclinic content. A sample set included both a grey and white portion of material cut from a brick removed from the pilot heater after Run 27. In addition, a few of the sample sets included a piece of 10.4 weight percent yttria-zirconia. The monoclinic content of the samples as a function of time at 3000°F is shownin Figure 39. Based on this data the decision was made to fire the pilot heater such that the zirconia/alumina interface would be maintained at 3000°F for 96 hours. To maintain 3000°F at the interface, under steady state conditions, it was necessary to hold 4000°F at the top of the matrix. Before beginning the 96 hour heat soak test additional cored block materials were placed on top of the matrix. These included several new 9.25 weight percent and 10.4 weight percent yttria-zirconia cored blocks.

At the completion of the 96 hour, 4000°F test, samples of the original destabilized 9.25 weight percent, the new 9.25 weight percent plus the new 10.4 weight percent yttria-zirconia material were removed from the heater. The microstructure of these samples were again closely examined for cracks as well as the crystalline structure for monoclinic content. The x-ray diffraction analysis, performed by ARL/WPAFB, showed less than one percent monoclinic for all three materials.

Photomicrographs of the three samples were prepared by Materials Consultants, Inc. Two photomicrographs were made of each sample. One showing the sample prior to etching and the second after etching. The photomicrograph before etching gave essentially no indication of microcracks in any of the three samples (Figures 40, 41 and 42).

Etching the same samples in hot hydrofluoric acid for 30 minutes revealed the grain boundary structure (Figures 40, 41 and 42). A large amount of grain growth was apparent. The photos also revealed a lower number of

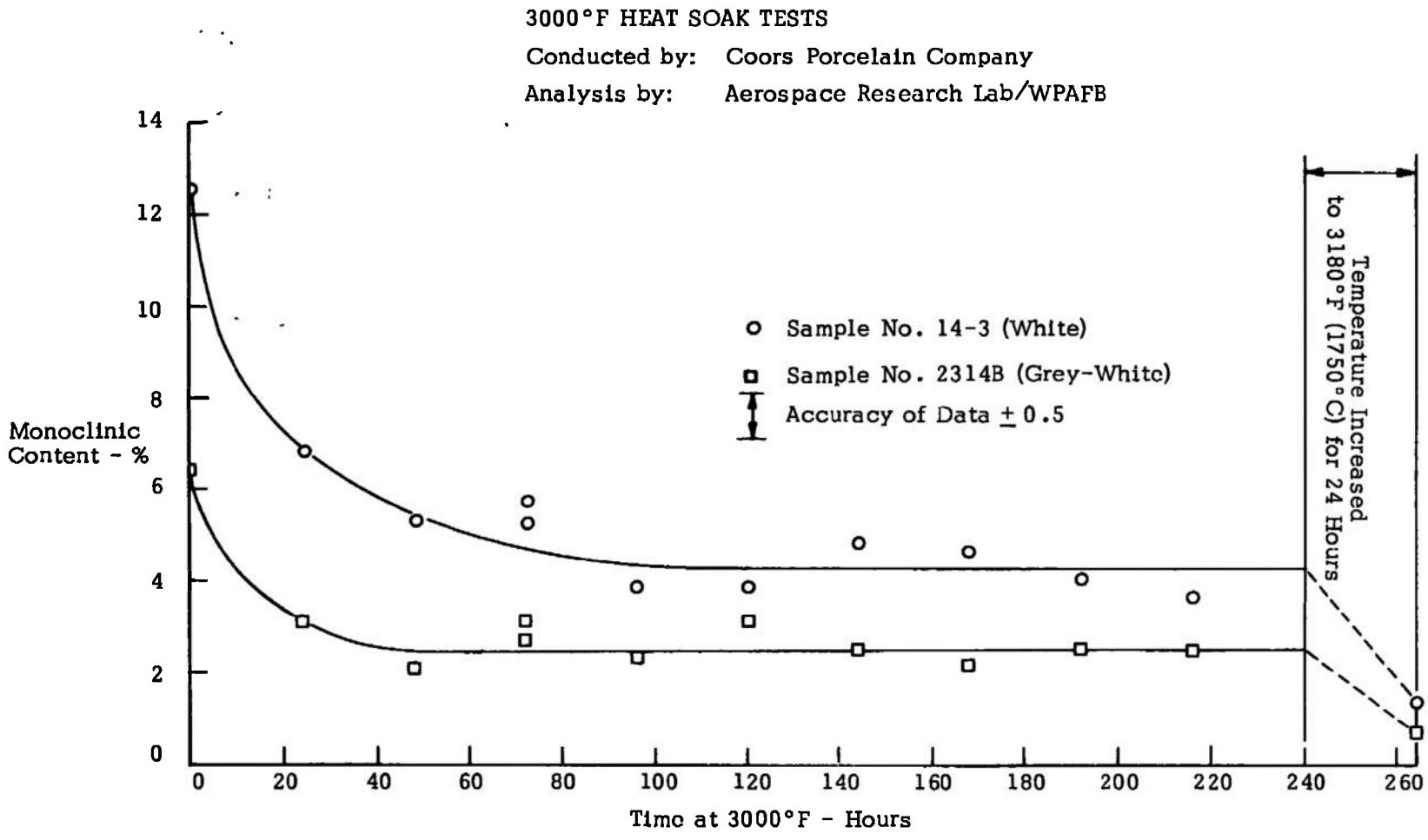

FIGURE 39. MONOCLINIC CONTENT OF SAMPLE OF 9.25 W/O YTTRIA-ZIRCONIA BRICK DURING FIRING AT 3000°F

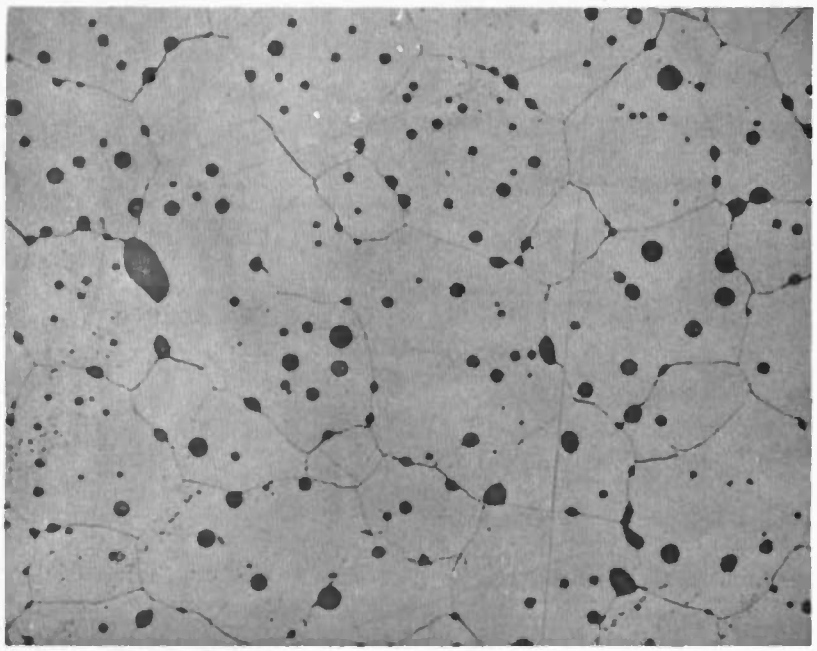

Unetched

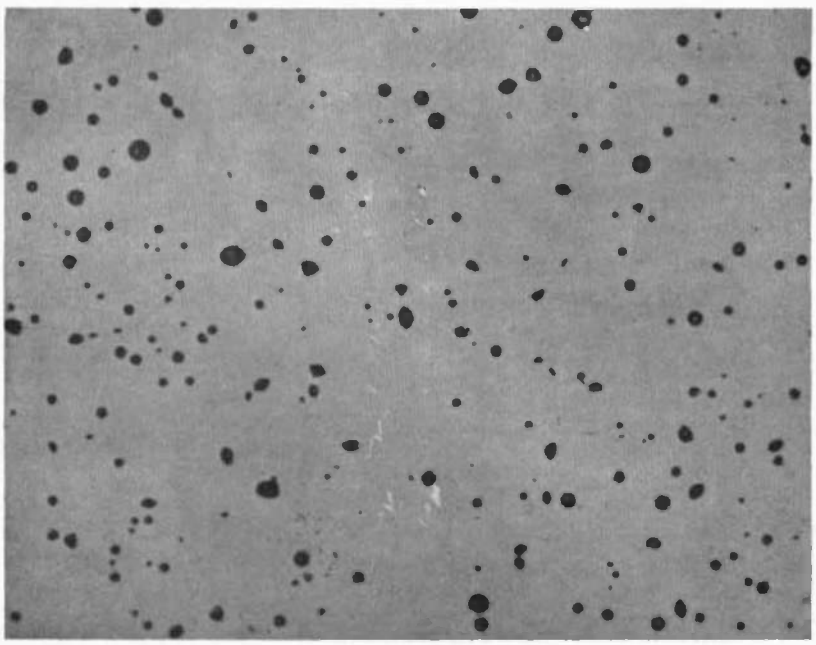

Etched

FIGURE 40. ORIGINAL 9.25 W/O YTTRIA-ZIRCONIA CORED BLOCK (SAMPLE 107) AFTER 96 HOURS AT 4000°F - MAGNIFICATION 200X

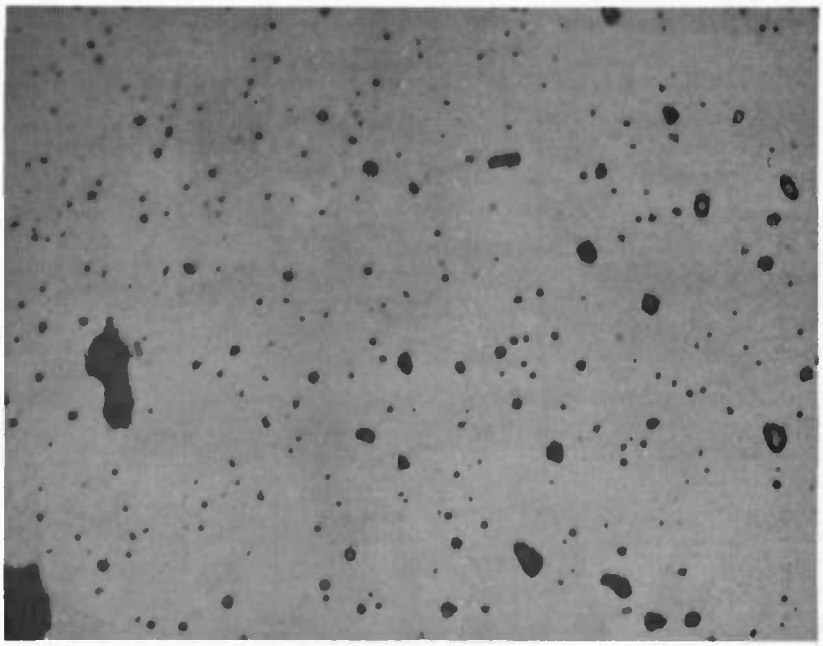

Unetched

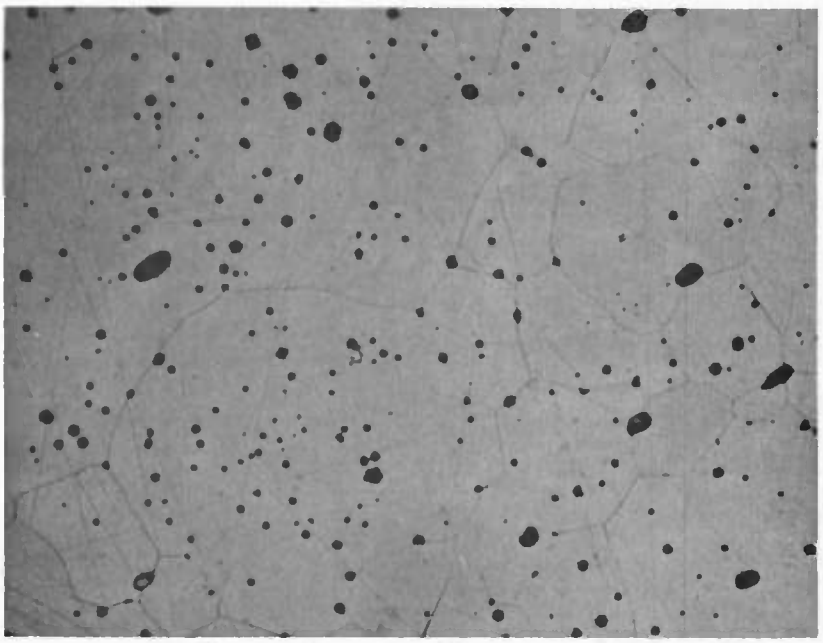

Etched

FIGURE 41. NEW 9.25 W/O YTTRIA-ZIRCONIA CORED BLOCK (SAMPLE 106) AFTER 96 HOURS AT 4000°F - MAGNIFICATION 200X

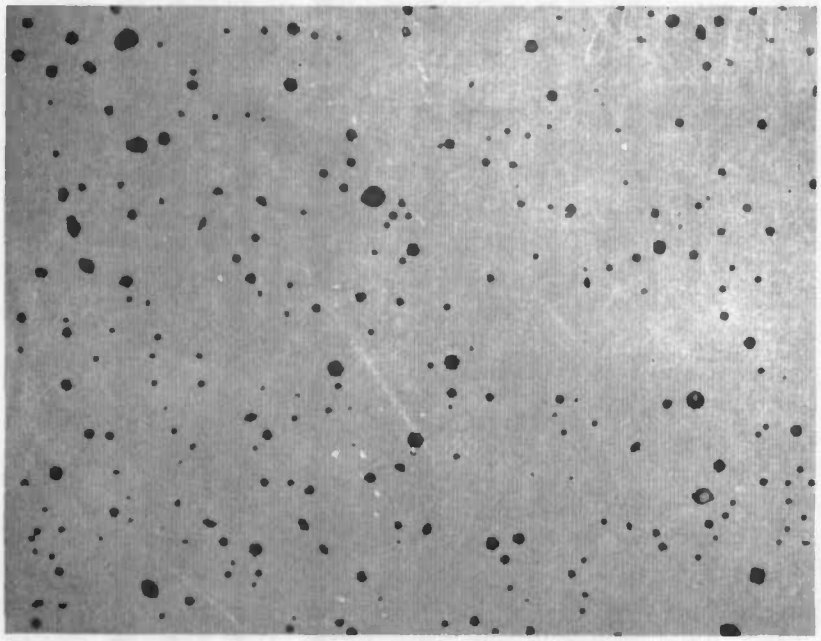

Unetched

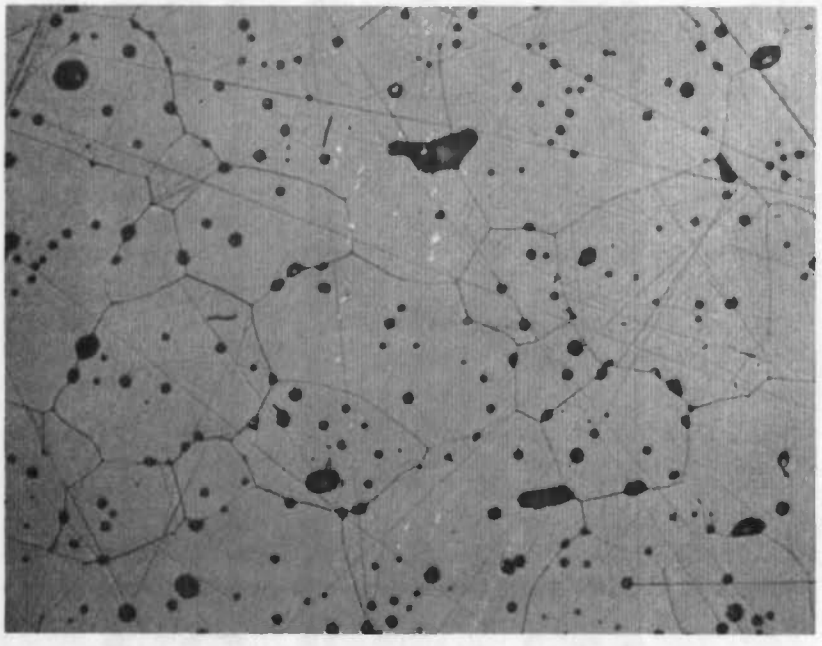

Etched

FIGURE 42. NEW 10.25 W/O YTTRIA-ZIRCONIA CORED BLOCK (SAMPLE 108) AFTER 96 HOURS AT 4000°F - MAGNIFICATION 200X

pores existing in the vicinity of grain boundaries. The pores were presumably removed by the sweeping grain boundaries. The samples were further examined at magnification as high as 500X in an unsuccessful attempt to identify cracking on a microscale.

The conclusion of these tests and analysis was that the 4000°F - 96 hour heat soak test had restored a large percentage of the useable strength to the previously destabilized, friable material.

In addition to the petrographic and x-ray analysis, a chemical analysis was performed on the destabilized yttria-zirconia cored block material prior to the 4000°F heat soak test. This analysis, performed by the AFML/WPAFB, revealed that the dispersion of yttria throughout the zirconia was very inhomogenous.

As mentioned previously the 9.25 weight percent yttria-zirconia material contained less than 5 percent monoclinic content as initially received from the manufacturer. It was found also that the yttria content throughout the block was more uniform indicating that portions of the block may be fully stabilized while others were not. Initial operation was also somewhat unusual in that four of the first 27 runs involved blowdown cycles during which the ceramics were force cooled through their inversion zone (i.e., cooled by blowdown air from temperatures above 2000°F to ambient).

Several differing hypothesis were set forth as to why the 9.25 weight percent material destabilized in the pilot heater. However, on several points, they were in agreement. In general they agreed that the yttria-zirconia blocks should be fully stabilized (i.e., devoid of any monoclinic content) and second, the heater should never be force cooled through the zirconia materials' inversion zone. Forced cooling of a zirconia storage heater below 2000°F is not forseen as a necessary operating condition, therefore, restricting blowdown to temperatures above 2000°F does not restrict the pilot heater's operating envelope. On the same basis the subsequent test program did not duplicate the initial operating conditions to determine if forced cooling below 2000°F was responsible for the destabilization problem encountered. Rather, additional test samples containing zero monoclinic content (produced by increasing the amount of yttria stabilizer) were installed in the heater and evaluated along with the original restabilized 9.25 weight percent yttria-zirconia under anticipated heater operating conditions.

A total of 85 cycles were made with the original material (58 cycles beyond the 4000°F - 96 hour heat soak test). Analysis of samples selected at various locations in the bed after Run 85 found no trace of monoclinic in the samples.

During the inspection of the ceramics following Run 85 it appeared that the strength of the yttria-zirconia cored blocks had been restored with the exception of the blocks in the vicinity of the alumina/zirconia interface. At this location some blocks were strong while others were quite friable. Monoclinic content was still present in the more friable blocks (~ 5%) but it should be noted that the strength of the blocks was adequate to hold them in position.

There was no indication that blocks had sagged or crushed to the point where air flow through the holes was restricted. There appeared to be no significant amount of surface abrasion or tendency for the material to dust with the exception of the blocks near the interface.

The alumina-zirconia interface reached a temperature, during the test program, that was adequate to reduce the materials' strength sufficiently to allow some deformation in the alumina cored blocks. A similar phenomena was not observed with the zirconia at the interface. Typically the interface temperature did not exceed 3000°F during the test program, however, during one operation upset the temperature did reach 3200°F. At temperatures less than 3000°F there appears to be no interface reaction problems between the alumina and yttria-zirconia.

Precise measurements were not made to determine if the yttria-zirconia had sustained any reheat shrinkage during the test program, however, reheat shrinkage of the material was not obvious during a close visual inspection.

7.3.3.1.2 Shape Related Factors

The dimensional tolerances specified on FluiDyne Drawing 7000-008 (Figure 29) and maintained during fabrication of the cored blocks were adequate to enable easy and satisfactory installation in the heater.

During the course of the test program a number of unkeyed blocks were installed on the top of the matrix. It was found extremely difficult to maintain good hole alignment during installation when the cored block were not keyed to one another. A new type of key was designed and included as an alternate in new material specification. This key design has the advantage of providing better alignment with the same dimensional tolerances because it extends to the outer edge of the block.

The thermal expansion gaps for the matrix provided during installation appeared to be adequate. There was no significant indication of cored blocks being crushed as a result of inadequate expansion allowance.

7.3.3.1.3 Material and Shape Related Factors

Two considerations which are important in determining a cored block's resistance to both the mechanical and thermal loads imposed on it, in a storage environment, are the material and the shape into which the material is fabricated. Mechanical stresses are generated by the force required to support a tall column of blocks, the forces produced in an externally restrained block by thermal expansion and the pressure forces imposed on a cored block during a high pressure blowdown cycle. The thermal stresses on the other hand are those generated by nonlinear temperature gradients leading to internally restrained nonuniform thermal expansion within individual cored blocks.

The mechanical loads generated in the individual blocks in a high column are typically quite small compared to the room temperature strength of the ceramic material. As the temperature is increased, however, the materials' strength decreases and eventually the column loads become significant. At high temperatures the brittle ceramic material can become plastic and experience hot load deformation, commonly termed creep. When comparing the creep parameters with the maximum temperature profiles typically established in the pilot heater it was found that creep, if it were to occur, would be expected in the upper few feet of the matrix. During this test program the cored block in the upper portion of the heater experienced temperatures up to 4000°F in excesses of 100 hours. During subsequent visual inspections there were no indications of high temperature deformation except on some of the coarse grained, lower density blocks at the top of the bed.

The mechanical loads due to external restraint of thermal expansion can be avoided by providing adequate gaps between adjacent blocks. Expansion gaps were provided during the initial installation. During inspection of the ceramics, at the completion of the test program, a number of blocks were found cracked and fractured. This cracking and fracturing was attributed to internal rather than external restraint of thermal expansion. Overall it appeared that the expansion gaps were adequate to prevent crushing of adjacent blocks and small enough to prevent any significant bypass flow channels.

During subscale tests a number of cored blocks were exposed to rapid pressurization and depressurization at room temperature. Under these tests, the blocks experience no structural degradation. Because of the high density (~ 95% of theoretical) and corresponding low porosity of the cored blocks installed in the pilot heater it was assumed that the cracking and fracturing observed was not a result of the high pressure loads imposed during heater blowdown.

Another important area in evaluating the cored blocks' performance is its resistance to the imposed thermal stresses. The cored blocks experience thermal stress loads during all phases of heater operation. The most important of these stresses are:

1. Tensile stresses induced around each hole during the storage heater blowdown cycle. These stresses are termed "web" thermal stresses because they occur in the web material between adjacent holes.

2. Stresses existing in the cored block due to nonlinear temperature distributions existing both across and along the cored block. The stresses induced by these temperatue gradients are termed "body" thermal stresses.

3. Stresses occurring at the top of the bed due to sudden heat loads from the reheat combustion process. This type of stress has been termed "thermal shock."

From the examination of material to date there has been no extensive indication of web stress damage. This result is not unexpected for two reasons. First, the approximate cooling rate at which cracking occurs in the yttria

stabilized zirconia cored blocks is about 40°F/sec determined during subscale tests. During heater operation the cooling rate has been limited to 20°F/second providing a safety margin of two. Secondly, this type of cracking, if it did occur, would be expected in the yttria-zirconia cored blocks nearest the interface between the alumina and yttria-zriconia material. The fracturing experienced by the material removed from this location in the heater was very extensive. The amount of fracturing which could be attributed to cooling, if any, was veiled by the destabilization problem encountered during the first 27 runs.

Figures 43 and 44 show four of the columns after their removal from the pilot heater. Figure 43 shows the top portion of the matrix (top to bottom from left to right) and Figure 44 shows the bottom portion of the zirconia matrix with the interface on the right. The short blocks on the left hand side of Figure 43 are the 12, 14 and 16 weight percent yttria-zirconia blocks installed in the heater following the 4000°F heat soak test. The blocks on the right in Figure 44 were quite weak, as mentioned in the last part of Section 7.3.3.1.1. In this instance it is difficult to separate what damage was due to thermal stresses and what was a result of the destabilization suffered during the first 27 runs. It should be noted that all the cored block holes were well aligned while the blocks were in the heater. Only after they were removed from the heater was the extensive fracturing, displayed in Figures 43 and 44, obvious. During the 85 run test program there was no significant increase in pressure drop across the matrix or excessive dusting that would have necessitated a facility shutdown.

Fracturing attributed to body thermal stresses was the most severe problem encountered during operation with the high density yttria-zirconia cored blocks, outside of the destabilization problem discussed in Section 7.3.3.1.1. Body stresses occur whenever nonlinear, axial or transverse temperature gradients exist across a cored block. Axial gradients are generated as the matrix is heated from the top by combustion products and transverse radial gradients are generated as heat is simultaneously lost from the heater vessel sidewalls. The destabilization suffered by the cored blocks during the first 27 runs hampered the interpretation of the body stresses and their correlation with the cracking and fracturing observed. Additional cored blocks were installed after Run 27 in the upper portion of the bed. During subsequent running, these blocks did encounter similar thermal stresses but did not undergo destabilization. The blocks have shown a variety of cracks which are very difficult to interpret. A particular crack pattern did emerge, however, with the dense ceramics which has also been observed on dense yttria-zirconia cored blocks in the NASA/Ames pilot heater. In both heaters the cored blocks displayed a tendency to fracture into shorter lengths. Examples of this are shown in Figures 45 and 46. One figure shows a 6-inch long block fracturing about 2-1/2-inches in from one end while the second figure shows a 3-inch block fracturing about 1-1/2-inches in from one end. This type of fracturing was evident on a number of blocks and was typically accompanied by several other cracks running at random through the blocks (Figures 43 and 44).

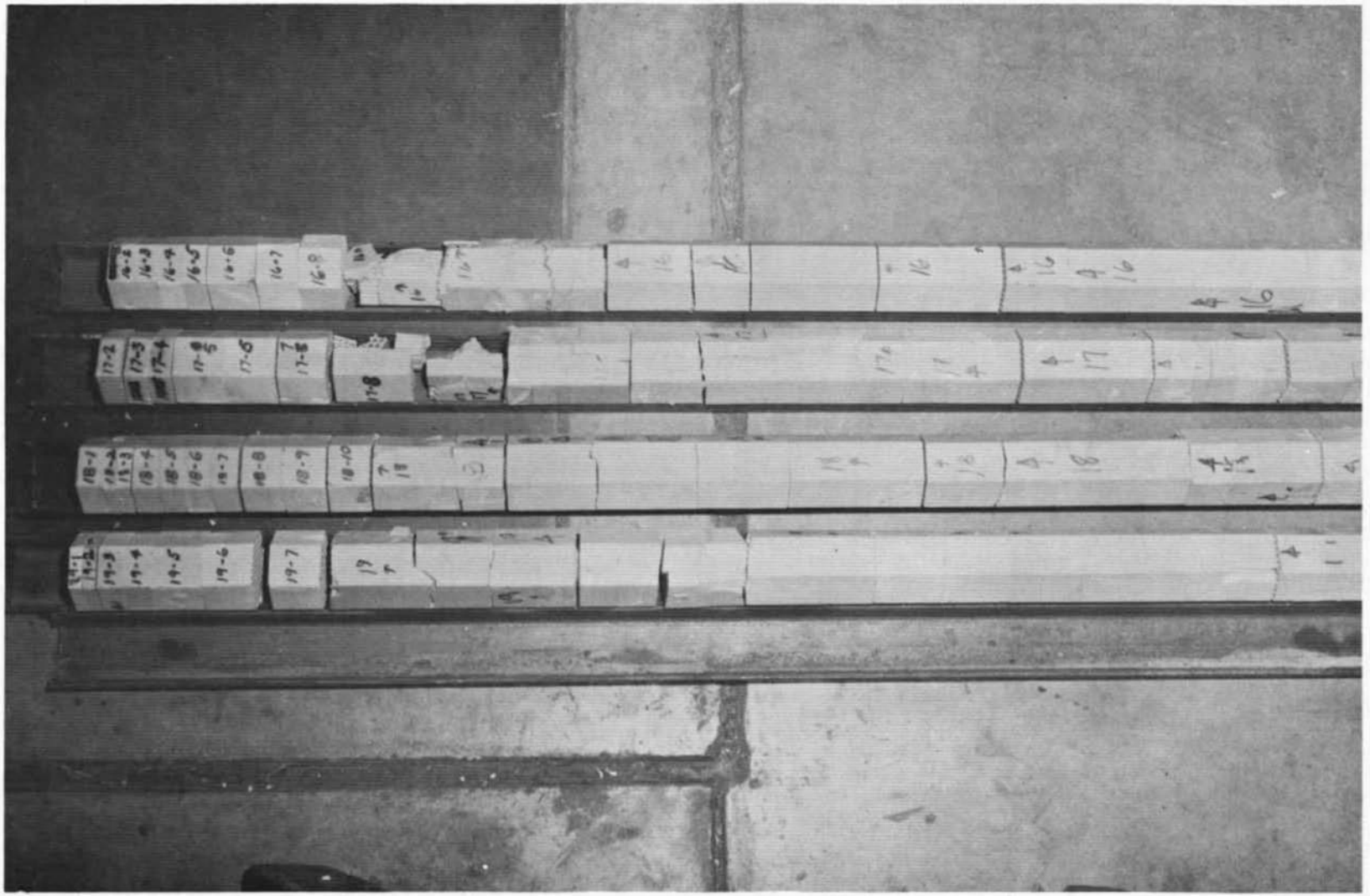

FIGURE 43. YTTRIA-ZIRCONIA CORED BLOCKS REMOVED FROM THE UPPER PORTION OF MATRIX AFTER RUN 85 - PILOT HEATER

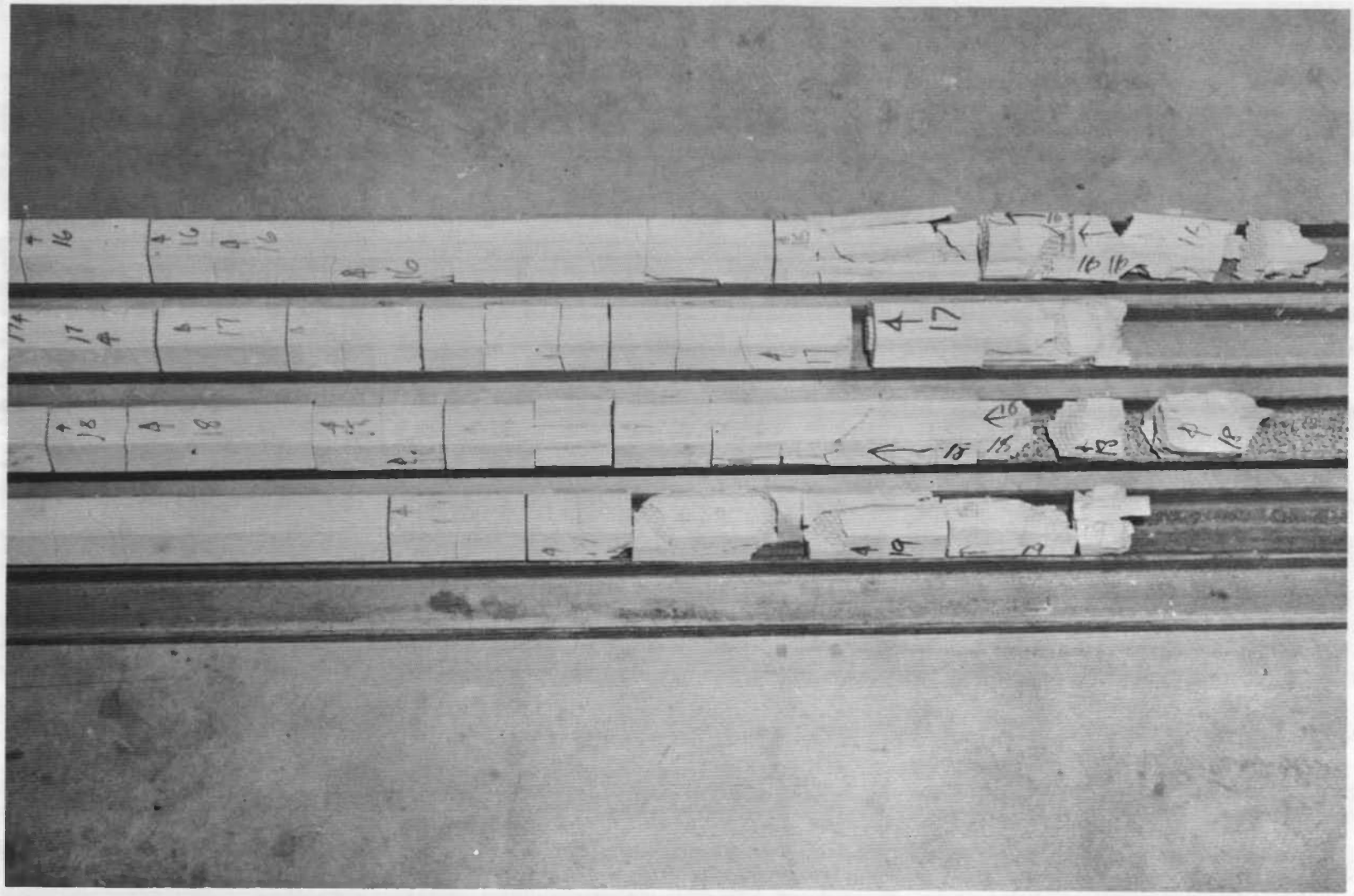

FIGURE 44. YTTRIA-ZIRCONIA CORED BLOCKS REMOVED FROM THE LOWER PORTION OF MATRIX AFTER RUN 85 - PILOT HEATER

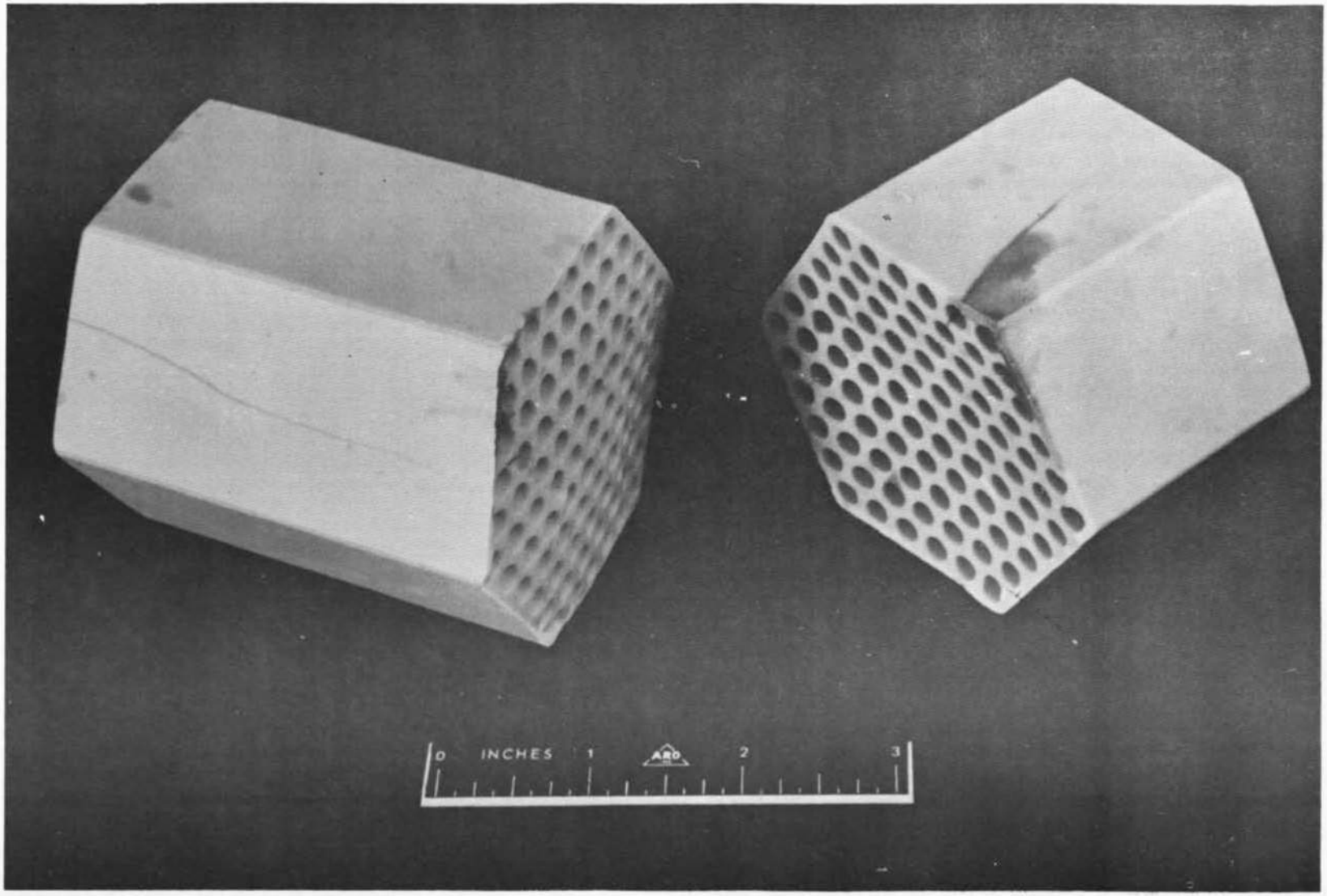

FIGURE 45. HIGH DENSITY CORED BLOCK REMOVED AFTER RUN 44 - PILOT HEATER

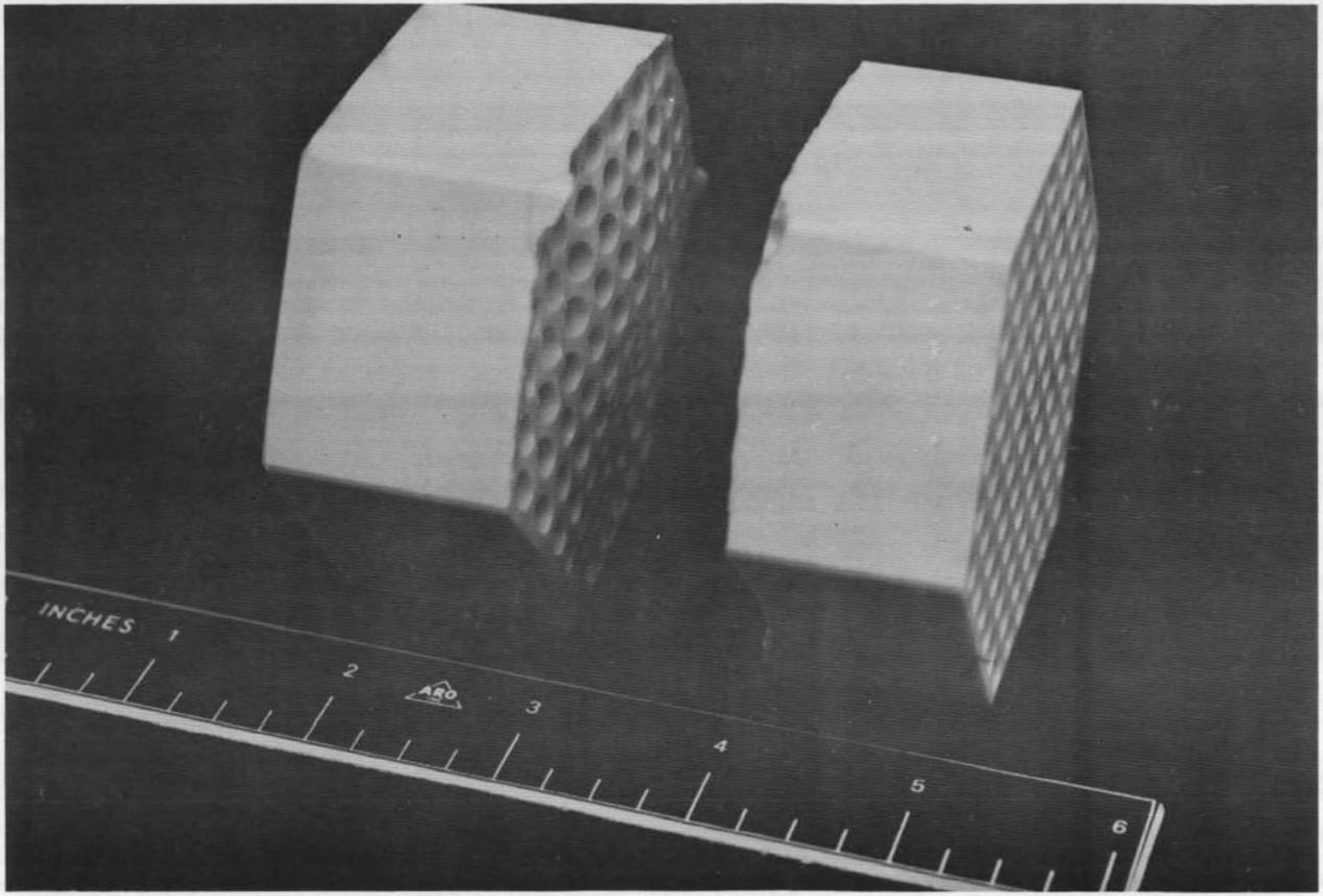

FIGURE 46. HIGH DENSITY CORED BLOCK REMOVED AFTER RUN 44 - PILOT HEATER

The effect of nonlinear temperature gradients can be reduced by decreasing the size of the block. From a design point, however, the size cannot be reduced without limit (Section 7.1.3.1.6). The width or flat-to-flat dimension of the block must be larger than the accumulated thermal expansion gaps plus the reheat shrinkage allowances. This consideration becomes more significant in a large heater. The long length on the other hand was originally thought desirable to avoid the potential for mismatch and the corresponding increased pressure drop. The long length also appeared as a useful means of reducing unit costs. The 9.25 weight percent yttria-zirconia blocks in the pilot heater were on the order of 8 to 10 inches in length. Comparing a 10-inch long block with the typical transient temperature profiles generated in the heater during the reheat cycle (Figure 47) it becomes apparent that the axial nonlinear temperature gradients can be quite severe. Severe radial temperature gradients can also exist due to heat loss out the side of the vessel. Temperature differences across the matrix center to side, can be as large at 600°F.

After examination of the cracked and fractured blocks removed from the heater, it appeared that a shorter block would suffer less thermal stress damage than the original long blocks. Furthermore, from the inspection it appeared that the optimum length was nominally 2-1/2-inches.

The third stress problem encountered in a storage heater is thermal shock. Thermal shock occurs in the upper portion of the heater as a result of sudden heat loads periodically imposed by the burner. The conditions typically occur during the initial ignition from ambient temperature and when returning to a reheat cycle following blowdown. Extreme thermal stress loads can also occur during unanticipated operational upsets. This problem was first identified in tests prior to operation of the pilot heater. It was found that the thermal stress loads to the matrix could be significantly reduced by placing a number of "sacrificial buffer layers" (i.e., short 1-inch long cored blocks) on top of the matrix. The pilot heater was initially designed with a minimum of three 1-inch buffer layers per column. Subsequent operation has shown three to be a minimum number and matrix cracking due to thermal shock could be further reduced by increasing this number of 1-inch buffer layers to about twelve.

7.3.3.2 High Density Zirconia - 12, 14, 12 Weight Percent Yttria

Following the destabilization problems encountered with the 9.25 weight percent yttria-zirconia material it was considered mandatory that any yttria-zirconia material used in the pilot heater matrix contain zero monoclinic. Analysis by AFML/WPAFB of the 9.25 weight percent yttria-zirconia material had disclosed the inhomogeneity of the material. Petrographic examination by ARL/WPAFB had also identified the presence of secondary phases within the material. The secondary phases were analyzed and found to be both deficient in yttria and consisted of a monoclinic solid solution. It was hypothesized that these phases could act as nuclei for the formation of additional monoclinic phase when exposed to the proper operating environment.

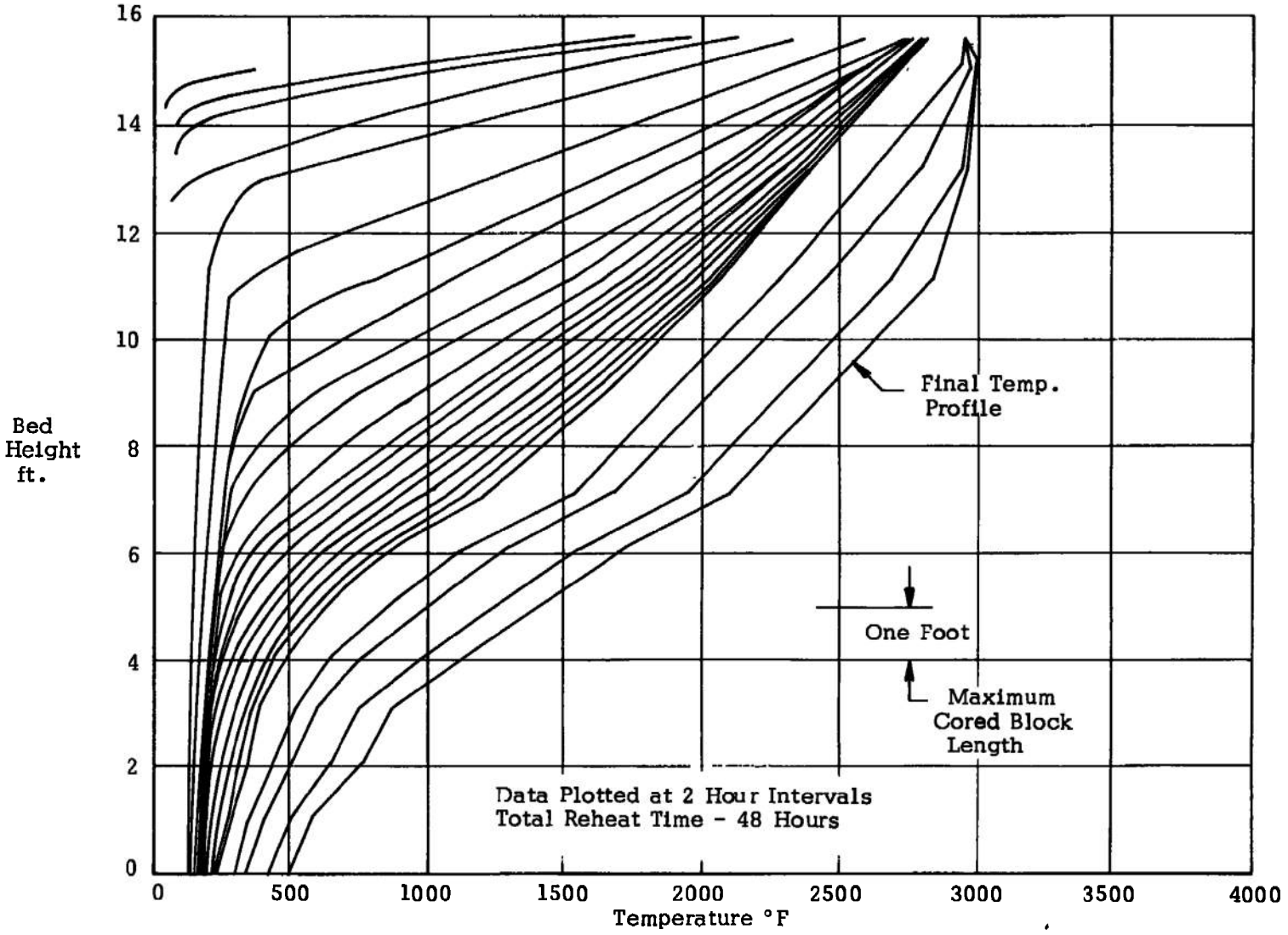

FIGURE 47. TEMPERATURE DISTRIBUTION THROUGH MATRIX DURING A HEATING CYCLE STARTING FROM ROOM TEMPERATURE (RUN 13) - PILOT HEATER

Cored blocks were also procured for a pilot heater at NASA/Ames shortly after the installation and prior to the operation of the pilot heater. To assure that the monoclinic content of the Ames blocks would be zero, the yttria content was increased to 10.4 weight percent. Following the destabilization problems with the 9.25 weight percent material, the 10.4 weight percent material was analyzed microstructurally and found to contain traces of secondary phase similar to that found in the 9.25 weight percent material supplied to AEDC. With these analysis as a basis, along with the requirement that monoclinic content be zero, small sample lots of zirconia cored blocks were procured with yttria contents of 12, 14 and 16 weight percent. Materials were procured from both Coors Porcelain Company and Zircoa Corporation. Coors supplied a number of high density zirconia cored blocks stabilized with 12, 14 and 16 weight percent yttria. Zircoa supplied both high density and low density yttria-zirconia cored blocks. The yttria content of the high density blocks were 11, 14 and 16 weight percent and that of the low density, 14 and 16 weight percent. The low density material is discussed in Section 7.3.3.3.

The test objectives for the pilot heater following the destabilization and subsequent resintering of the original 9.25 weight percent yttria-zirconia, were directed toward two goals; first to continue evaluation of the resintered material to determine its permanence of stability under heater operating conditions and; secondly, to seek additional information to form a basis for writing a material specification for successive procurements of yttria-zirconia cored blocks.

A number of high level yttria-zirconia cored blocks were installed following the 4000°F - 96 hour heat soak test, in the upper two feet of the matrix. The test program is summarized in Section 7.3.2.

X-ray diffraction analysis of the high yttria-zirconia samples after Run 85 have indicated an undetectable level of monoclinic content (i.e., less than 0.5%). In addition to the absence of monoclinic content, the material examined exhibited no loss in strength or abrasion resistance as compared with the "as manufactured" condition.

The dense higher yttria level blocks from both Coors and Zircoa experienced no significant amount of reheat shrinkage during the test program. The total time exposed to 4000°F temperatures, however, was less than 100 hours.

The majority of the blocks supplied by both Coors and Zircoa were in the 2 - 4-inch length range, considerably shorter than the initial 9.25 weight percent material initially installed in the pilot heater. The shorter blocks contained less cracks than the longer blocks. It was also observed that the longer blocks tended to fracture or crack into shorter length blocks; lengths on the order of 2-inches. The few blocks shorter than 2-inches that fractured were typically fractured in half in the axial direction.

Based on the tests with the higher level yttria-zirconia blocks, it appears that a stable zirconia cored block can be provided by increasing the level of yttria stabilizer and eliminating the monoclinic content. Furthermore, it appears that by reducing the length of the cored block to something on the order of 2.5-inches, while keeping the cross sectional dimensions the same, will significantly reduce the amount of cracking and fracturing experienced by the cored blocks.

7.3.3.3 Low Density Zirconias Stabilized with Increased Levels of Yttria

Low density yttria-zirconia cored blocks were also procured following the destabilization problem experienced with the 9.25 weight percent yttria-zirconia high density material (discussed in Section 7.3.3.2). The density level of these blocks was about 70 percent compared with the high density blocks which ranged from 90 and 95 percent of theoretical (theo = 6.0 gms/cc). The low density material was procured from the Zirconium Corporation of America in 14 and 16 weight percent yttria-zirconia compositions.

As discussed in Section 6.1.1, the crack initiation theory was used in designing with a dense ceramic for the matrix whereas the damage resistance criteria was used for the lower density material in the insulation. In designing with the damage resistance criteria the assumption is made that cracks will be initiated but the energy required to propagate them will be large tending to reduce the overall thermal stress damage. This would be the criteria used when designing with a low density material in the matrix of a storage heater. Owing to the damage incurred by the high density cored blocks during operational upsets and in some of the high stress regions of the matrix, a number of trial low density cored blocks were procured. Evaluation of the low density material took place in conjunction with the high density material in the pilot heater. This was accomplished by placing a few of the low density cored blocks alongside the high density blocks in the top portion of the heater.

Cored blocks of both 14 and 16 weight percent yttria-zirconia were installed in the heater, as shown in Figure 48 prior to Run 45. During the duration of the test program, these blocks were exposed to a total of 46 runs, reaching maximum conditions of 4000°F and 1850 psi. A complete visual examination of the blocks was performed following Run 85. During the test program the blocks changed in color from a yellowish-brown to a brillant white. The low density blocks experienced no fracturing during the test program, although one of the blocks did exhibit a few very tight hairline cracks.

One rather disturbing phenomena observed with the low density material was its tendency to deform under high temperatures. In one instance when a block was not resting uniformly on its supporting surface the material deformed until an adequate surface was in contact to support the load (Figure 49). As mentioned in Section 6.1.1.1, the strength of a ceramic is a function of its porosity.

$$S = S_o e^{-7p}$$

Therefore, it may be possible, by increasing the density into the 80-85% range, to reduce the deformation experienced with the 70% material and yet retain a sample that is relatively thermal shock and thermal stress resistant.

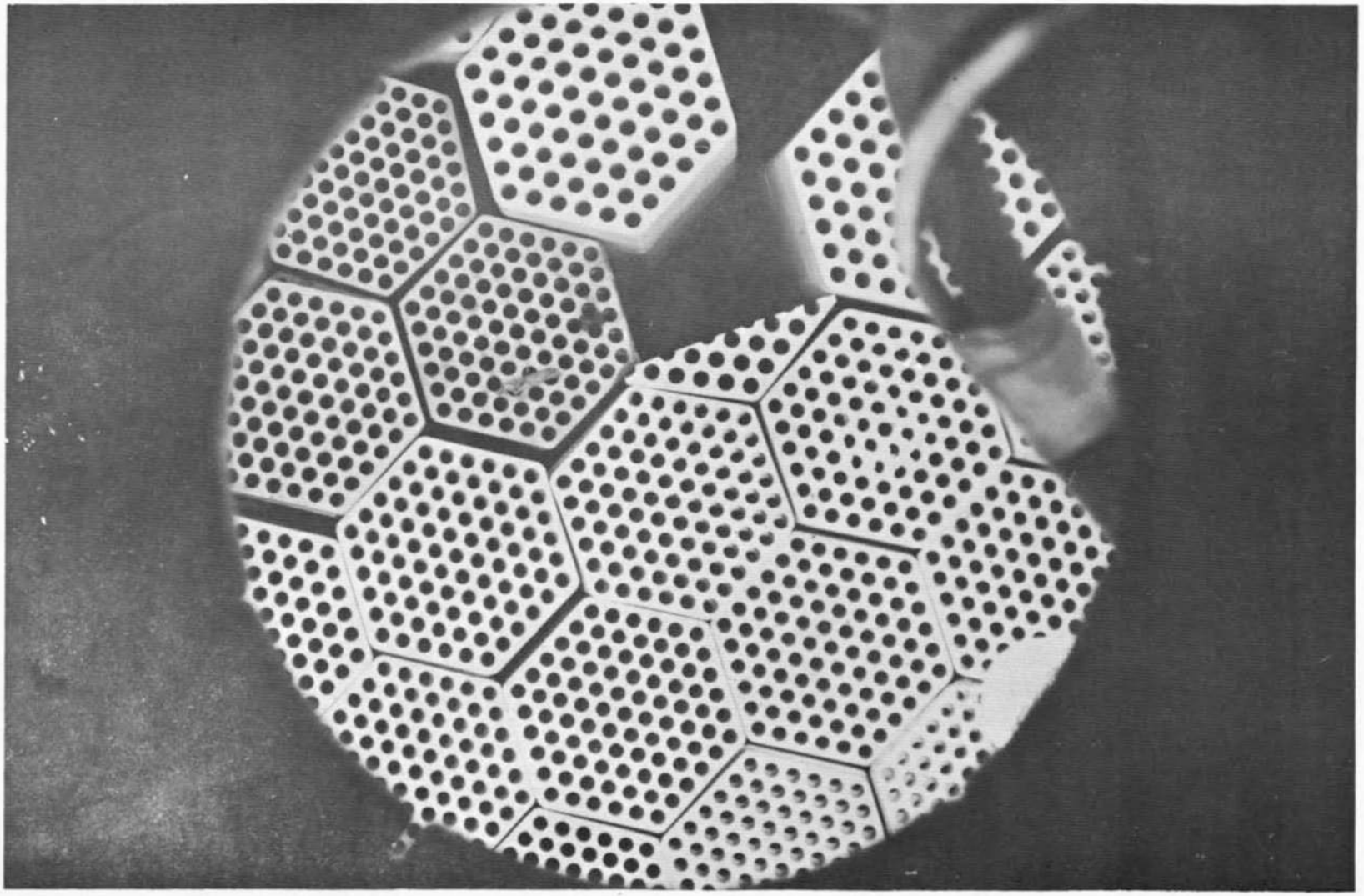

FIGURE 48. TOP OF MATRIX PRIOR TO RUN 45. (LOW DENSITY CORED BLOCKS ARE LOCATED IN UPPER PORTION OF PHOTO) - PILOT HEATER

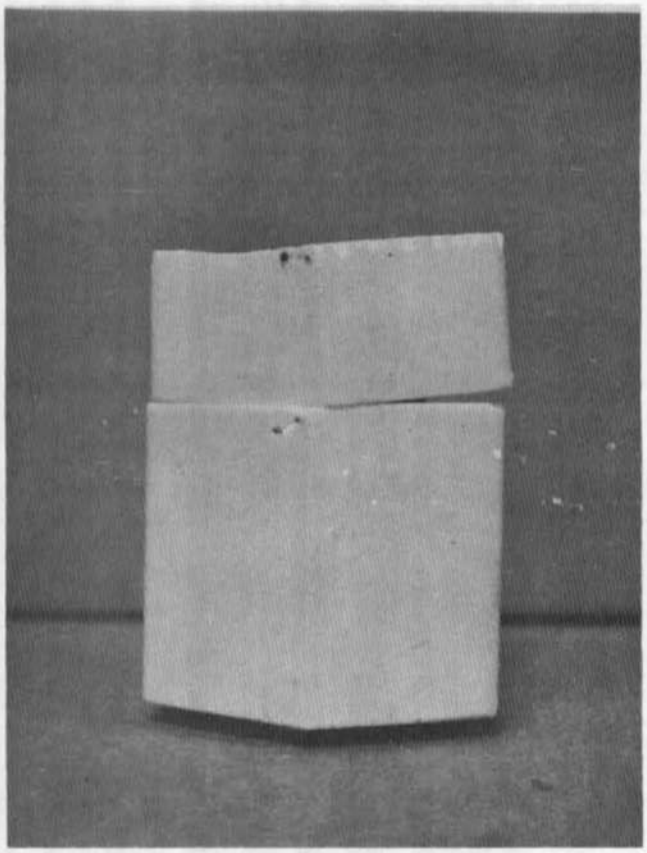

FIGURE 49. DEFORMATION OF LOW DENSITY YTTRIA-ZIRCONIA MATERIAL OBSERVED ON SAMPLES 11-3 AND 11-4 AFTER RUN 85 - PILOT HEATER

Although the data obtained on the low density material is quite limited, both in terms of samples tested and hours at temperature, it is quite encouraging. Additional testing may unveil the low density material as a usable alternative to the high density material in heaters, where lower mass flows per unit area can be tolerated.

7.3.3.4 Alumina

The alumina cored blocks were located in the bottom portion of the heater extending from the metal support grate up to the 7.5 foot level (Figure 21). The alumina blocks were produced by Coors Porcelain Company (Section 7.1.3.1.8). They were manufactured from a 99% pure alumina and possessed a fired density of about 95% of theoretical (theoretical density for alumina is 4.0 gms/cc). Due to their deep location in the bed, inspection of the alumina blocks was not possible until after Run 85 when the zirconia matrix was removed.

A close visual inspection disclosed a number of cracks and some fractures in the alumina. The blocks appeared to have suffered no reheat shrinkage or hot load deformation with the exception of the material in the immediate vicinity of the alumina/zirconia interface. The face of the alumina blocks, forming the interface, had taken on a slightly deformed appearance (Figure 50). The deformation, however, was not severe enough to cause any significant restriction of air flow through the matrix. This deformation has been attributed to an operational upset when the interface temperature exceeded the maximum of 3000°F and reached 3200°F. Judging from the conditions of the remaining alumina blocks there appears to be no significant deformation at 3000°F.

Approximately one foot of alumina blocks was removed. The condition most typical of the alumina cored blocks is shown in Figure 51.

The holes in the alumina matrix remained clear and aligned indicating there is no serious degradation of the alumina ceramics in the lower portion of the heater. The lodging of particles in the holes of the blocks shown in Figures 50 and 51 occurred during the removal of ceramics following Run 85.

Based on the inspection the condition of the alumina blocks appeared adequate to justify their remaining in the heater for the next test series. When new blocks are procured, for some subsequent test program, the replacement blocks would be reduced in length to the 2-1/2-inch range.

7.3.4 Performance of Insulating Material

The insulation material installed in the pilot heater was selected both on the basis of their thermal conductivity, maximum service temperature, and structural integrity. In a wind tunnel heater application it is important that the insulation provide adequate protection for the pressure vessel and, in the process, generate a very minimum of dust. The insulation installed in the pilot heater is described in Figure 21. The inner most layer of insulation exposed to the high temperature combustion gases is commonly termed the hot

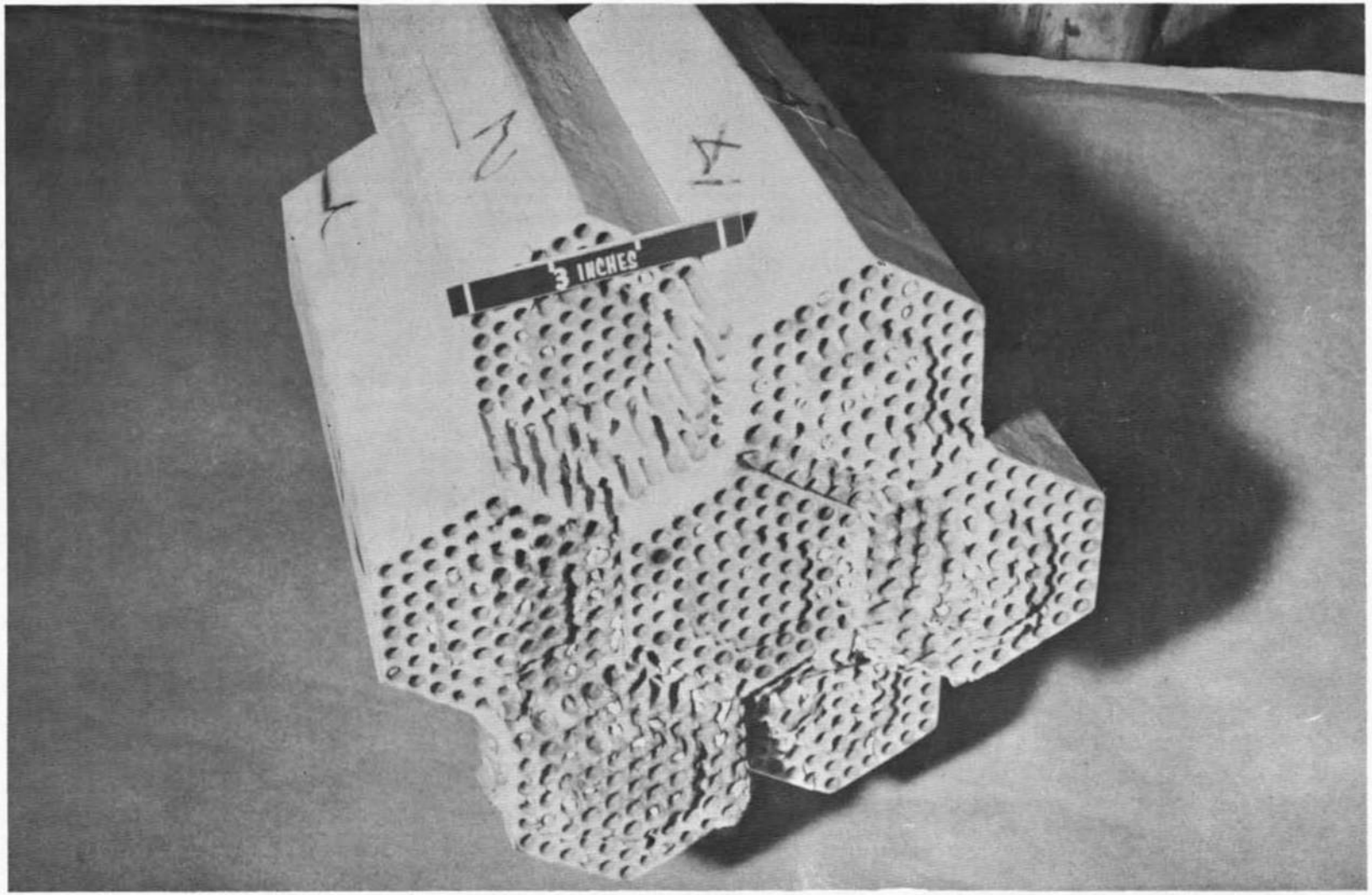

FIGURE 50. ALUMINA CORED BLOCKS REMOVED FROM THE CENTER OF THE MATRIX AT THE INTERFACE LEVEL AFTER RUN 85 - PILOT HEATER

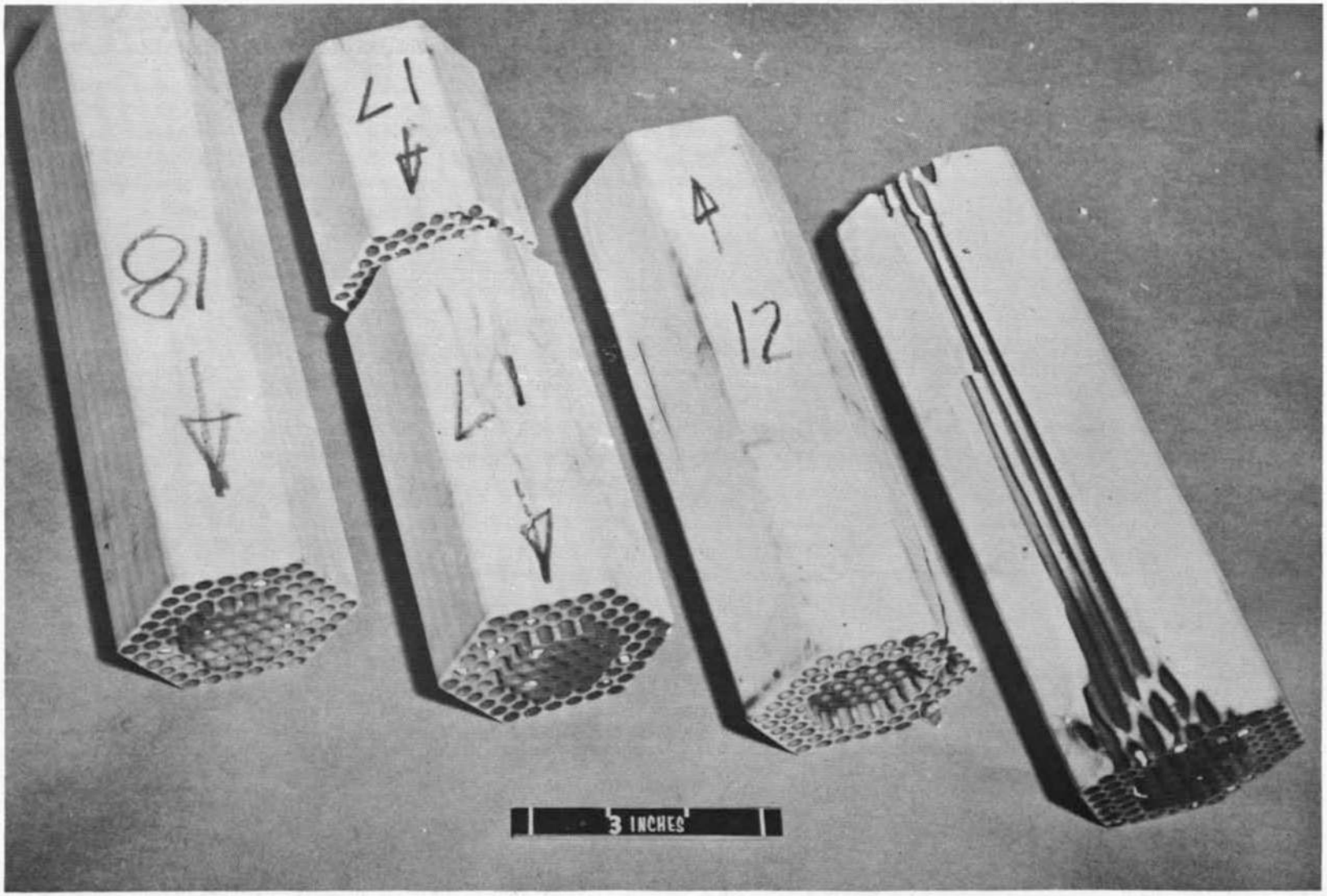

FIGURE 51. TYPICAL ALUMINA CORED BLOCKS AFTER RUN 85 - PILOT HEATER

liner. As illustrated in Figure 21, the hot liner material in the dome and outlet regions of the heater is an 8.5 weight percent yttria-zirconia (density between 250-280 lb/ft^3). The hot liner forming the cylinder above and around the matrix contains two compositions; two-thirds 8.5 weight percent and one-third 9.5 weight percent yttria-zirconia. In the combustion chamber all light weight 8.5 weight percent yttria-zirconia insulating material (density between 150-180 lb/ft^3) was used.

7.3.4.1 Combustion Chamber Hot Liner

Inspection of the light weight combustion chamber blocks during the various inspection intervals found material spalling from the front face of the blocks. The degradation was severe enough to warrant their replacement after Run 37. The light weight material had been specified for this location because of the minimum exposure to hot combustion products and the lower mechanical loads the light weight material would impose on the dome structure.

Failure of the light weight material was attributed to the rapid change in temperature which the front face would experience during heater pressurization. During the reheat cycle, the front face of the light weight combustion chamber blocks viewed the cool metal surface of the burner. During reheat this surface would operate at about 200°F. During the pressurization cycle, however, blowdown air at temperatures about equal to the bed temperatures was forced into the annulus between the burner and the ceramics, raising the temperature further from compressive heating as the air pressure went from ambient up to 2000 psi. This high temperature, high pressure air imposed a severe thermal load on the light weight refractories in this area. The heat load was adequate to spall the front surface of the ceramics. Spalling in this area is very undesirable because the resulting fragments fall directly onto the matrix where they may be blown out of the heater in the form of dust during subsequent blowdown cycles.

The light weight material was replaced by a higher density 8.5 weight percent yttria-zirconia material in the 250 to 280 lb/ft^3 range. This material was the same as that used in the dome region of the heater. The denser material remained in the heater from Run 37 to Run 69. During this period it did not experience any spalling or fracturing. Following Run 69, the first generation burner was replaced with the second generation burner.

In terms of the combustion chamber refractories the major difference between the first and second generation burner was the replacement of the metal, water cooled combustion chamber of the first burner with a refractory lined combustion chamber. The diameter of the second burner was slightly smaller than the first. Consequently, a new set of combustion chamber refractories were designed, procured and installed.

The new refractories were procured in an 8.5 weight percent yttria composition and installed prior to Run 70. Inspection of these refractories following Run 85 found no indications of fracturing or spalling. Tight cracks were visible about 1-inch in from the hot face on the blocks in the lower

portion of the combustion chamber that were exposed to the reacting gases. The surfaces exposed to the products of combustion possessed a bleached appearance indicating a loss of impurities.

7.3.4.2 Dome Hot Liner

The dome hot liner refractories were an 8.5 weight percent yttria-zirconia composition. These refractories were installed at the beginning of this test program and remained in position during the entire 85 runs. Inspections performed midway through the test program found some of the blocks extending in toward the heater centerline. This was an indication that the blocks had fractured at some location about halfway through the block allowing the front portion to fall out of position. Removal of the dome material after Run 85 established that nearly every dome brick was fractured at the tongue and groove location (Figures 52 and 53). The strength of the blocks after Run 85 was essentially unchanged from the "as manufactured" condition. X-ray analysis performed on the material at the fracture plane revealed essentially no monoclinic. The blocks "as manufactured" contained an undetectable level of monoclinic.

It is uncertain at the present time as to why the dome refractories have suffered such severe deterioration. Several hypotheses have been set forth but as yet have not been substantiated. Additional analyses are presently underway which may give additional insight into the problem. Despite the severe deterioration experienced by the dome ceramics, the heater remained operational. The dome refractories must, however, be replaced for the next test series in the pilot heater.

7.3.4.3 Matrix Hot Liner

The matrix hot liner comprises the insulation material immediately adjacent to the matrix. In the pilot heater installation, the hot liner consisted of four different materials:

1. 8.5 weight percent yttria-zirconia.
2. 9.5 weight percent yttria-zirconia.
3. Calcia-zirconia, fully stabilized.
4. Alumina.

The yttria-zirconia was located in the upper portion; the calcia-zirconia in the mid portion; and the alumina in the lower portion of the heater (Figure 21).

After Run 85, the yttria material was cracked and in several instances fractured in the tongue and groove region (Figure 54). The cracking and fracturing was most predominant in the region above the top of the matrix and

FIGURE 52. 8.5 W/O YTTRIA-ZIRCONIA HOT LINER DOME INSULATION AFTER RUN 85 - PILOT HEATER

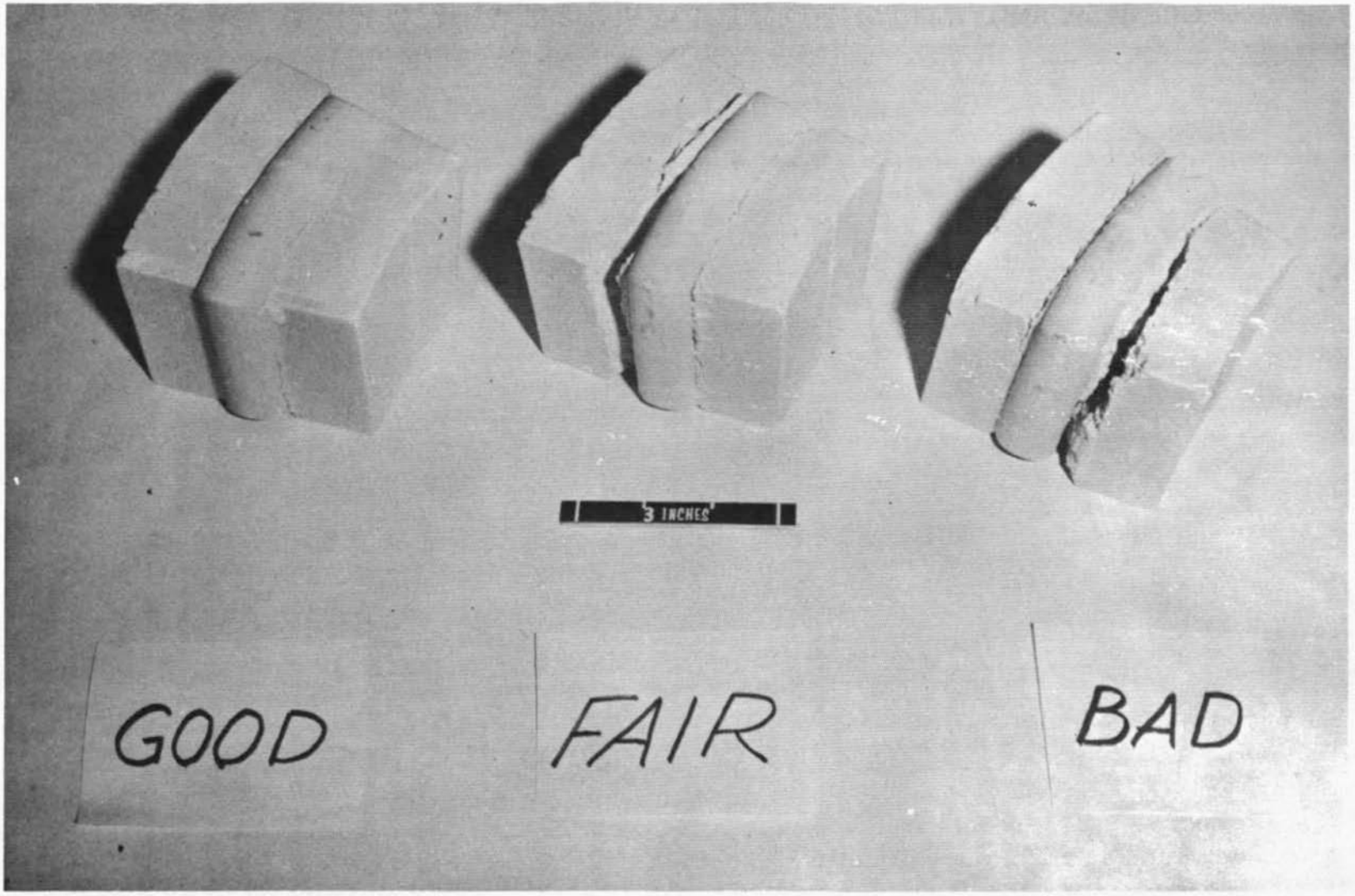

FIGURE 53. TYPICAL 8.5 W/O YTTRIA-ZIRCONIA DOME HOT LINER REMOVED AFTER RUN 85 - PILOT HEATER

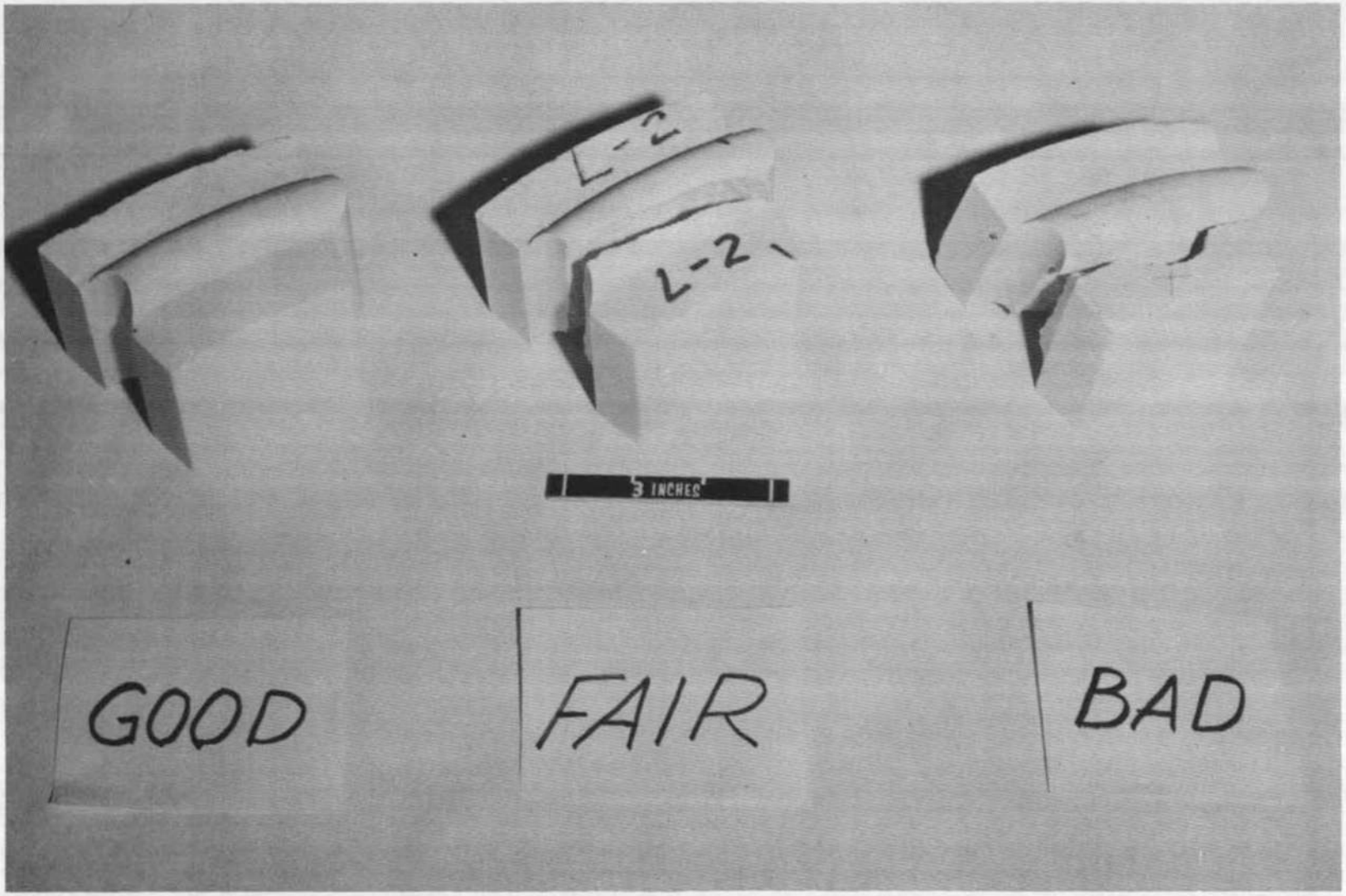

FIGURE 54. YTTRIA-ZIRCONIA MATRIX HOT LINER REMOVED AFTER RUN 85 - PILOT HEATER

gradually decreased in severity until at approximately one foot below the top surface of the matrix the cracking disappeared. The strength and abrasion resistance of the blocks appeared to remain unchanged although no quantitative measurements were made. X-ray diffraction analysis were made at various locations in the block but failed to detect any monoclinic content.

The calcia-zirconia experienced a considerable amount of fracturing. The material appeared to have suffered no loss in strength or abrasion resistance or any significant amount of destabilization during the 85 run test program. The nature of the fracturing (Figure 55) indicates an inadequate amount of room was provided for thermal expansion such that the resulting mechanical forces were sufficient to fracture the blocks.

The inspection following Run 85 did not proceed down past the calcia-zirconia bed liner blocks. Consequently, the alumina matrix hot liner blocks were not inspected. There is no indication, however, that these blocks have deteriorated. From past experience with other heaters these blocks are exposed to a relatively mild thermal environment and as a result typically suffer no deterioration.

7.3.4.4 Heater Outlet and Stilling Chamber

The refractories forming the hot heater outlet and stilling chamber were fabricated in an 8.5 weight percent yttria-composition. The outlet was comprised of an inner and backup outlet, each consisting of four pieces (Figure 21). The stilling chamber was made up of discrete rings. The outlets as well as the stilling chamber rings suffered no apparent loss in either strength or abrasion resistance. The outlets did contain a number of tight hairline cracks but sustained no fractures. The outlet rings fractured into two and in some cases three separate pieces. This is not unexpected when a solid ring of brittle material is heated on its inner surface only. In future installations it would be useful to saw a gap along one of the radii in an axial direction to accommodate the thermal expansion. These refractories could be reinstalled for the next test program.

7.3.4.5 Backup Insulation

The backup insulation consisted of a number of different materials ranging from a light weight calcia-zirconia behind the dome in the upper portion of the heater to a 2600°F firebrick at the base of the heater. The various materials and their location in the heater are described in Figure 21.

The insulation behind the dome was constructed such that it rested on the back side of the dome. The thermal expansion of both the dome and the backup insulation was accommodated by providing a gap between the backup insulation and the heater vessel. This gap was loosely filled with alumina-silica ceramic fiber.

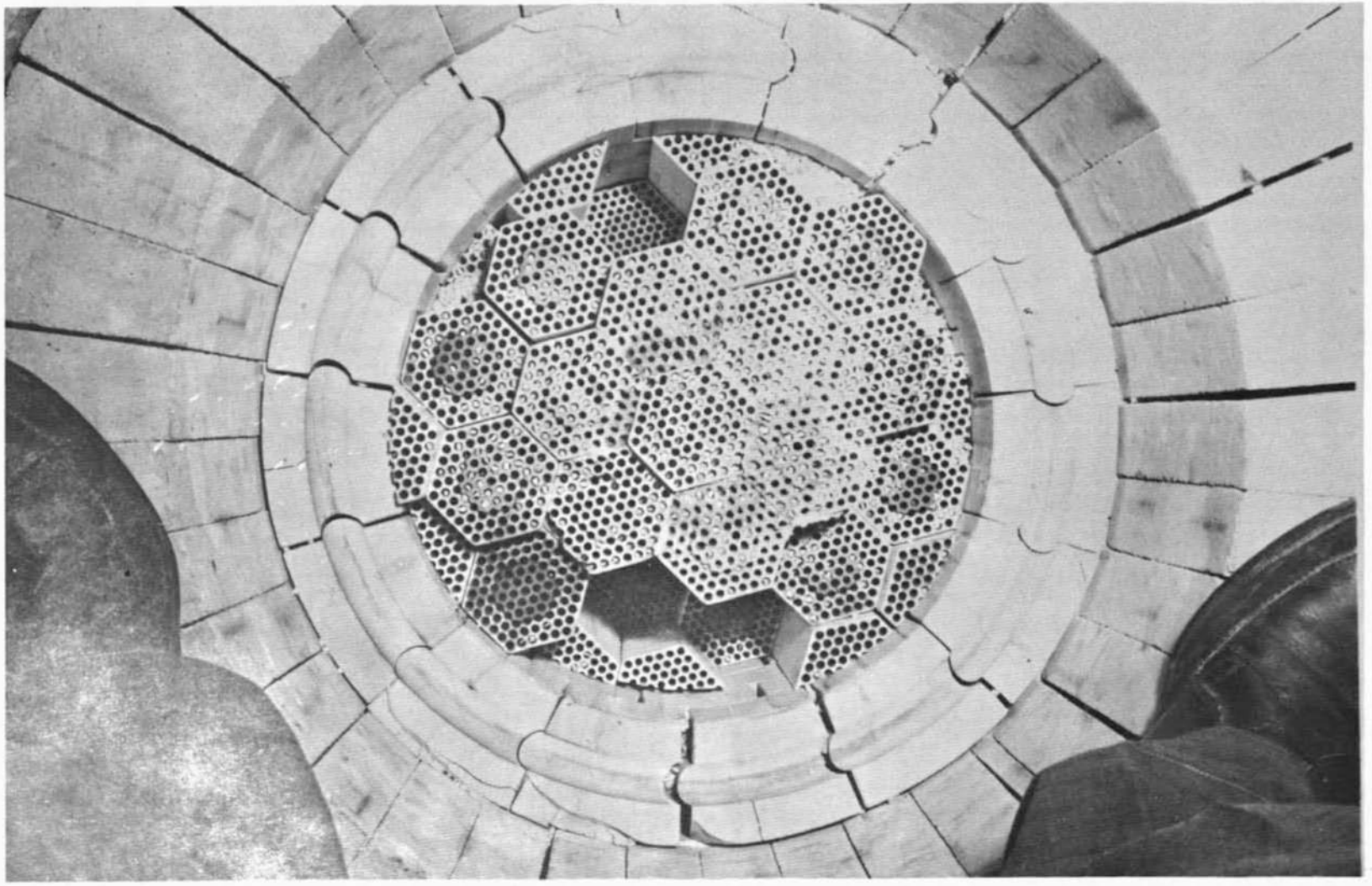

FIGURE 55. FULLY STABILIZED CALCIA-ZIRCONIA MATRIX HOT LINER AT THE ALUMINA/ZIRCONIA INTERFACE AFTER RUN 85 - PILOT HEATER
(NOTE: The plugging of cored block holes occurred during the ceramic removal after Run 85.)

The light weight insulation material used behind the dome did experience large amounts of fracturing (Figure 56). The material, however, did not appear to lose strength or destabilize. It appeared, during the inspection, that this problem could be significantly reduced by redesigning the backup insulation as a self supporting structure.

The backup insulation behind the matrix liner and above the shelf consisted of the same material. This material also suffered some fracturing and crushing from inadequate allowance for thermal expansion (Figure 57).

The backup insulation below the shelf displayed no signs of deterioration with the exception of the material in the vicinity of the side viewports and immediately under the shelf. The temperatures in these locations appeared to have exceeded the maximum service temperatures of the material. These areas should be redesigned prior to the next installation.

7.3.4.6 Shelf Insulation

The metal shelf located in the upper portion of the heater provides a support for the dome refractories and eliminates the large accumulative expansion which would occur if the entire structure was supported from the base of the heater (Figure 21). To prevent the shelf from overheating, it is surrounded by special insulating shapes and is wrapped with several layers of alumina-silica ceramic fiber. During the inspection of the shelf, following Run 85, it was evident that the shelf fiber insulation had been overheated on the underside. This was also evidenced by excessive thermocouple temperature readings during the high temperature 4000°F runs.

This problem will be solved by adding more insulation and redesigning the insulation thermal expansion gaps in the vicinity of the shelf.

7.3.5 Performance of Heat Generation System

During the first test program in the AEDC pilot heater, two burner concepts were evaluated. Both were premix designs using metal water cooled walls, but differing in other design areas. The major design differences between the first and second generation burner were:

1. Change from a water cooled to a refractory lined combustion chamber.
2. Change from gold plated zirconium copper to high grade stainless steel construction.
3. Reduce maximum mass flow from 1000 to 500 lb/hr.

The second generation burner contained a number of additional refinements based on operating experience gained with the first burner concept.

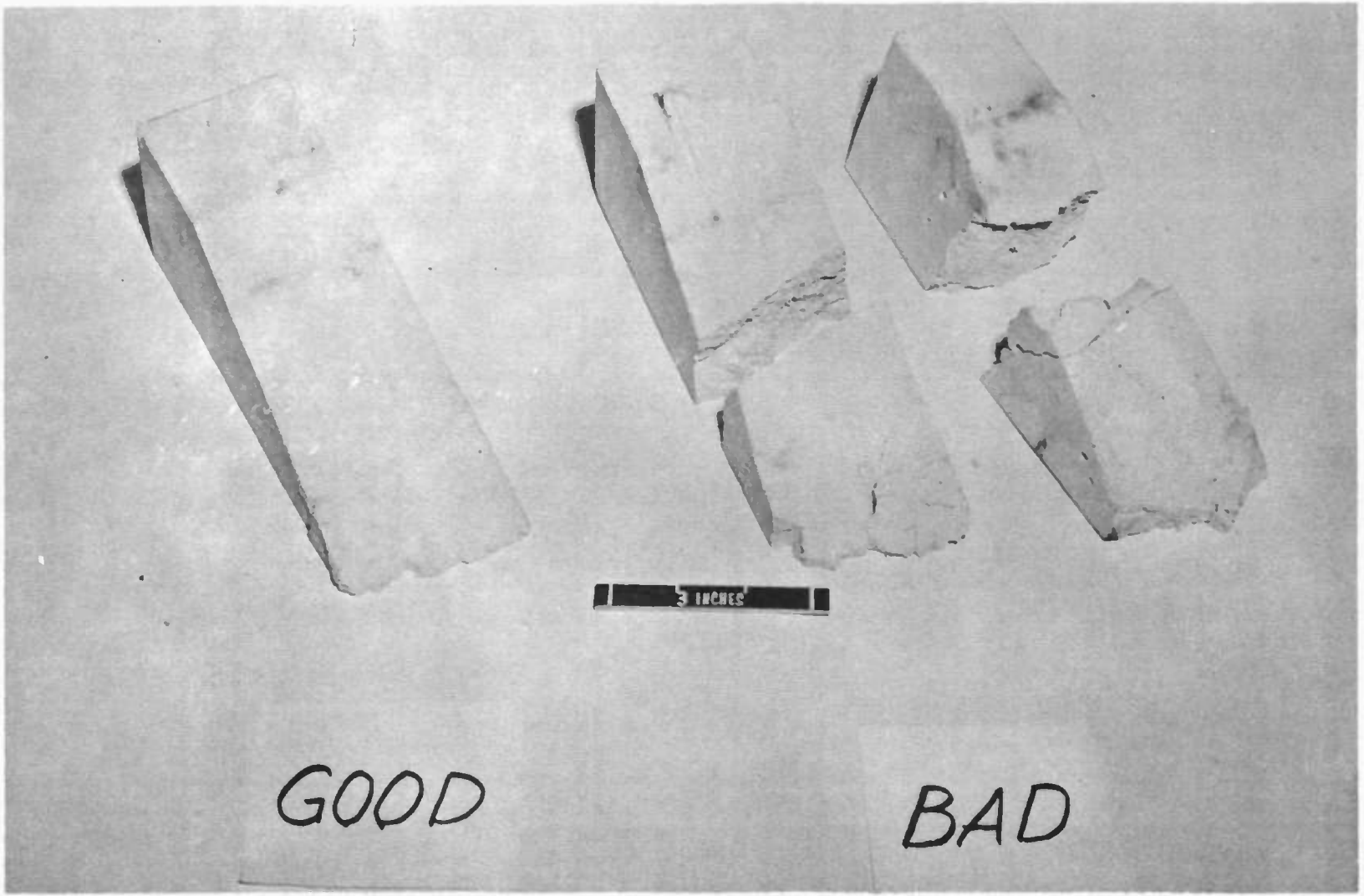

FIGURE 56. FULLY STABILIZED, LIGHTWEIGHT CALCIA-ZIRCONIA DOME BACKUP INSULATION REMOVED AFTER RUN 85 - PILOT HEATER

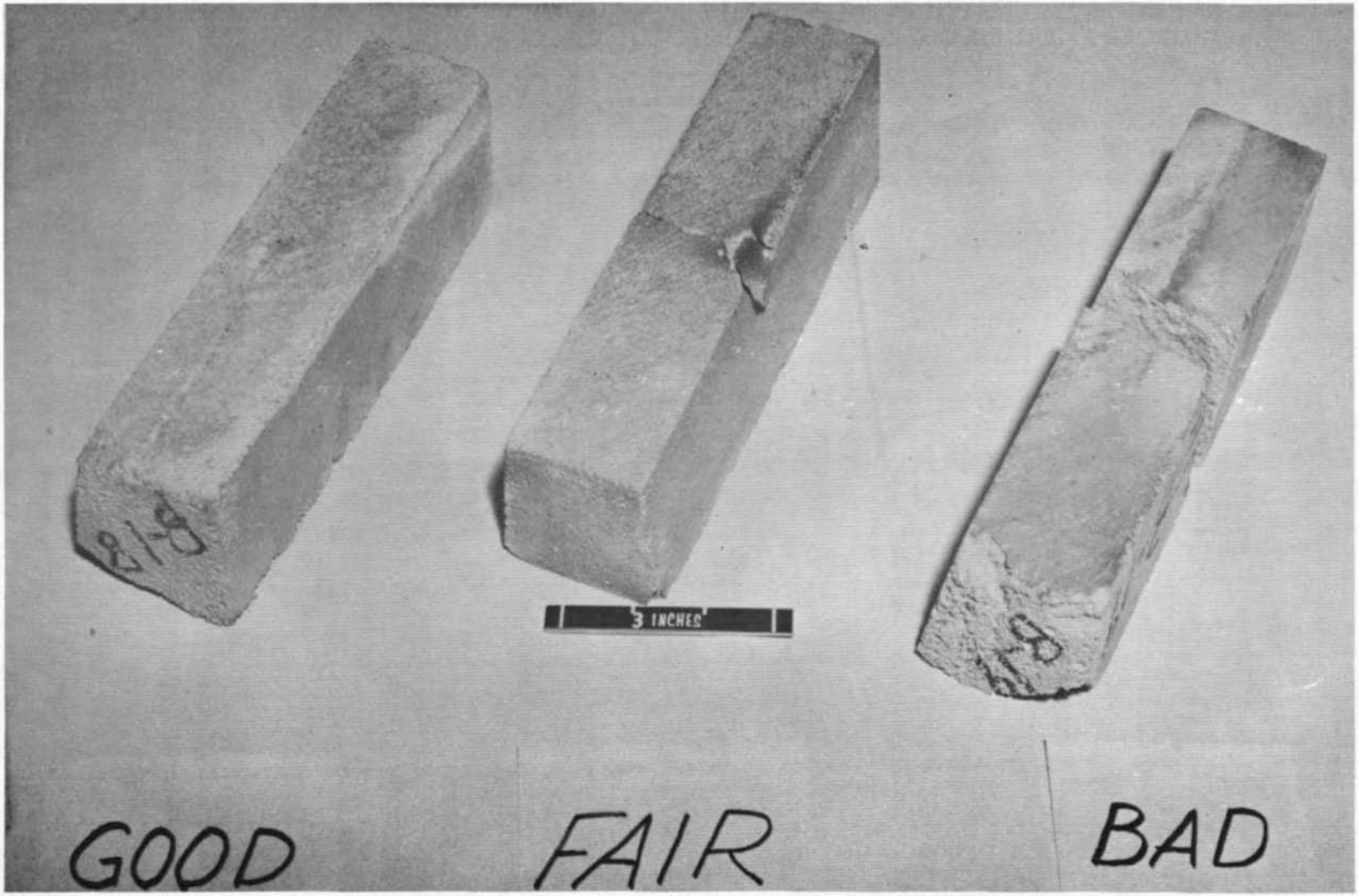

FIGURE 57. FULLY STABILIZED, LIGHTWEIGHT, CALCIA-ZIRCONIA BACKUP INSULATION REMOVED AFTER RUN 85 - PILOT HEATER

7.3.5.1 First Generation Burner

The first generation burner was installed and used during the first 69 runs in the AEDC pilot heater test program. Its performance was quite satisfactory in that the desired temperature profiles could be established in the heater. The major problem that arose with the first generation burner and eventually lead to its being discarded was corrosion.

The design of the first generation burner employed a water cooled, metal combustion chamber. The need for a metal combustion chamber stemmed from the deterioration and frequent replacement experienced with calcia-zirconia combustion chambers in previous storage heaters. An effort to eliminate the refractory problem was attempted with the first generation burner by providing a metal, water cooled combustion chamber incorporated as part of the burner. The material used for the walls of the combustion chamber in the first generation burner was zirconium-copper because of its high heat transfer capability. The material used for the injector head was nickel. All of the areas exposed to reacting combustion products were plated with gold to provide a corrosion barrier.

Following the 4000°F heat soak test, corrosion was observed on the combustion chamber walls (Figure 58). The burner was repaired by rebuilding the surface with copper plate, machining and replating with gold. addi-tional runs and repairs were made. In general, it appeared that corrosion was almost insignificant at temperatures below 3000°F, however, above 3500°F the corrosion became quite severe. It was concluded that the major factor contributing to the burner corrosion problem was the nitric acid generated by the combustion process. Secondary corrosion problems may have been galvanic corrosion within the copper-nickel-gold system.

Operation continued with the first generation burner through Run 69 during which the burner began leaking. Up to that point in the test program, the burner had been repaired several times and its operation restricted to maximum temperatures and pressures of 3500°F and 1000 psi. A design was underway at that time for a second generation burner, consequently, the decision was made to retire the first burner from service and delay the test program until the second generation burner was available.

7.3.5.2 Second Generation Burner

The design for a second generation burner was initiated under a separate contract with FluiDyne Engineering Corporation (AF Contract F40600-70-C-0009). The design was completed by FluiDyne and fabrication carried out by ARO/AEDC.

The primary criteria for the design of a second generation burner was to use to the maximum extent possible corrosion resistant materials. The design evolved with a stainless steel burner employing the original premix and high pressure concepts plus a modified mixer design and the use of a hot refractory combustion chamber. Stainless steel was used for the burner and a 9.25 weight percent yttria stabilized zirconia was used for the refrac-tory combustion chamber.

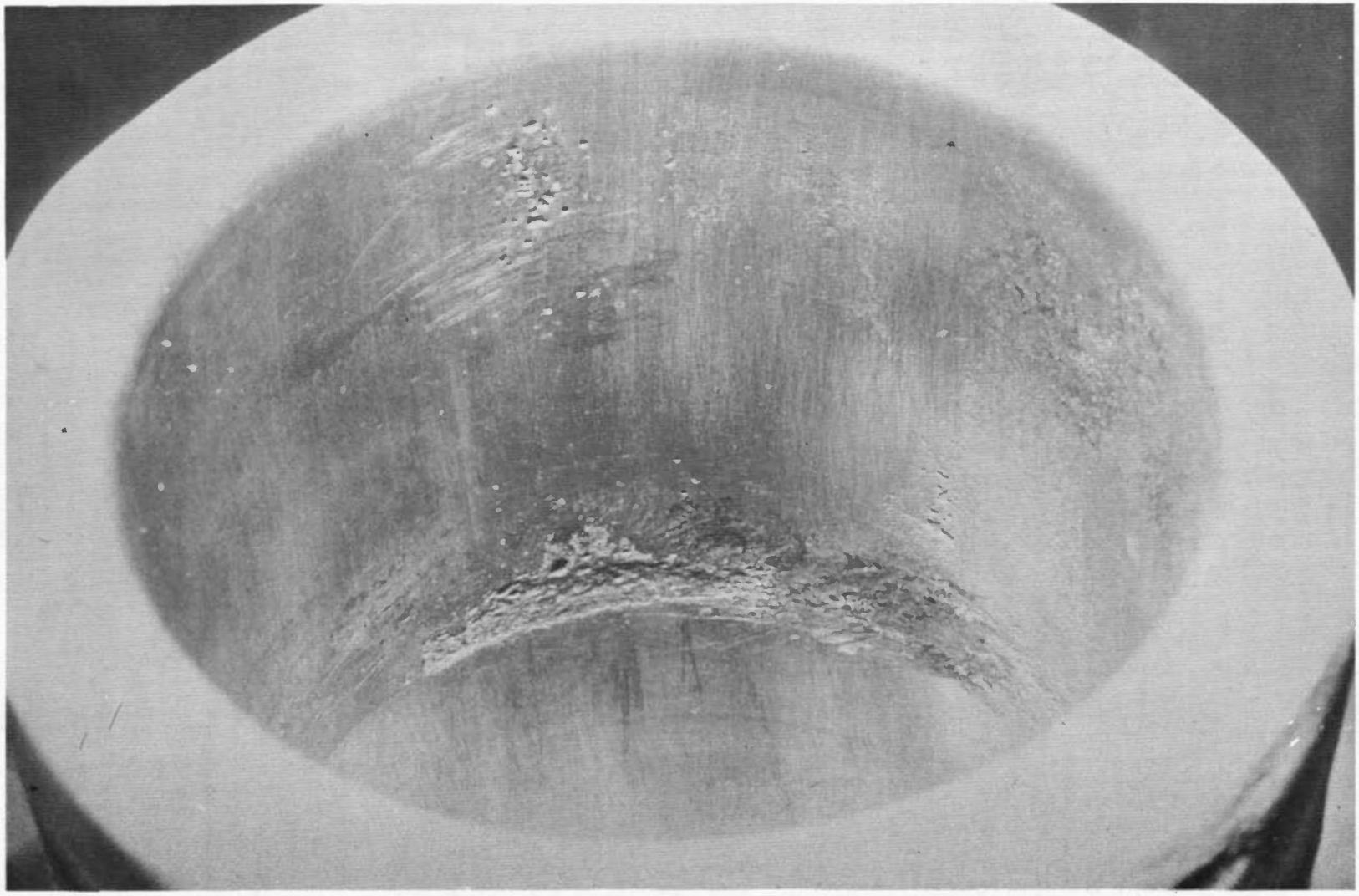

FIGURE 58. CORROSION OBSERVED ON FIRST GENERATION BURNER AFTER 96 HOUR HEAT SOAK AT 4000°F - PILOT HEATER

The burner was put into pilot heater service beginning with Run 70. After a preliminary shakedown period the burner was found to operate quite satisfactorily. The corrosion problem, from experience acquired to date, has been eliminated. The burner has operated for a total of 16 runs during which maximum conditions of 4000°F and 1850 psi have been encountered. During these runs the burner accumulated a certain amount of deposits from the combustion products (Figure 59). There were no indications of corrosion, however, when these deposits were removed. It is difficult to predict the life of the second generation burner, due to the limited amount of operating data accumulated with it thus far. The superiority of stainless steel over zirconium copper in a storage heater environment was quite obvious after only a small number of runs. The refractory combustion chamber employing 9.25 weight percent yttria-zirconia appears, thus far, to be performing quite satisfactorily. Once again, however, the amount of operating data accumulated is relatively small.

7.3.6 Performance of Instrumentation Systems

The instrumentation used to record temperatures in the AEDC pilot heater were of two basic types: thermocouples and optical pyrometers. Prior to the pilot heater, storage heaters were typically designed with thermocouple instrumentation in the matrix below 3000°F, the backup insulation and various locations on the shell and grate support structure. The AEDC pilot heater included this type of instrumentation along with an optical pyrometer-viewport slot system that allowed the operators to view and make temperature measurement at four locations at the center of the matrix. The pyrometer-slot temperature system was designed and fabricated under a separate Air Force contract with FluiDyne Engineering Corporation (AF Contract F40600-68-C-0002). The system consisted of a number of slots through adjacent insulation and matrix blocks that would align at temperatures between 2000°F and 4200°F. The geometry of these sight holes is shown in Figure 31. An optical pyrometer of the disappearing filament type, especially designed for viewing small targets, was provided under the contract. The instrument provided was a Micro-Optical Pyrometer manufactured by the Pyrometer Instrument Company of Bergenfield, New Jersey.

To aid in the original checkout and calibration of the combination pyrometer-slot system, a number of thermocouples were installed within the bed at the slot locations to provide simultaneous readings at the lower temperatures. The thermocouples were Pt-6Rh/Pt-30Rh which have a maximum service temperature of about 3100°F. Once high temperatures were reached these thermocouples were lost. During the design it was estimated that the system would provide an accuracy of 1% for temperature measurements made at the center of the matrix.

Temperature data were gathered during the initial portion of the test program. These raw data, in their uncorrected form, are given in Table 5. The data presented are for simultaneous readings of both the thermocouples and the pyrometer. Readings are tabulated in degrees Fehrenheit for the 9, 11 and 13-foot levels.

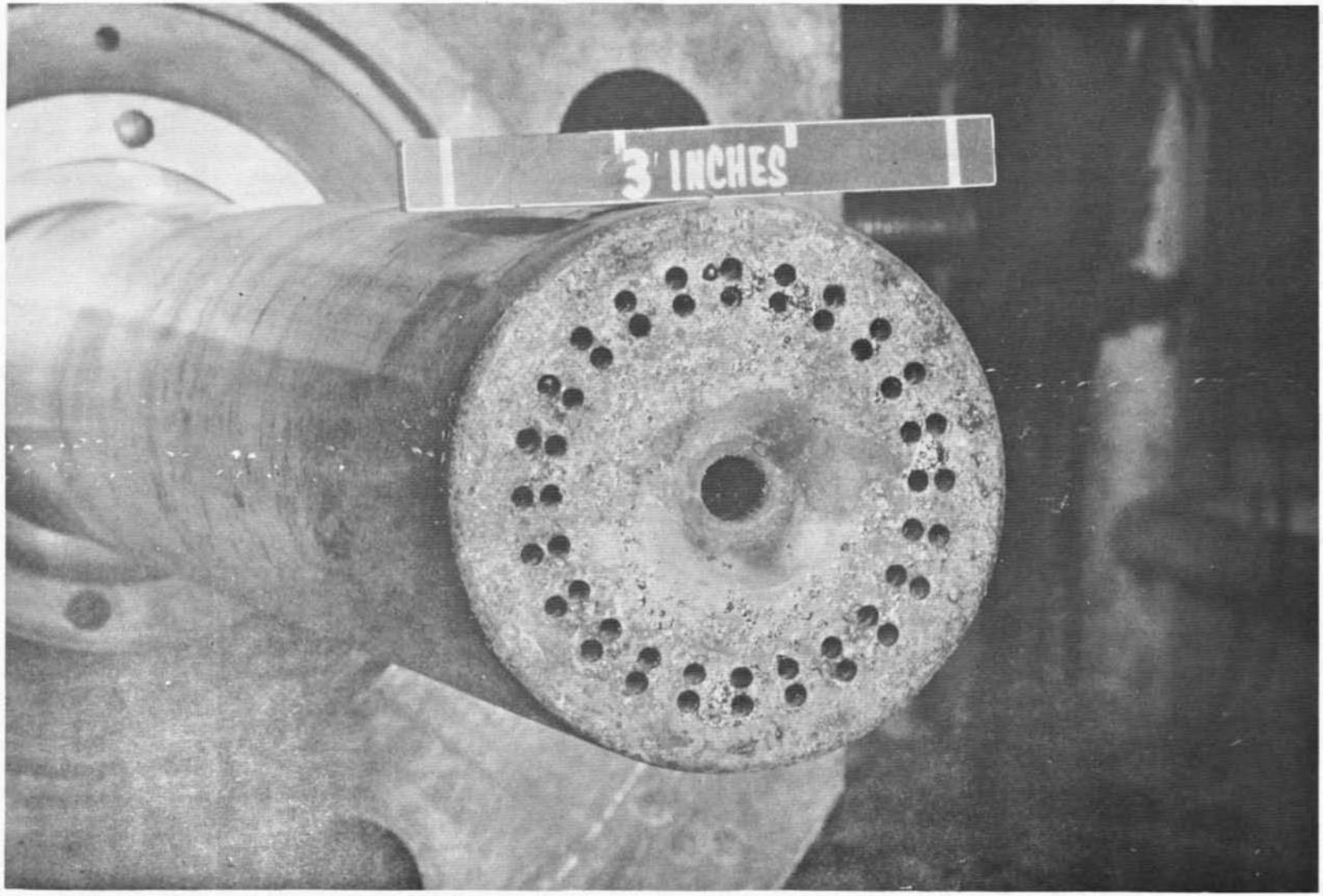

FIGURE 59. SECOND GENERATION BURNER AFTER RUN 85 - PILOT HEATER

The viewport slots were designed such that emissivity corrections would be unnecessary for temperature readings made at the center of the bed. This was accomplished by providing a wide slot in the center block and a relatively narrow slot in the adjacent block. This design formed a black cavity in the center block where the temperature measurements were taken. The data of Table V has not been corrected for the pyrometer calibration and for losses encountered through the glass viewport window.

The data in its raw form show agreement with the thermocouple readings within $\pm$ 5%. This is well within the accuracy required to establish blowdown rates for the storage heater.

The system could be improved by providing slightly wider slots through the outer insulation blocks for better hole alignment.

TABLE V

COMPARISON OF THERMOCOUPLE AND PYROMETER MEASUREMENTS - PILOT HEATER

Date	Time, Hr.	9-Foot Level T/C Temperature °F	9-Foot Level Pyro Temperature °F	11-Foot Level T/C Temperature °F	11-Foot Level Pyro Temperature °F	13-Foot Level T/C Temperature °F	13-Foot Level Pyro Temperature °F
9/27	0000	1939	1905	2603	2580	3228	----
	0200	2006	1960	2640	2610	3228	3180
	0400	2068	1990	2669	2620	3238	3190
	0600	2114	2070	2697	2660	3246	3210
	0800	2150	2100	2710	2685	3250	3240
	1000	2180	2105	2730	2650	3270	3230
	1200	2200	2160	2750	2710	3280	3270
	1400	2225	2165	2760	2710	Out	3250
	1600	2250	2190	2785	2695		
	1800	2280	----	2810	----		
	2000	2350	2240	2870	2780		
	2200	2415	2365	2915	2910		
9/28	0000	2460	2350	2950	2910		
	0200	2520	2440	2980	2960		
	0400	2550	----	3010	----		
	0600	2575	2490	3020	2990		
	0800	2575	2540	3025	3000		
	1000	2590	2550	3040	3030		
	1200	2600	2565	3060	3020		
	1400	2625	2610	3100	3090		
	1600	2640	2770	3130	3150		
	1800	2715	2750	3250	3250		
	2000	2790	2850	Out	3360		
	2200	2960	2980				
9/29	0000	3070	3100				
	0200	3160	3160				
	0400	3210	3200				
	0600	Out	3240				

8.0 FINAL MATERIAL SPECIFICATION

The purpose of the materials development program, was to evaluate various materials and shapes for potential use in the full scale storage heater. The first phase of this program involved the evaluation of sample materials on a subscale basis where small samples were evaluated under simulated heater operating conditions. The most promising materials from these tests were then procured in full scale cored brick shapes. These shapes were evaluated in the pilot heater where they experienced actual storage heater operating conditions. The materials exhibiting the most promising performance in the pilot heater became candidate materials for the full scale heater. This implies, however, that materials which exhibit satisfactory performance in the pilot heater can be adequately described to enable procurement of material for the full scale heater with reasonable assurance of similar performance. To provide the reasonable assurance, it was essential that a comprehensive material specification be written to describe the material.

A material specification was prepared and is included in Appendix B. The material specified is a 6 m/o high purity, high density, yttria stabilized zirconia. The block length was reduced to lengths ranging from 1 to 2.5-inches. An alternate key design was also included which will replace the hex design on material supplied for the full scale heater. The material specification was written based on the experience gained from both the subscale tests, the pilot heater tests and the associated analysis.

During the writing of the specification open communications were maintained with all interested potential suppliers. It was felt extremely important that suppliers be allowed to comment on the specification during various phases of its writing to assure that the resulting specification was realistic in terms of their manufacturing capabilities.

From the AEDC pilot heater tests a number of things were learned with regard to material performance. The original 9.25 weight percent yttria-zirconia did destabilize early in the test program masking the performance of the material at the higher operating temperatures and pressures. In addition to the original material, a number of samples of zirconia with increased levels of stabilizer were installed and evaluated in the last half of the test program. From the test and analysis of these samples along with the original 9.25 weight percent material, the subject specification was written. The material specified, however, has not been tested as yet in the pilot heater. Present plans are to procure the matrix to the subject specification and evaluate the material in the pilot heater for approximately one year. If the material performs successfully during this test, it would then become the candidate for the full scale storage heater.

In the writing of the specification there were a number of areas where the suppliers lacked sufficient production experience, with the specified material, to enable them to quote realistically on a fixed price basis. The

specification, therefore, was broken into two general catagories: a pilot heater order and a production order. It was felt necessary to include the production order specification as part of the pilot, such that the suppliers would be aware of what would be expected on subsequent production orders. On the pilot order the suppliers are required to meet the pilot order specification on a fixed price basis and the production order specification on a best effort basis only.

REFERENCES

1. Duwez , P., Odell, F., and Brown, F.H. Jr., "Stabilization of Zirconia with Calcia and Magnesia," J. Amer. Cer. Soc., 35(5) 107-13 (1952).

2. Weber, B.C. and Schwartz, M.A., "Zirconia; Its Crystallographic Polymorphy and High Temperature Potentials," WADC TR 58-646, WPAFB, Ohio, July 1958.

3. Weber, B.C., Garrett, H.J., Mauer, F.A., and Schwartz, M.A., "Observations on the Stabilization of Zirconia," J. Amer. Ceram. Soc. 39)6) 197-207, 1956.

4. Fehrenbacher, L.L., Jacobson, L.A., and Lynch, C.T., "Sintering Behavior of Stabilized ZrO_2 Compositions," AFML-TR-65-394, Air Force Materials Laboratory, WPAFB, Ohio, Dec. 1965.

5. Buckley, J.D. and Wilson, H.H., "Destabilization of Zirconia by Cyclic Heating," J. Amer. Cer. Soc., 46 (Oct. 1963) 510.

6. DeCoursin, D.G., et al, "Recent Development of Storage Heaters to Provide Flight Simulation for Air Breathing Propulsion Systems," AIAA Third Propulsion Joint Specialist Conference, Washington, D.C., 17-21 July 1967.

7. Schwartz, B., "Thermal Stress Failure of Pure Refractory Oxides," J. Amer. Cer. Soc., 35 (Dec. 1952) 325-333.

8. Lowrance, D.T., "A Correlation of Properties for Various Formulations of Sintered Zirconia-Unpublished Data," Chance Vought Corp., ASTIA AD 273802 (March 1962).

9. Ryshkewitch, E., Oxide Ceramics. New York: Academic Press, 1960.

10. Coble, R.L. and Kingery, W.D., "Effect of Porosity on Thermal Stress Fracture," J. Amer. Cer. Soc., 38 (Jan. 1955) 33-37.

11. Hasselman, D.P.H., "Elastic Enery at Fracture and Surface Energy as Design Criteria for Thermal Shock," J. Amer. Cer. Soc., 46 (Nov. 1963) 535-540.

12. Nakayama, J., "Direct Measurement of Fracture Energies of Brittle Homogeneous Materials," J. Amer. Cer. Soc., 48 (Nov. 1965) 583-587,

13. Nakayama, J. and Ishizuka, M., "Experimental Evidence for Thermal Shock Damage Resistance," J. Amer. Cer. Soc., 45 (July 1966) 666-669.

14. "High Temperature Volatization of Special Refractories," The Refractories Journal, Dec. 1964, 498-500.

15. AEDC-TDR-64-48.

16. Hagford, D.E., "Research Study and Development of Refractories for a Pilot Heater," AEDC-TR-69-108, May 1969.

APPENDIX A

PILOT HEATER MATERIAL SPECIFICATIONS

YTTRIUM-RARE EARTH OXIDES MIXTURE

1. The minimum Y_2O_3 concentration shall be 88 percent by weight.

2. The total percentage of lanthanum, cerium, praseodymium, neodymium, promethium, samarium, and europium oxides shall not exceed 1 percent by weight.

3. The minimum concentration of yttria and rare earth oxides shall be 99.5 percent by weight.

4. At least 90 percent of the oxide powder shall be composed of particles with average diameter less than 4 microns (Fisher sub-sieve sizer).

5. Weight loss of oxide powder shall not exceed 2 percent in air at 1400°F.

Yttria Stabilized Zirconia

1. Primary stabilizer to be 6.0 to 6.5 weight percent of yttria or yttria-rare earth oxides mixture with total of lanthanum, cerium, praseodymium, neodymium, promethium, samarium, and europium oxides not to exceed one weight percent. Minimum concentration of yttria plus rare earth oxides to be 99.5 weight percent.
2. Secondary stabilizers of the RO oxide group permitted to a maximum of 2.0 weight percent.
3. Maximum individual impurities (weight percent):

Titania	0.2	Ferric Oxide	0.2
Silica	0.3	Alumina	0.3

4. Maximum total impurities not to exceed 1.0 weight percent (excluding hafnia and RO group secondary stabilizers).
5. Minimum bulk density of fired shapes to be 5.40 grams per cubic centimeter.
6. Shapes to be fired at cone 35 (3250°F) or higher.
7. Fired shapes to be essentially free of monoclinic phase.

Yttria Stabilized Zirconia

1. Primary stabilizer to be 8.0 to 8.5 weight percent of yttria or yttria-rare earth oxides mixture with total of lanthanum, cerium, praseodymium, neodymium, promethium, samarium, and europium oxides not to exceed one weight percent. Minimum concentration of yttria plus rare earth oxides to be 99.5 weight percent.
2. Secondary stabilizers of the RO oxide group permitted to a maximum of 2.0 weight percent.
3. Maximum individual impurities (weight percent):

Titania	0.2	Ferric Oxide	0.2
Silica	0.3	Alumina	0.3

4. Maximum total impurities not to exceed 1.0 weight percent (excluding hafnia and RO group secondary stabilizers).
5. Minimum bulk density of fired shapes to be 5.40 grams per cubic centimeter.
6. Shapes to be fired at cone 35 (3250°F) or higher.
7. Fired shapes to be essentially free of monoclinic phase.

YTTRIA STABILIZED ZIRCONIA

1. Stabilizer to be 9.0 to 9.5 weight percent of yttria or yttria-rare earth oxides mixture with total of lanthanum, cerium, praseodymium, neodymium, promethium, samarium, and europium oxides not to exceed one weight percent. Minimum concentration of yttria plus rare earth oxides to be 99.5 weight percent.

2. Maximum individual impurities (weight percent):

Titania	0.2	Ferric Oxide	0.2
Silica	0.3	Alumina	0.3
Calcia	0.4	Magnesia	0.4

3. Maximum total impurities not to exceed 1.8 weight percent (excluding hafnia).

4. Minimum bulk density of fired shapes to be 5.40 grams per cubic centimeter.

5. Shapes to be fired at Cone 35 (3250°F) or higher.

6. Monoclinic content of fired shape not to exceed one percent.

Yttria Stabilized Zirconia

1. Stabilizer to be 8.2 to 8.6 weight percent of yttria or yttria-rare earth oxides mixture with total of lanthanum, cerium, praseodymium, neodymium, promethium, samarium, and europium oxides not to exceed one weight percent. Minimum concentration of yttria plus rare earth oxides to be 99.5 weight percent.
2. Maximum individual impurities (weight percent):

Titania	0.2	Ferric Oxide	0.2
Silica	0.2	Alumina	0.2
Calcia	0.4	Magnesia	0.4

3. Maximum total impurities not to exceed 1.2 weight percent (excluding hafnia).
4. Minimum bulk density of fired shapes to be 5.40 grams per cubic centimeter.
5. Shapes to be fired at cone 33 (3170°F) or higher.
6. Fired shapes to be essentially free of monoclinic phase.

Yttria Stabilized Zirconia

1. Stabilizer to be 9.0 to 9.5 weight percent of yttria or yttria-rare earth oxides mixture with total of lanthanum, cerium, praseodymium, neodymium, promethium, samarium, and europium oxides not to exceed one weight percent. Minimum concentration of yttria plus rare earth oxides to be 99.5 weight percent.
2. Maximum individual impurities (weight percent):

Titania	0.2	Ferric Oxide	0.2
Silica	0.2	Alumina	0.2
Calcia	0.4	Magnesia	0.4

3. Maximum total impurities not to exceed 1.2 weight percent (excluding hafnia).
4. Minimum bulk density of fired shapes to be 5.40 grams per cubic centimeter.
5. Shapes to be fired at cone 33 (3170°F) or higher.
6. Fired shapes to be essentially free of monoclinic phase.

Yttria Stabilized Zirconia

1. Primary stabilizer to be 8.0 to 8.5 weight percent of yttria or yttria-rare earth oxides mixture with total of lanthanum, cerium, praseodymium, neodymium, promethium, samarium, and europium oxides not to exceed one weight percent. Minimum concentration of yttria plus rare earth oxides to be 99.5 weight percent.
2. Secondary stabilizers of the RO oxide group permitted to a maximum of 2.0 weight percent.
3. Maximum individual impurities (weight percent):

Titania	0.2	Ferric Oxide	0.2
Silica	0.3	Alumina	0.4

4. Maximum total impurities not to exceed 1.0 weight percent (excluding hafnia and RO group secondary stabilizers).
5. Bulk density of fired shapes to be in range 150 to 180 pounds per cubic foot.
6. Shapes to be fired at cone 35 (3250°F) or higher.
7. Fired shapes to be essentially free of monoclinic phase.

Yttria Stabilized Zirconia

1. Primary stabilizer to be 8.0 to 8.5 weight percent of yttria or yttria-rare earth oxides mixture with total of lanthanum, cerium, praseodymium, neodymium, promethium, samarium, and europium oxides not to exceed one weight percent. Minimum concentration of yttria plug rare earth oxides to be 99.5 weight percent.
2. Secondary stabilizers of the RO oxide group permitted to a maximum of 2.0 weight percent.
3. Maximum individual impurities (weight percent):

Titania	0.2	Ferric Oxide	0.2
Silica	0.3	Alumina	0.4

4. Maximum total impurities not to exceed 1.0 weight percent (excluding hafnia and RO group secondary stabilizers).
5. Bulk density of fired shapes to be in range 250 to 280 pounds per cubic foot.
6. Shapes to be fired at cone 35 (3250°F) or higher.
7. Fired shapes to be essentially free of monoclinic phase.

Yttria Stabilized Zirconia

1. Stabilizer to be 9.0 to 9.5 weight percent of yttria or yttria-rare earth oxides mixture with total of lanthanum, cerium, praseodymium, neodymium, promethium, samarium, and europium oxides not to exceed one weight percent. Minimum concentration of yttria plus rare earth oxides to be 99.5 weight percent.
2. Maximum individual impurities (weight percent):

Titania	0.2	Ferric Oxide	0.2
Silica	0.3	Alumina	0.4
Calcia	0.4	Magnesia	0.4

3. Maximum total impurities not to exceed 2.0 weight percent (excluding hafnia).
4. Bulk density of fired shapes to be in range 250 to 280 pounds per cubic foot.
5. Shapes to be fired at cone 35 (3250°F) or higher.
6. Fired shapes to be essentially free of monoclinic phase.

YTTRIA-RARE EARTH STABILIZED ZIRCONIA

1. Stabilizer to be 9.0 to 9.5 weight percent of yttria-rare earth oxides mixture with total of lanthanum, cerium, praseodymium, neodymium, promethium, samarium, and europium oxides not to exceed one weight percent. Minimum concentration of yttria to be 88 weight percent. Minimum concentration of yttria plus rare earth oxides to be 99.5 weight percent.

2. Maximum individual impurities (weight percent):

Titania	0.2	Ferric Oxide	0.2
Silica	0.2	Alumina	0.2
Calcia	0.4	Magnesia	0.4

3. Maximum total impurities not to exceed 1.2 weight percent (excluding hafnia).

4. Minimum bulk density of fired shapes to be 5.40 grams per cubic centimeter.

5. Shapes to be fired at Cone 35 (3250°F) or higher.

6. Monoclinic phase of fired shapes not to exceed 3.0 percent.

APPENDIX B

SPECIFICATION FOR 6 MOLE PERCENT YTTRIA-ZIRCONIA CORED BLOCKS FOR THE AEDC PILOT HEATER

(AEDC NO. ETF-71-1)

SPECIFICATION FOR 6 MOLE PERCENT YTTRIA ZIRCONIA CORED BLOCKS FOR THE AEDC PILOT HEATER

1.0 PURPOSE AND SCOPE

1.1 PURPOSE

The purpose of this specification is to define the requirements for supplying yttria-stabilized zirconia cored blocks for use as matrix elements in the AEDC Pilot Heater. The blocks are to replace those which have been previously operated and tested in the Pilot Heater.

1.2 SCOPE

Sufficient cored blocks (FluiDyne Drawing No. 7003-008D) of total length of 180 lineal feet and segments (FluiDyne Drawing No. 7003-604C) of total length of 115 lineal feet shall be fabricated. (This total does not include those blocks required for inspection in paragraph 3.1.) Included in these amounts will be 16 blocks of nominal length 1/2" and 144 blocks of nominal length 1". Out of the total length of blocks the Contractor may, at his option, produce not more than 16 blocks of length 4", 16 blocks of length 5", and 16 blocks of length 6". The remainder of the 180 lineal feet of blocks will be of random length between 1" and 2-1/2". (This supersedes item 1 of FluiDyne Drawing No. 7003-008D.) The total 115 lineal feet of segments shall be of random lengths between 1" and 2-1/2" or longer. (This supersedes item 2 of FluiDyne Drawing No. 7003-604C.) This production is called the Pilot Heater Order. The objective of this procurement is to verify and refine fabrication procedures and techniques, followed by long term testing, by others, of the procured blocks in the pilot heater to yield service life data of the blocks. Dependent on the results of such long term operation of the blocks in the pilot heater, the Government may consider, at some future date, a production order of such or similar blocks. These production order blocks would be used in a large storage heater. It is anticipated that the fabrication procedures and techniques developed by the supplier in the course of the Pilot Heater Order would be used for the production order. The Contractor shall attempt to meet the Appendix 1 specifications on the Pilot Heater Order but is required to meet only the basic specification, exclusive of Appendix 1.

2.0 REQUIREMENTS AND INSPECTION

2.1 GENERAL

The following describes the material specifications, the detailed requirements for the cored blocks, and the method of selecting blocks and samples for inspection and tests. The dimensions of the required blocks are shown

on FluiDyne Drawings Nos. 7003-008D and 7003-604C attached hereto and made a part of this specification (except item 6 in Drawing 7003-008D).

2.2 QUALITY ASSURANCE TESTING

The purpose of these tests is to assure compliance of the fabricated blocks with these specifications. The Contractor shall make available to the Government, in addition to the blocks called for in paragraph 1.2, the cored blocks and material samples called for in paragraphs 2.4.3 and 3.1 for quality assurance tests. Results of the tests will be provided to the Contractor. Appendix 2 describes, for the Contractor's information only, the procedures to be used for these quality assurance tests.

2.3 INSPECTION LOTS

2.3.1 The Pilot Heater Order shall be divided into two inspection lots of approximately equal weight by sequence of fabrication, i.e., the first half completed and the second half completed.

2.3.2 Each of the two lots will be inspected as specified in paragraph 3.0 and Appendix 2.

2.4 IDENTIFICATION

2.4.1 Each block and sample required by this specification shall be permanently identified by individual code numbers that are traceable to the following:

a. Drawing Number
b. Material
c. Grain Batch (raw material)
d. Kiln Load and Kiln Firing Conditions.

2.4.2 Representative samples of mixed raw materials shall be retained by the Contractor for submission to the Government as required.

2.4.3 An approximate one cubic inch portion of one cored block from each kiln load will be delivered to the Government as each kiln load is produced.

2.5 DIMENSIONS AND TOLERANCES

2.5.1 All dimensions shall be within the tolerances as specified on the drawings listed in paragraph 2.1. (See paragraph 3.1 for inspection procedure.)

2.6 SURFACE CHARACTERISTICS

2.6.1 All die flash and feather edges must be removed from holes and periphery. (Die flash and feather edges are mean projections of material beyond the solid boundaries as specified by applicable drawings.)

2.6.2 All surfaces must be smooth and free of loose grains.

2.6.3 Blocks with open visible cracks (width 0.002 inch or greater) are not acceptable.

2.6.4 Blocks with chips larger than 1/4-inch diameter by 1/8-inch deep from any surface are not acceptable.

2.7 DENSITY AND INTERNAL STRUCTURE

2.7.1 Density of the solid material of the fabricated cored blocks shall be greater than 5.4 grams per cubic centimeter.

2.8 CHEMICAL COMPOSITION

2.8.1 The concentration of yttrium oxide stabilizer to be added to pure zirconium dioxide shall be $6.0\ ^{+0.5}_{-0.0}$ mole percent on a Y_2O_3 basis accounting for the stabilizer's loss on ignition value. The total purity of the yttria powder shall not be less than 99.5 weight percent with Y_2O_3 content being at least 99 atomic percent of the total rare earth oxides present.

2.8.2 The total of the following impurities in the fabricated block shall not exceed 1.0 percent by weight. Maximum limits (weight percent) for individual impurities are:

Al_2O_3 - 0.2%	MgO - 0.4%
SiO_2 - 0.2%	CaO - 0.4%
FE_2O_3 - 0.2%	TiO_2 - 0.2%

The total of all impurities shall not exceed 1.2 percent by weight (excluding hafnia).

2.8.3 All shapes shall be fired at Cone 35 (3250°F reference) or higher.

2.9 MONOCLINIC PHASE CONTENT

2.9.1 Monoclinic zirconia phase concentrations greater than 0.5% as detected by X-ray diffraction analysis will not be accepted. Any indicated monoclinic phase shall be confirmed by metallographic determination. (Test procedure, sample preparation, test equipment, and calculations to be used in determining monoclinic content are described, for information only, in Appendix 2. With the procedures described, the minimum detectable limit is 0.5% with 95% confidence limit for experimental determination.)

3.0 INSPECTION QUANTITIES

3.1 Approximately 1/3 of the blocks (randomly selected) will be inspected for compliance with dimensions, tolerances, and surface characteristics. They will be inspected as follows:

Hole diameter	Three randomly selected locations on each end face.
Distance between adjacent holes	Six randomly selected locations on each end face.
Distance across flats	One randomly selected locations per flat.
Flatness and parallelism of sides and end faces	Each surface.
Perpendicularity of sides to end faces	One randomly selected location for each end face.
Rounds and fillets	Visually inspected.

A minimum of two blocks of each inspection lot will be inspected and tested for density and internal structure and chemical composition. These tests may be performed on pieces of the same two cored blocks selected at random from each inspection lot. In addition, cored block portions furnished under paragraph 2.4.3 will be tested by the Government for monoclinic phase content and the results for each Contractor's sample given to that Contractor.

2 Atchs
1. FluiDyne Drawing No. 7003-008D
2. FluiDyne Drawing No. 7003-604C

(NOTE: As per paragraph 1.2 of the basic specifications, the Contractor is not required to meet the specifications in Appendix 1 for the Pilot Heater Order. The Contractor should, however, attempt to meet as many of these specifications as possible.)

APPENDIX 1
PROPOSED SPECIFICATIONS FOR PRODUCTION ORDER

1.0 GENERAL

1.1 GENERAL

Specifications for the major production order are expected to include those for the Pilot Heater Order plus the following additional specifications.

2.0 REQUIREMENTS AND INSPECTION

2.1 SURFACE CHARACTERISTICS

2.1.1 Blocks having up to three hairline cracks no greater than 1/2" x 1/2" will be acceptable. (Hairline cracks are cracks of width less than 0.002 inch.)

2.1.2 Blocks with a network of surface cracks or surface checking are not acceptable.

2.1.3 Blocks having surface stains with indented or glassy areas exceeding 1/8 inch diameter are not acceptable.

2.2 DENSITY AND INTERNAL STRUCTURE

2.2.1 Blocks with lamination cracks are not acceptable.

2.2.2 Blocks with visible black coring or internal discoloration are not acceptable.

APPENDIX 2
QUALITY ASSURANCE TEST PROCEDURES

1.0 DIMENSIONS

The block dimensions which will be measured are listed in the following table:

	Description of Measurement	Location
1.	Hole diameter	Three randomly selected locations on each end face.
2.	Distance between adjacent holes	Six randomly selected locations on each end face.
3.	Distance between outside holes (across flats)	Six randomly selected locations on each end face.
4.	Distance across flats	One randomly selected location per flat.
5.	Flatness and parallelisms of sides and end faces	Each surface.
6.	Perpendicularity of sides to end faces	One randomly selected location for each end face.

The rounds and fillets shall be visually inspected.

2.0 SURFACE CHARACTERISTICS

Blocks will be inspected for hairline cracks using the following dye check method:

2.1 The block shall be totally immersed in a dye check solution for a period of 5 seconds.

2.2 The block shall then be totally immersed in two baths to remove excess dye from the block surfaces. The block should be immersed perpendicularly to the holes a total of 4 times in each bath. Each immersion involves simply covering the entire block with the cleaning agent and removing immediately.

2.3 The excess cleaning agent can be removed by exposing the block surfaces to a 1-2 sec, 30 psig air stream delivered from a 1/32-inch orifice at a distance of 6 inches.

3.0 DENSITY AND INTERNAL STRUCTURE

3.1 Density may be measured by ASTM C20-46(1967) or equivalent methods. The C20-46(1967) test will be modified to include a 10 second exposure to 30 psi compressed air from a 1/32-inch orifice at a distance of 6 inches to blow water droplets from inside surfaces of holes. Piece will be held with holes in vertical position and air blast directed downward.

4.0 CHEMICAL COMPOSITION

4.1 Analytical method for determining chemical composition will be atomic absorption, optical and/or mass spectroscopy.

5.0 MONOCLINIC PHASE CONTENT

5.1 Determination of monoclinic phase content will be by X-ray quantitative diffraction using Norelco X-ray diffraction equipment. Equipment operating parameters will be 40 KV, 10 Ma with a scan rate of 1/2° per minute, a divergence slit of 1°, and a receiving slit of 0.1°. Ni filtered CuKα line radiation will be used with a Geiger Counter detector.

5.2 Sample will be prepared by crushing, using a mortar and pestle until all fragments pass through a 325 mesh sieve. The powder will then be passed into a sample holder using a glass slide and spatula. Collodian binder will be used in small quantities.

5.3 Monoclinic content will be calculated as follows. Peaks to be scanned are:

$\text{Monoclinic}_{(1,1,1)}$	M-1 = 28.3°	(2θ)
$\text{Monoclinic}_{(1,1,1)}$	M-2 = 31.6°	(2θ)
$\text{Cubic}_{(1,1,1)}$	30°	(2θ)

Percentage monoclinic is calculated using the following formula:

$$\% \text{ Monoclinic} = \frac{P.H._{M-1} + P.H._{M-2}}{P.H._{C} + P.H._{M-1} + P.H._{M-2}}$$

where P.H. is the respective peak height.

5.4 The instrument count controls will be adjusted to cause the cubic peak to essentially fill the recorder chart. All three peaks will then be scanned. Peak heights will be measured above the average background.

6.0 REHEAT SHRINKAGE, WEIGHT LOSS, HOT LOAD DEFORMATION

6.1 The Government will also examine representative blocks for the percentage of reheat shrinkage, reheat weight loss, and hot load deformation.

7.0 RESULTS OF QUALITY ASSURANCE TESTS

7.1 The Government will provide to the Contractor the results of the Quality Assurance Tests on his blocks.

APPENDIX 3
TEST AND INSPECTION PROCEDURES FOR PRODUCTION ORDER

The technical provisions of specifications for the major production run of yttria-zirconia cored blocks are expected to be the same or similar to those for the Pilot Heater Order, except for modifications necessitated by the larger production. Such anticipated modifications are outlined in the following.

1.0 INSPECTION LOTS

1.1 The production order shall be divided into inspection lots of 500 blocks each by sequence of fabrication. These lots shall be numbered sequentially.

1.2 A plan for selecting these inspection lots is described in the following. (An alternate inspection plan is MIL-STD-105D 2.5 AQL II Single-Normal Inspection Plan. However, the Government may, at its option, choose to inspect and test fewer than or more than the number of lots identified in these plans.)

1.2.1 Lot 1 will be inspected.

1.2.2 If Lot 1 fails inspection, Lot 2 will be inspected, etc.

1.2.3 After a lot passes inspection, three of the following nine lots will be selected at random for inspection.

1.2.4 If one or more of these lots fail inspection, the earliest manufactured lot (lowest number) that was not inspected will be inspected. The next lots in sequence will be inspected until three consecutive lots pass. The succeeding nine lots will be inspected according to paragraph 1.2.3.

1.2.5 After the three lots of paragraph 1.2.3 pass inspection, a single lot will be selected at random from the succeeding ten lots for inspection.

1.2.6 If the lot of paragraph 1.2.5 fails inspection, paragraph 1.2.4 will be repeated starting with the earliest manufactured lot in the group of ten.

1.2.7 If the lot of paragraph 1.2.5 passes inspection, paragraph 1.2.5 will be repeated with the next group of ten lots, etc., until completion.

1.2.8 The minimum number of lots inspected under this plan will be ten lots for production quantities in the range 20,000 to 50,000 blocks.

1.3 A lot that is rejected may, at the Government's option, be divided into smaller lots with each to be inspected.

1.4 The blocks supplied under the production order shall be made by processes and materials that do not differ in any basic respects fromthose used to produce blocks accepted under the pilot order and subsequently successfully evaluated in the AEDC Pilot Heater. That is, the values obtained for the arithmetic mean (1) and the mean deviation (2) in the production of the Pilot Heater Order for such properties as density and purity shall become the arithmetic mean and mean deviation for the production order. The arithmetic mean and mean deviation for the pilot and production orders shall be similar within a 90% confidence limit using standard statistical methods. These values shall supersede the values called out in this specification for the pilot order. The monoclinic requirements for the production order shall remain as written in this specification for the pilot order.

$$(1)\ \text{Arithmetic Mean} = \bar{X} = \frac{\sum_{j=1}^{N} X_j}{N}$$

$$(2)\ \text{Mean Deviation} = \text{M.D.} = \frac{\sum_{j=1}^{N} | X_j - \bar{X} |}{N}$$

where X = Sample
N = Total Number of Samples.

2.0 DIMENSIONS AND TOLERANCES

2.1 Inspection shall be by MIL-STD-105D 2.5 AQL II Single-Normal Inspection Plan. Thus, 50 blocks will be inspected in each lot of 500 blocks. A lot will be accepted if 3 or fewer blocks are rejected. A lot will be rejected if 4 or more blocks are rejected.

3.0 SURFACE CHARACTERISTICS

3.1 Each block will be inspected.

4.0 DENSITY AND INTERNAL STRUCTURE

4.1 A minimum of two blocks from each inspection lot will be tested.

5.0 CHEMICAL COMPOSITION

5.1 A minimum of two blocks from each inspection lot will be tested.

6.0 MONOCLINIC CONTENT

6.1 A minimum of 2 blocks selected at random from each inspection lot, in addition to 2 small samples from each kiln load, will be analyzed.

APPENDIX C

THERMAL STRESS DESIGN CONSIDERATIONS

THERMAL STRESS DESIGN CONSIDERATIONS

Thermal stress failure is the major limitation in the use of ceramic materials in heat exchangers because ceramic materials are brittle. Therefore, locally high stress levels are not relieved through plastic deformation (except at temperatures near the service limits). Thermal stress considerations were dominant factors in much of the heater design and in the establishment of operating procedures. These design considerations were particularly important to the bed. The discussion will therefore be directed primarily to the bed, and comments regarding the insulation will be made where appropriate.

Thermal stresses arise from restraint of thermal expansion and/or contraction. The restraint may be external to the brick or it may be internal (within the brick). Consider a brick that is part of the bed or the insulation. If the brick is not free to expand when heated from room temperature, the external restraint of the neighboring bricks will cause thermal stresses. Excessive stresses from this source are avoided by providing space for the thermal expansion. Accommodation of overall thermal expansion does not constitute a serious problem in design or operation.

On the other hand, thermal stresses arising from internal restraint cannot be controlled by simply providing space for expansion. These stresses depend only upon the temperature distribution within the brick and its physical properties (primarily, thermal expansion coefficient, modulus of elasticity, and Poisson's ratio). In general, these stresses decrease as the size of the brick is decreased. The use of small bricks to minimize stresses is very effective and has been applied for many years to the design of insulation assemblies. In this case, there is a backlog of experience regarding brick sizes and shapes, and excessive thermal stress conditions can usually be avoided. The situation with respect to the cored bricks is different. Here, experience is very limited, and the highest feasible performance was desired. Development of procedures for designing cored brick beds within thermal stress limitations was begun only recently (Refs. 1 and 3). The operation of the present heater and the Air Force pilot heater (Ref. 4) have provided further understanding, but a complete design procedure that would provide the confidence normally associated with heat exchanger construction is not yet available.

Design of the bed in terms of thermal stress limitations requires consideration of: (1) thermal stress failure modes, (2) material selection as related to failure modes, and (3) magnitude of the stresses. Each will be discussed in turn, and, as noted above, it is necessary to consider only stresses resulting from internal restraint.

Thermal Stress Failure Modes

Ceramic materials are much weaker in tension than in compression. Both tensile and compressive stresses exist in a brick thermally stressed

by internal restraint, i.e., with stresses arising only from the temperature distribution. Thus, most thermal stress failures are tensile failures. Shear failures sometimes develop, especially in areas of high compressive stress.

A brick exposed to thermal stresses greater than its strength can fail in several ways. A crack (or cracks) can develop but not propagate through the brick, leading to reduced overall strength. Cracks can propagate through the brick, fracturing it into one or more pieces. Cracks can propagate and intersect to spall the surface but not necessarily fracture the brick. The readiness with which cracks propagate differs greatly among ceramic materials. Most ceramics can be compared either to glass at room temperature, where cracks extend swiftly and usually lead to fracture, or to concrete, where cracks meander and branch, causing loss of strength and usually leading to spalling.

Consideration of these two modes of failure has led to two thermal stress resistance criteria (Ref. 5). The first is to avoid the initiation of cracks by keeping the stress levels below the material strength. The second is to allow thermal stresses greater than the strength, thus permitting cracks to be initiated but to minimize the resulting damage to the brick, such as loss of strength or loss of material through spalling.

The first criterion is the one commonly seen in the thermal stress literature. The procedure is to calculate the temperature field in the body, then calculate the stress field, then compare stress and strength. The results have been applied successfully to those materials in which cracks propagate readily to produce fracture. For ceramics these are typically the low porosity, fine grain materials that have high strength. As discussed later, this kind of material was chosen for the bed and therefore, this criterion was applied.

The second criterion applies to those materials in which cracks meander and branch, typically the coarse grain ceramics having a pore volume of roughly 20% or more. These materials can be exposed to conditions where the tensile stress at the surface exceeds the strength but without fracture or spalling providing the conditions are not too severe. The only effect, then, is the development of cracks. Cracks do weaken the brick but not necessarily to a level where it is no longer serviceable. This situation is common in insulation brickwork where the thermal stresses cannot be kept below the strength. This design approach has been used for many years and relies heavily on test data, such as from the ASTM panel spalling test, and experience. Experience was the major guide in the present design of the insulation. Essentially, the approach is to make the individual bricks as small as possible without compromising the structural integrity of the assembly and without excessive cost (which increases with the number of bricks).

Material Selection as Related to Failure Modes

The material selection will determine which mode of thermal stress failure is dominant: complete fracture or damage caused by cracking (without fracture). The choice is between a fine grain material of low porosity

and a coarse grain material of higher porosity. In this context, low porosity means a total pore volume of not more than about 10% (therefore, 90% or more of the theoretical density), and high porosity is roughly 20% to 30% pore volume. The term, density, will not be used in the absolute sense -- to compare different materials -- but only as a measure of the porosity of a given material, i.e., how close the material is to its theoretical density (zero porosity). A low porosity (high density) material offers performance advantages, specifically, the highest service temperature, highest mass flow capability, and lowest dust production. The disadvantages are cost and susceptibility to thermal fracture. These factors are discussed in the following paragraphs.

The maximum temperature of the bed is ultimately limited by deformation of the bricks through creep. Creep resistance increases as the pore volume is reduced, which thereby increases the service temperature.

The mass flow rate capability of the bed (for a given run time) is limited by flotation, the amount of energy stored, and the rate at which the stored energy can be removed to heat the air. Flotation is frequently the most restrictive limitation for pebble beds but with cored brick, thermal stress limitations are usually the most restrictive. The amount of stored energy increases as the material porosity is reduced, both directly and because the higher creep resistance allows a greater depth of bed to be heated to the maximum temperature.

Extraction of the energy at high rates requires that the product of heat transfer coefficient and heat transfer surface area be large. Large values are achieved in cored brick by use of small, closely spaced holes. The effect on surface area per cubic foot of bed is given below. Values for spherical pebbles are included for comparison.

	Hole or Sphere Diameter inches	Web Thickness inches	Surface Area ft^2/ft^3
Spheres	.38		122
	.5		86
	1.0		43
Cored Brick	.25	.25	44
	.20	.10	97
	.194	.085	108

The fine grain versus coarse grain choice enters into the web thickness selection because coarse grains cannot be used to fabricate thin webs. Coarse grain materials have been limited to a minimum web thickness of about 0.25 inch, providing a surface area equivalent to one inch spheres. The hole and web sizes chosen were .194 and .085, respectively, giving a surface area between those for 3/8 and 1/2 inch spheres.

The heat extraction rate is also dependent upon the resistance to heat conduction in the web. Thin webs of high conductivity give up their

heat more readily. Both factors are improved by use of a low porosity (high density) material.

Dust is produced in the bed by the rubbing of adjacent surfaces. Dense, fine grain materials have smooth, hard surfaces with tightly bonded grains. These produce less dust than the rough textured, coarse grain materials.

As described above, the failure modes are different between the low and high density materials. Overstressing the dense (low porosity) bricks will result in fractures. The seriousness of such fractures depends upon the number and their orientation. Fracturing usually relieves thermal stress levels; therefore, the fractured bricks may not progressively fracture into smaller parts upon exposure to repeated temperature conditions. Fractures in horizontal planes are considered less damaging than those inclined to the vertical. Vertical fractures may produce pieces which could fall downward and become wedged in the bed, enhancing the conditions for additional fracture during repeated cycling. Basically, some fracture in a bed of dense bricks is tolerable, provided it relieves a local condition and does not lead to progressive deterioration. The fracture behavior can only be determined from an operating bed.

Exposure to the same conditions will also crack the bricks in a bed of the lower density, coarse grain material. The cracks will reduce the strength and may cause spalling. Progressive deterioration may occur because of the loss of strength and because the cracks will tend to propagate upon repeated temperature cycling.

At this time, there is not sufficient information to allow comparison of the two kinds of materials in terms of allowable bed flow rates and bed life except to state that the dense materials have the greatest potential. This potential for high performance was the reason for selection of dense ceramics for the bed.

Thermal Stresses in the Bed

This section describes the problems of predicting the thermal stress levels in the bed and of relating these stresses to the bed design and operating conditions. The intent will be to predict the maximum tensile stresses, then estimate the tensile strength (or modulus of rupture) of the material, and apply the criterion: stress less than strength. In this analysis, stresses due to the weight of the bed are negligible and are ignored. Also, thermal stresses that would arise from "pinching" of the bricks due to restraint of overall expansion are ignored. It is assumed that adequate expansion space has been provided. Only thermal stresses from internal restraint within each cored brick will be discussed.

A brief qualitative summary of thermal stresses of this type will be useful. Cooling of all surfaces of a block produces tensile stresses in the surface and compressive stresses in the interior. Failure is initiated by surface cracks that usually enter at 90°. Heating has the reverse effect. Rapid heating may cause tensile failures in the interior or shear failures at the surface, usually entering the surface at about 45°.

The thermal stress level is strongly dependent on the nonlinearity of the temperature distribution within the brick. If the temperature distribution through the brick is linear in Cartesian coordinates and if the properties are constant (independent of temperature), no thermal stresses will develop (Ref. 6, p. 271 and Ref. 7, p. 403). However, no simple relationship exists between the temperature distribution and the stress levels for "brick" shaped bodies, as opposed to shapes such as plates, spheres, tubes, etc. (The simple equation that applies to tubes will be used later.) Calculations for "brick" shapes require numerical solutions by computer on a case-by-case basis. Insofar as the authors are aware, no such calculations have been made for three-dimensional temperature and stress distributions.

A simpler case of a one-dimensional temperature distribution and a three-dimensional stress field led to the following conclusions (Ref. 8):

1. Temperature distributions having negative second derivatives produce tensile stresses on the surface of the block and compressive stresses near the center of the block.

2. Temperature distributions having positive second derivatives produce the reverse effect: compressive stresses on the surface and tensile stresses inside of the block.

3. Thermal stresses are roughly proportional to the deviation of the temperature distribution from linearity.

4. Thermal stresses can be reduced significantly by changes in size and/or shape. Reducing overall size is a common approach to reduction of stresses. But if only one or two dimensions can be reduced, the orientation with respect to the temperature distribution is important. For example, the stresses can be reduced by decreasing the dimension of the block in the direction along which the temperature varies and/or by decreasing the dimensions of the block which lie perpendicular to the temperature variation (i.e., reducing the cross-sectional area by reducing both dimensions of which it is comprised).

With this background we will now examine the temperature distribution in the heater to qualitatively assess the thermal stress conditions. An idealized sketch of the temperature distribution is shown in Figure 1 (text). Not shown in this figure is the radial distribution of temperature. The cored bricks in contact with the insulation are cooler than those in the center of the bed. This distribution is caused by heat loss through the insulation and can be quite significant, 300° to 600°F from the center to the edge of the bed.

Thus, individual bricks have a vertical temperature distribution and a horizontal temperature distribution even without the added effect of gas flow through the bed. During reheat the bricks are heated at the surface of the holes, and during blowdown they are cooled. These flows produce

temperature distributions within the webs between the holes. The thermal stresses are, of course, determined by the entire temperature distribution within the brick. For discussion purposes, however, it is convenient to separate these into two kinds of stresses: "body stresses" caused by the vertical and horizontal temperature distributions acting alone and "web stresses" caused by the temperature distribution in the web acting alone. The separation is convenient because the temperature distribution in the webs (and, therefore, the web stresses) is dependent upon the heater flow conditions over which the operator has control, while the horizontal distribution is controlled by the insulation design. Thus, only the vertical temperature distribution is controlled through the reheat process.

The vertical temperature distribution has, for the most part, a negative second derivative which will cause body stresses that are tensile at the surface. In the ideal case of a linear ramp and linear plateau, the linear portions would produce stresses only because the material properties are temperature dependent. The maximum second derivatives would be produced at the cold air entrance to the bed and at the "intersection" of the ramp and plateau. This suggests that the maximum stresses caused by the vertical temperature distribution will be at these locations also, but a detailed analysis that included the effects of temperature dependent properties and creep would be needed to establish stress level with certainty.

The radial temperature distribution within the bed also has a negative second derivative. Therefore, both the vertical and radial distributions tend to produce tensile stresses in the surface of the bricks. Calculations of the stress field would require a substantial programming and digital computer effort. This was not done. It was hoped that the heater operation would provide information in this area, recognizing that interpretation would be difficult because of the presence of the web stresses.

The vertical and radial temperature distributions do not depend upon the size of the individual cored bricks. Rather, these distributions are related primarily to the length and diameter of the bed, coupled with the insulation design and heater flow conditions. For a given bed, the "body stresses" can be reduced by making the cored bricks smaller. Cracking and fracture reduce stresses by effectively making the bricks smaller. Thus, if some of the bricks are overstressed they will crack or fracture. This process will not be progressive unless the broken pieces tend to plug holes in the bed.

Web stresses caused by the reheat gas flow are much lower than those caused by the blowdown air flow with the exception of the top foot or so of matrix, because the rate at which the bed is heated is much lower than the rate at which the bed is cooled. Also, the air flow produces tensile stresses at the surface of the holes, whereas the reheat flow produces tensile stresses inside the webs. The former condition is more critical. Consequently, air flow conditions that would produce excessive web stresses must be avoided. The analysis used to establish the air flow limitations is described in the following section, Web Stress Analysis.

The web tensile stress is proportional to the rate at which the web is cooled, which, in turn, is proportional to the air flow rate. A bed designed to give maximum performance will have a large fraction of its cored bricks operated at the design stress level. Therefore, excessive flow rates could cause wide scale web cracking throughout the bed. Further, this would happen during the blowdown process when structural failure of the bed could result in broken pieces being blown out of the heater. Consequently, operational safety and bed life were judged to be more dependent upon the web stresses than upon other conditions, such as body stresses and creep.

Many of the bricks in the bed will be cooled through a temperature range of several hundred degrees during a tunnel run. (It is interesting to note, in comparison, that the temperature difference within the webs is only at 40°F at the maximum conditions.) Nonuniform cooling can produce large temperature variations within a brick and therefore, large "body" stresses. Uniform flow through the holes is needed, which requires that the bricks be held in alignment. This was achieved through the use of tongue and groove keys.

Thermal stress levels are also influenced by creep deformation at high temperatures. Deformation will reduce both tensile and compressive stresses. If the brick is than cooled rapidly so that reverse creep does not occur, residual stresses will develop that are reversed in sign from the initial stresses. The magnitude of the residual stresses depends upon the completeness of the high temperature stress relaxation and the modulus of elasticity at the low temperature. Under some conditions the residual stresses are larger than the initial stresses.

Creep deformation requires stress and time. The reheat web stresses exist for long times but are very low in magnitude. The cooling web stresses are high, but their duration is very short. Therefore, it is unlikely that the web stresses will be relaxed significantly.

On the other hand, the body stresses can be large and are of long duration and therefore, could be relaxed by deformation. Rapid cooling to below the creep temperature range would then introduce reversed stresses. For the cored bricks, this would mean, for the most part, residual stresses with tension in the interior and compression in the exterior.

Estimation of these effects requires knowledge of the creep characteristics of the material. This information is currently not available for the zirconia material used in the bed. This remains an area for further work.

The top and the bottom of the bed deserve mention. At the bottom the cold air causes rapid cooling and tensile stresses. The grate structure and the metal grate plates provide support and also receive the frontal blast of the air. The alumina bricks at the grate are never operated at high temperature but always in a range where the thermal conductivity and strength are high. The actual condition of the bricks near the grate will not be known until the bed is disassembled sometime in the future.

The top of the bed receives the hot combustion gases from the burner. Failure from too rapid heating is definitely possible. For this reason, the upper layers of the bed are thin (1/2 to 1 inch) cored bricks (called buffer layers) which develop lower stresses than the long bricks. Burner flow rates and temperatures are controlled to limit rapid temperature changes and therefore, limit thermal stresses during the reheat process.

Web Stress Analysis

The web stresses caused by the air flow were analyzed on the basis of an idealized model (Ref. 1, Appendix H). The stresses that would be caused by the vertical and radial temperature distributions were ignored (i.e., the body stresses). This is equivalent to assuming that the radial temperature across the bed is uniform and that the vertical temperature distribution does not contribute to the stresses. Remembering that a linear temperature distribution existing across a material with temperature-independent properties does not create stresses, makes the latter assumption fairly reasonable except at the ramp-plateau junction.

Under these assumptions, a single cored brick becomes equivalent to a nest of tubes, each with a circular hole and a hexagonal outer surface. The hexagonal tube was further simplified to an equivalent round tube having the same cross-section area in the tube wall. The hole pattern used is one with a hole diameter of 0.194 inch and a web thickness of 0.085 inch. The equivalent circular diameters are 0.194 I.D. and 0.293 O.D. For the circular tube, the elastic stress at the surface is (plane strain with tube ends not restrained, Refs. 6 and 7):

$$S = \frac{\alpha E}{1 - \nu} (T_{ave} - T_{surf}) \tag{1}$$

where S is the surface stress, T_{ave} is the average temperature of the tube wall, and T_{surf} is the temperature of the surface in question (inner or outer). In this application, the inner wall stress is desired, and T_{ave} is also equal to the average temperature through the web of the cored brick.

The relationship of the ΔT of Eq. (1) to the hole pattern dimensions and the heater operating conditions is presented in Ref. 1 (Appendix H). Equating the heat transferred from the ceramic (i.e., from the equivalent circular tube) to the air gives the following equations:

$$T_{ave} - T_{surf} = \frac{R_3}{8} D^2 \frac{C_p}{k_s} \frac{\dot{m}}{A} \frac{dT}{dZ} \tag{2}$$

$$T_{ave} - T_{surf} = -\frac{R_1}{8} \frac{D^2}{a} \frac{dT}{d\theta} \tag{3}$$

R_1 and R_3 are functions of the hole spacing-to-hole diameter ratio and are equal to .22 and .38, respectively, for the geometry used. The temperature on the right hand side is the temperature at any location within

the web. Examination of computer solutions for the temperature distribution through the bed has shown that this is a good approximation for the ramp portion of the bed temperature distribution, except near the cold air inlet.

Eqs. (1), (2), and (3) provide the desired relations among the ceramic properties, the tube inner and outer diameters (or cored brick hole diameter and web thickness), and the bed operating conditions: mass flow per unit area, slope of the temperature ramp, and temperature rate of change. The equations can be applied to any vertical location in the bed using material properties corresponding to the local temperature. By setting the stress in Eq. (1) equal to the tensile strength, the maximum allowable temperature difference is obtained. Eq. (2) will then give the maximum allowable flow rate and temperature ramp, and Eq. (3) will give the corresponding time rate of change of temperature.

This procedure was applied in Ref. 1 to alumina and calcia-stabilized zirconia through use of property data from the literature. In order to apply literature data to design, it is necessary to account for the strong dependence of strength and modulus of elasticity on material density. The relations used are (Ref. 1, p. 96):

$$S = S_o e^{-7p}$$

$$E = E_o e^{-4p}$$

where p is the porosity and the subscript zero denotes zero porosity. With these relations, the corresponding result from Eq. (1) is:

$$\Delta T = T_{ave} - T_{surf} = (T_{ave} - T_{surf})_o e^{-3p}$$

A plot of this temperature difference versus material temperature (using Eq. 1) is shown as Figure 7c in Ref. 1. The lowest temperature differences occur in the range, 500° to 2500°F, for both alumina and calcia-stabilized zirconia. The porosity levels of interest in the present program are approximately 5% for alumina and 10% for zirconia. Corresponding minimum values of ΔT from Ref. 1 are 40°F for alumina and 60°F for zirconia.

From Eq. (2) the allowable mass flow is proportional to $k_s \Delta T/C_p$ With an increase in temperature, the conductivity of alumina decreases rapidly (for temperatures to about 2500°F, the specific heat of air increases, and, therefore, $k_s \Delta T/C_p$ decreases. Hence, the critical temperature for alumina is the highest value which occurs at the alumina-zirconia interface in the bed.

The thermal conductivity of zirconia increases slightly with temperature (Ref. 1, Figure 3c). Using the property values of Ref. 1, the parameter $k_s \Delta T/C_p$ varies only 12% in the temperature range, 500° to 2500°F, and rises for temperatures above and below this range. The actual minimum occurs at 2000°F, but this is not too significant because of the uncertainty in the properties. The mass flow limit from Eq. (2) can be determined by using zirconia properties within the temperature range, 500° to 2500°F, or the

minimum temperature if it is above 2500°F. This requirement is satisfied by using the temperature at the alumina-zirconia interface.

Comparison of alumina and zirconia shows that zirconia will have the lowest allowable flow rate from Eq. (2). Consequently, estimates of the web stress limited flow rates have been based upon the zirconia portion of the bed and specifically, by use of properties at the interface temperature. As noted above, the property values combine to give $k_s \Delta T/C_p$ values that are nearly independent of temperature in the range, 500° to 2500°F. The minimum values, together with the chosen hole pattern dimensions, give the following results from Eqs. (2) and (3) for zirconia of 10% porosity:

$$\frac{\dot{m}}{A}\frac{dT}{dZ} = 5800 \frac{\text{lb °F}}{\text{sec ft}^3}$$

$$\frac{dT}{d\theta} = 50°\text{F/sec.}$$

The web thickness at the outer surface of the hexagonal bricks is the same as that between the holes (Figure 29 - text). However, the outer web will be cooled from only one side when adjacent bricks are in contact. This will increase the local stresses. An approximate correction for this effect was made by increasing the wall thickness of the equivalent tube. The larger value was calculated by using the true ratio of open area to total area of the hexagonal brick, which is 0.40 (the repeating hole pattern gives .44). The equivalent tube with this ratio of open to total area has an O.D./I.D. of 1.58. This increases the value of R_3 used in Eq. (2) from 0.38 to 0.47, which then gives:

$$\left.\frac{\dot{m}}{A}\frac{dT}{dZ}\right]_{\text{fracture limit}} = 4700 \frac{\text{lb °F}}{\text{sec ft}^3}$$

R_1 increases from 0.22 to 0.29, giving

$$\left.\frac{dT}{d\theta}\right]_{\text{fracture limit}} = 38°\text{F/sec.}$$

These results provide a basis for determining operational limits for the heater. It is emphasized that they are based on property data from the literature for calcia-zirconia and upon an elastic stress analysis that considered only the stresses produced by the web temperature distribution during blowdown, i.e., that does not include the "body" stresses. In applying these results, a factor of safety is introduced to account for the various uncertainties. Tests were also made to confirm these results. Based upon those tests (discussed in the section, Web Stress Tests) operational limits of one-half the above values were selected.

Since the completion of the work described in this report, another reference (Ref. 9) dealing with a similar thermal stress problem has come

to the authors' attention and provides additional, useful information. Reference 9 describes a thermal stress analysis of a gas-cooled nuclear reactor. The reactor elements studied were tubes with circular holes and a hexagonal exterior. The additional stress caused by the hexagonal shape, as compared with the equivalent circular tube (as used above), was calculated. The maximum tensile stress occurred on the inner surface and at the thinnest part of the tube wall. The stress was 40% larger than that given by Eq. (1) for the dimensions of interest here. Application of this result reduces the numerical values given above to 3600 lb °F/sec ft^3 and 36°F/sec but does not affect the test results discussed in the section, Web Stress Tests.

The relationship between mass flow and the vertical temperature gradient (dT/dZ) within the bed indicates that a linear vertical temperature distribution will allow maximum performance. This distribution is controlled through design of the insulation around the bed (i.e., control of heat losses) and through control of the reheat gas temperature and mass flow rate. The effect on the insulation design was to require less thermal resistance at the low temperature end of the bed (see Ref. 1 for discussion).

Web Stress Tests

As discussed in the text, the high temperature material chosen for the matrix was yttria-stabilized zirconia. The results described above were based upon published properties of calcia-zirconia. This difference, combined with the dependence of ceramic properties upon manufacturing methods, required that additional information be developed. One approach could have been to measure the high temperature properties and then use the method presented in the section, Web Stress Analysis, or even a more complete analysis. It was decided instead to perform subscale tests and to use Eqs. (1) through (3) to scale the results to the full-scale size. Tests were made (Ref. 4) in two steps. Both steps involved heating and cooling a small bed of cored bricks (or pieces cut from cored bricks) in a way similar to the large heater operation. Heating was relatively slow, but cooling was fast and at controlled rates with the web temperatures measured with platinum/rhodium thermocouples.

The first step employed a bed 1-1/2 inches in diameter by 6 inches long. Specimens were heated to 2700°F and then cooled by blowing air. Runs were made in groups of five with the cooling rate increase successively at roughly 5°F/sec intervals. The specimens fractured early in the test because of the large radial and axial temperature variations (body stresses). But the onset of web cracking was clearly evident as the cooling rate was increased. The results gave a wide range for the three yttria-zirconia materials tested: 20°F/sec, 50°F/sec, and 65°F/sec.

The second test employed a bed 5 inches in diameter by 6 feet long. The bed contained alumina at the cooler end and the remainder was zirconia (three kinds, side-by-side). This test was made at a cooling rate of 25°F/sec.

The hole pattern was identical to the .194 x .085 used in the heater. These results were qualitatively similar to those obtained with the smaller set-up. That is, the bricks fractured because of the large radial temperature variations, but there was very little evidence of web cracks.

The conclusion drawn from these tests was that 25°F/sec represented a reasonable design value in terms of minimizing web cracking; however, excessive radial and vertical temperature gradients could be damaging. Further, it was recognized that both the radial and vertical temperature variations would be less severe as the overall size of the bed increased in relation to the individual cored brick size. It was apparent, however, that some fracturing could occur without impairing the usefulness of the bed.

Upon review of both the subscale test results and the limited amount of property data available from the literature, the decision was made to limit pilot heater operation to one-half (i.e., safety factor = 2) the more conservative fracture limit, i.e.,

$$\frac{\dot{m}}{A}\frac{dT}{dZ} = \frac{4700}{\text{factor of safety}} = \frac{4700}{2}$$

which was based on the true ratio of open-to-total area of the hexagonal brick. The corresponding cooling rate is approximately 20°F/sec.

Application of this limit to the actual operation of the pilot heater, however, is more complicated. During pressurization a finite time and volume of air is required to fill the heater vessel and raise its pressure to the desired value. Thus, it becomes necessary that the mass flow entering the heater exceed that exiting the heater during the pressurization process. Consequently, the maximum flow rate occurs during pressurization, and hence, the limit must be applied to the pressurization flow rate.

To enable pressurization to occur within a reasonable time period, the pressurization mass flow was set 10% higher than steady state:

$$\frac{\frac{\dot{m}}{A}\frac{dT}{dZ}_{\text{steady state}}}{\text{safety factor}} = \frac{0.9\,\frac{\dot{m}}{A}\frac{dT}{dZ}}{\text{safety factor}} = \frac{(0.9)(4700)}{\text{safety factor}} = \frac{4230}{\text{safety factor}}$$

This equation is plotted in Figure 28 (text).

The pressurization rate is controlled by limiting the pressure drop across the bed.

REFERENCES

1. AEDC-TDR-64-48.

2. Hasselman, D.P.H. and Crandall, W.B., "Thermal Shock Analysis of Spherical Shapes, II," J. Amer. Cer. Soc., 46 (September 1963), 434-437.

3. DeCoursin, D.G., et al, "Recent Developments of Storage Heaters to Provide Flight Simulation for Air Breathing Propulsion Systems," Presented at AIAA Third Propulsion Joint Specialists Meeting (July 17-21, 1967).

4. Air Force Contract AF 40(600)-1094.

5. Hasselman, D.P.H., "Elastic Energy at Fracture and Surface Energy as Design Criteria for Thermal Shock," J. Amer. Cer. Soc., 46 (November 1963), 535-540.

6. Boley, B.A. and Weiner, J.H., Theory of Thermal Stresses, J. Wiley & Sons, 1960.

7. Timoshenko, S. and Goodier, J.N., Theory of Elasticity, 2nd Ed., McGraw-Hill, 1951.

8. Hasselquist, P.B., et al, "Study of an Uncooled Nozzle Throat for a Large Hypersonic Wind Tunnel," AEDC-TR-70-92 (May 1970).

9. Chandler, B.A. and McConnelee, J.R., "Thermal Stress Evaluation of Ceramic Fuel Elements," J. Nuclear Materials, 11, 3 (1964), 273-301.

UNCLASSIFIED

Security Classification

DOCUMENT CONTROL DATA - R & D

(Security classification of title, body of abstract and indexing annotation must be entered when the overall report is classified)

1. ORIGINATING ACTIVITY (Corporate author)	2a. REPORT SECURITY CLASSIFICATION
FluiDyne Engineering Corporation 5900 Olson Memorial Highway Minneapolis, Minnesota 55422	UNCLASSIFIED
	2b. GROUP N/A

3. REPORT TITLE

RESEARCH ON STORAGE HEATERS FOR HIGH TEMPERATURE WIND TUNNELS - FINAL REPORT

4. DESCRIPTIVE NOTES (Type of report and inclusive dates)

Final Report - January 1964 to September 1971

5. AUTHOR(S) (First name, middle initial, last name)

D. E. Hagford and D. G. DeCoursin

6. REPORT DATE	7a. TOTAL NO. OF PAGES	7b. NO. OF REFS
February 1972	177	16

8a. CONTRACT OR GRANT NO.	9a. ORIGINATOR'S REPORT NUMBER(S)
F40600-70-C-0006 also F40600-68-C-002 b. PROJECT NO. 3012 AF 40(600)-1054 c. Program Elements 62402F and 63723F d. Task 07	AEDC-TR-71-258
	9b. OTHER REPORT NO(S) (Any other numbers that may be assigned this report) N/A

10. DISTRIBUTION STATEMENT

Approved for public release; distribution unlimited.

11 SUPPLEMENTARY NOTES	12. SPONSORING MILITARY ACTIVITY
Available in DDC	Arnold Engineering Development Center, Air Force Systems Command, Arnold AF Station, Tenn. 37389

13. ABSTRACT

The results from the materials development program for the ceramics of the storage heater system for high temperature wind tunnels are presented. A number of ceramic oxides were evaluated including magnesia, zirconia, and alumina. Magnesia was dropped as a candidate early in the program because of the high vaporization rate experienced in a flowing combustion gas atmosphere. Zirconia was evaluated in its stabilized form using calcia, magnesia, and yttria as the stabilizing oxides. Yttria-stabilized zirconia evolved as the candidate material for the upper portion of the heater matrix (2800°F to 4200°F) and alumina for the lower portion (1000°F to 2800°F). The development program evaluated materials in both subscale and pilot scale tests. The performance of the individual materials during the various subscale tests is discussed. The design basis for a pilot facility is presented along with the material performances following the 85 run, pilot heater test program. Specifications for materials used in the pilot facility are presented along with a cored block specification prepared based on the development program.

DD FORM 1 NOV 68 1473

UNCLASSIFIED

Security Classification

14. KEY WORDS	LINK A ROLE	LINK A WT	LINK B ROLE	LINK B WT	LINK C ROLE	LINK C WT
hypersonic wind tunnels						
high temperature						
heat exchangers						
storage heaters						
heaters						
materials tests						
performance						
ceramics						
1 zirconium oxides						
2 yttrium oxides						
2 aluminum oxides						
3 magnesium oxides						
temperature						
pressure						
mechanical properties						

4. Heat exchangers.
5 Heaters.

AFSC
Arnold AFS Tenn